4 December 2012

Report to Prince William Sound Citizen's Regional Advisory Council:
Future Iceberg Discharge from Columbia Glacier, Alaska

Reference PWSRCAC Project #8551
Contractor: W. T. Pfeffer Geophysical Consultants, Nederland, Colorado

Report #1
Part I: Data Report

1. Overview

Columbia Glacier has the world's longest and most detailed observational record of an ocean-terminating glacier in rapid retreat. The complexity and volume of data requires that its organization and archiving be managed with care. This report provides a compact overview of the available information, from raw data and imagery to maps, technical reports, and papers published in the scientific literature. The data is organized geographically, with observations of the sea floor and glacial bed followed by observations at the glacier surface and meteorological observations of the local atmosphere. Within each geographic section, observations are categorized by type or source (e.g. ship-borne sonar, aerial photography, ground-based time-lapse camera), and wherever possible, a citation or hyperlink to the data is provided. Finally, certain ancillary data, such as geodetic datum adjustments and photogrammetric control, are listed.

A full discussion of the scientific literature on the Columbia Glacier is beyond the scope of this summary. However, a compact bibliography is included, and references are cited whenever necessary to explain the origin of a listed data quantity.

History: Credit for the initiation of the Columbia Glacier data record goes to the U.S. Geological Survey (USGS), in particular the efforts of Mark Meier and Austin Post, who anticipated as early as the mid-1960s that Columbia Glacier was likely to begin a rapid retreat. The USGS research program produced a significant body of analysis, most notably the USGS Professional Paper Series 1258 A-H (1982-1989), and archived data, much of which was cataloged digitally and summarized by Robert Krimmer (2001).

Following the end of the first period of major USGS participation, in the mid-1980s, research continued, supported mainly by National Science Foundation (NSF) awards to the Institute of Arctic and Alpine Research (INSTAAR) at the University of Colorado. A field program in 1987, funded by NSF and led by Mark Meier (who by that time had moved to the University of Colorado) and Barclay Kamb of Cal Tech, marked the last on-site investigation at the glacier, until resumption of the field program in 2004, funded by NSF and led by W. Tad Pfeffer at the University of

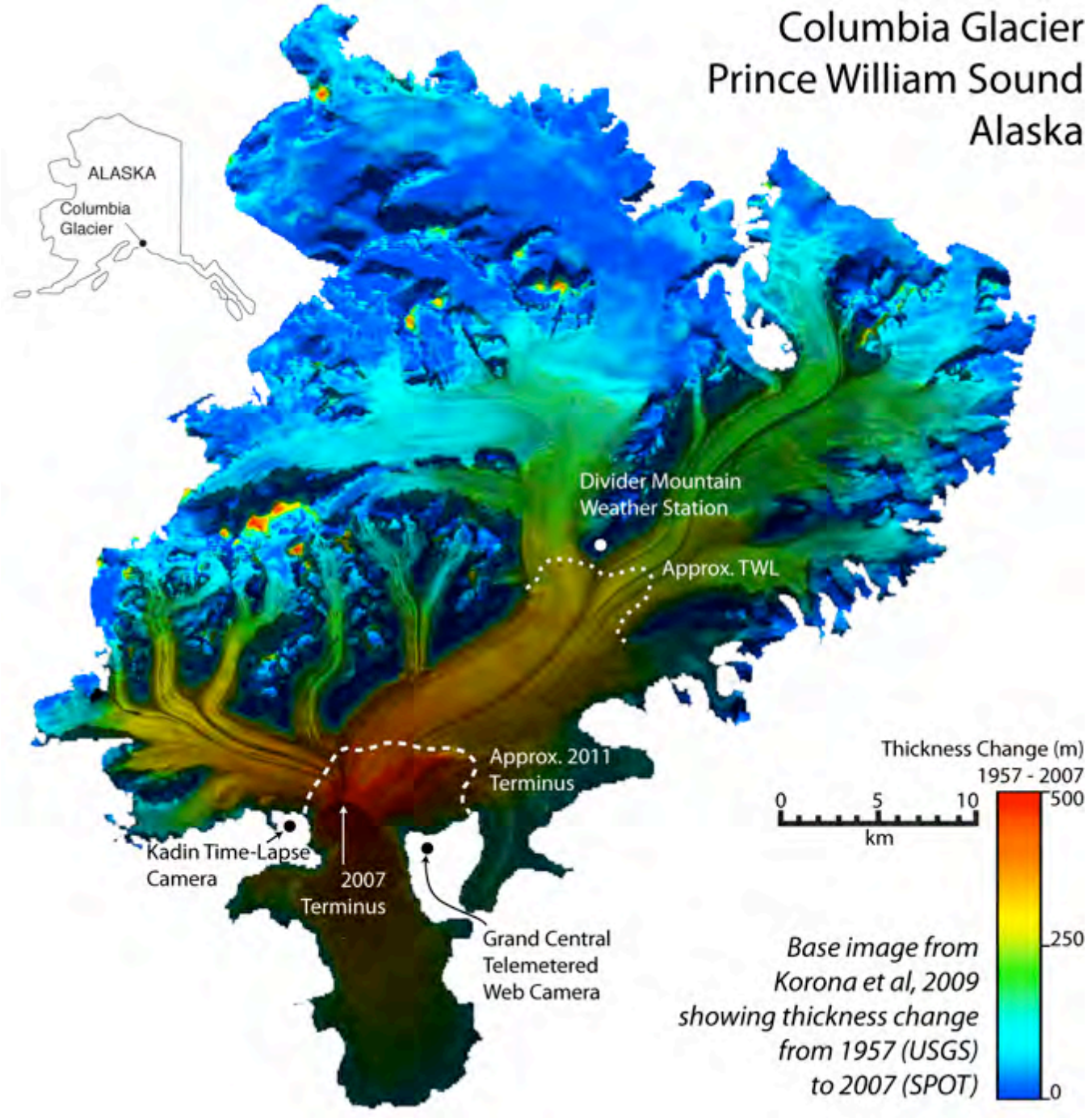

Figure 1a: Columbia Glacier Overview Map. Image shows surface elevation change from 1957 (
retreat geometry) to 2007. *Base image from Korona et al, 2009*

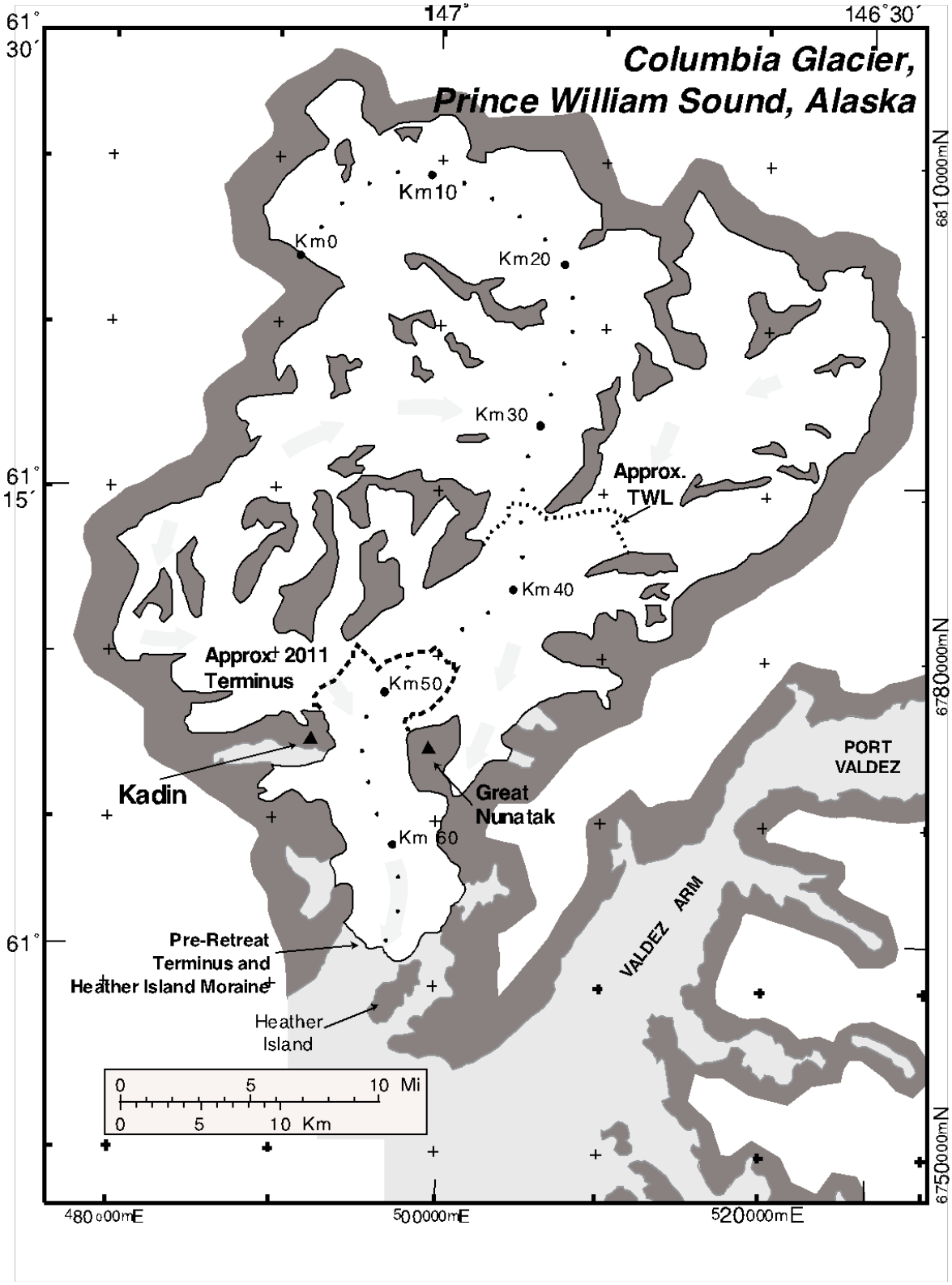

Figure 1b: Columbia Glacier, showing centerline coordinate system. Adapted from Krimmel, 2001.

Colorado. Regular acquisition of aerial stereo photography continued throughout the 1990s and 2000s, but was terminated in 2010. Data acquired and analyzed since the resumption of field operations in 2004 has been published in a variety of sources, and portions of that data (most notably the aerial and time-lapse photography) is archived at the National Snow and Ice Data Center (NSIDC) in Boulder, Colorado.

In 2005, the National Oceanographic and Atmospheric Administration (NOAA) research ship *Rainier* conducted a marine bathymetric survey of the Columbia forebay (the waters between the Heather Island moraine shoal and the glacier terminus at that time); the data from that survey is archived by the National Geophysical Data Center (NGDC).

In 2004, Shad O'Neel (then a graduate student at the INSTAAR research group and now at the USGS in Anchorage, Alaska) started making digital time-lapse camera observations of the Columbia Glacier terminus. Austin Post, Robert Krimmel, and others at the USGS had made time-lapse observations at Columbia Glacier as early as 1978, and in 1996-2000, Post and Wendell Tangborn (Hydromet, Inc. of Seattle, Washington) captured several sequences of the glacier terminus and iceberg drift in the forebay as part of the Iceberg Monitoring Project (IMP). The INSTAAR time-lapse program was expanded in 2006 when Pfeffer and O'Neel built high-resolution digital single-lens-reflex (DSLR) time-lapse systems for the British Broadcasting Corporation (BCC) and acquired time-lapse sequences for BBC producers. The sequences shot at Columbia Glacier were used in the television series *Earth: The Power of the Planet*, broadcast in Britain in 2007, and in the US in 2008 (under the title *Earth: The Biography*). These developments led, by 2007, to collaborations with US photographer James Balog and the formation of the Extreme Ice Survey (EIS). One of the missions of EIS has been to acquire time-lapse photography of glacier changes that are both compelling imagery for public communication and detailed quantitative documentation of events at glacier termini, including iceberg calving. Our terrestrial photogrammetric analysis at Columbia Glacier, drawing on (as of this writing) more than 160,000 images taken from more than 30 different camera positions surrounding the lower glacier, gives us direct quantitative measures of such quantities as terminus position, terminus height, near-terminus ice velocity, iceberg flux, iceberg size distribution and drift rate, and the presence and concentration of ice in the forebay, at regular intervals ranging from seconds to hours. Most of the images and accompanying metadata are archived at NSIDC; analysis of the data is in progress, but is reported on in some of the INSTAAR and USGS publications.

In 2010, David Finnegan of the U.S. Army Cold Regions Research and Engineering Laboratory (CRREL) in Hanover, New Hampshire, built and deployed a telemetered web camera at "Grand Central" (see Figure 1a) and a telemetered weather station at "Divider." After some early equipment failures and vulnerabilities to weather and snow loads, these installations are now operating reliably and available to the public

at www.glacierresearch.com. The images and meteorological data are archived and available to us for analysis. Both the camera and weather station are installed and maintained by CRREL at no cost to our project.

2. Data Types

2a. Ocean Bathymetry

Analyses of terminus retreat and iceberg discharge rely on knowledge of the bathymetry over the entire Columbia Glacier fjord, from the tidewater limit at approximately Km 35 (See Figure 1b) to the Heather Island moraine shoal at Km 69. The tidewater limit, marked as "TWL" in Figure 1b, marks the point at which the elevation of the glacier bed rises above sea level. (If the glacier were removed entirely, the coastline would reach the tidewater limit.) This tidewater reach, approximately half of the glacier's full length, is in direct contact with the ocean, and the evolving balance of stresses here are a primary control on the speed of ice flow, rate of vertical thinning, and rate of iceberg calving. The englacial and subglacial hydrology in the tidewater reach also influence the hydrology (and thus the flow dynamics) of the glacier lying above the tidewater limit. This linkage is hypothesized to be a primary control on the transfer of ice down over the tidewater limit from the upper glacier, a transfer that provided approximately 95% of the volume of ice lost from Columbia Glacier in 1995-2007. Understanding the dynamics and hydrological connection between the upper and lower glacier is thus a crucial part of making robust projections of future calving losses.

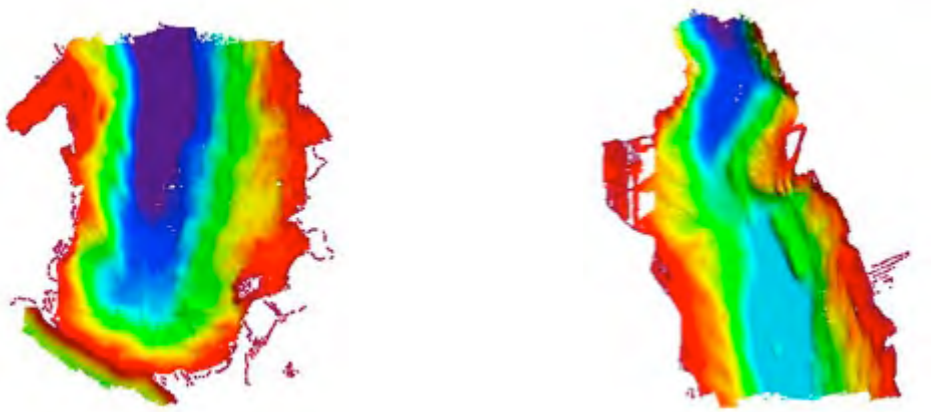

Figure 2a: Columbia Glacier forebay bathymetry, measured by NOAA (Noll, 2005) *Left*: Lower forebay; *Right*: Upper forebay. Note change in color coding of depths between panels; depth scale not available for these images. Maximum depths are ca. 400 m near join between images. *Source: Columbia Bay Hydrographic Survey RAP Sheets H11493/H11494. National Oceanographic and Atmospheric Administration. National Geophysical Data Center, National Ocean Service, Boulder, CO*

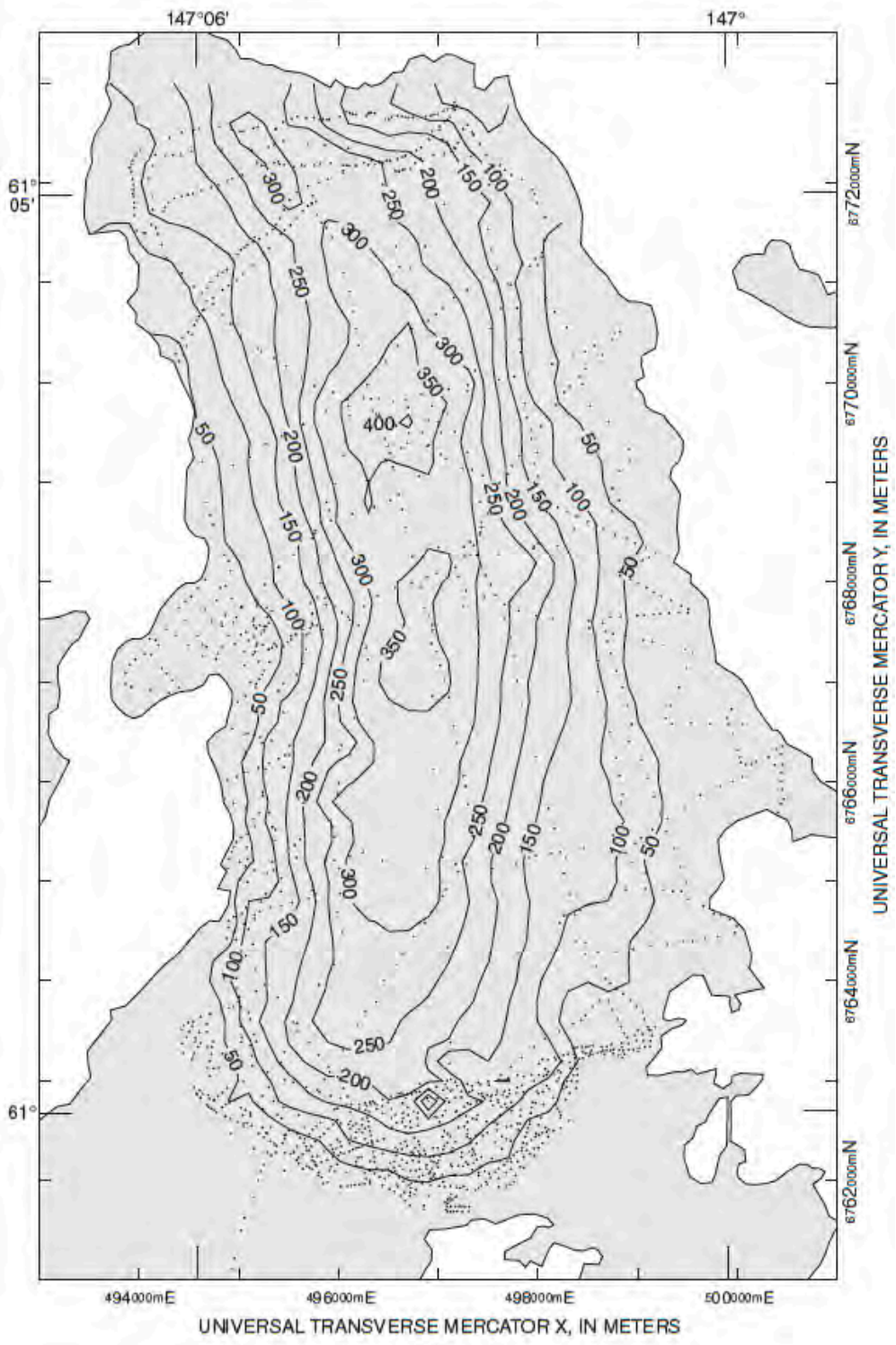

Figure 2b: Columbia Glacier forebay bathymetry from Krimmel (2001), based on USGS profiling.

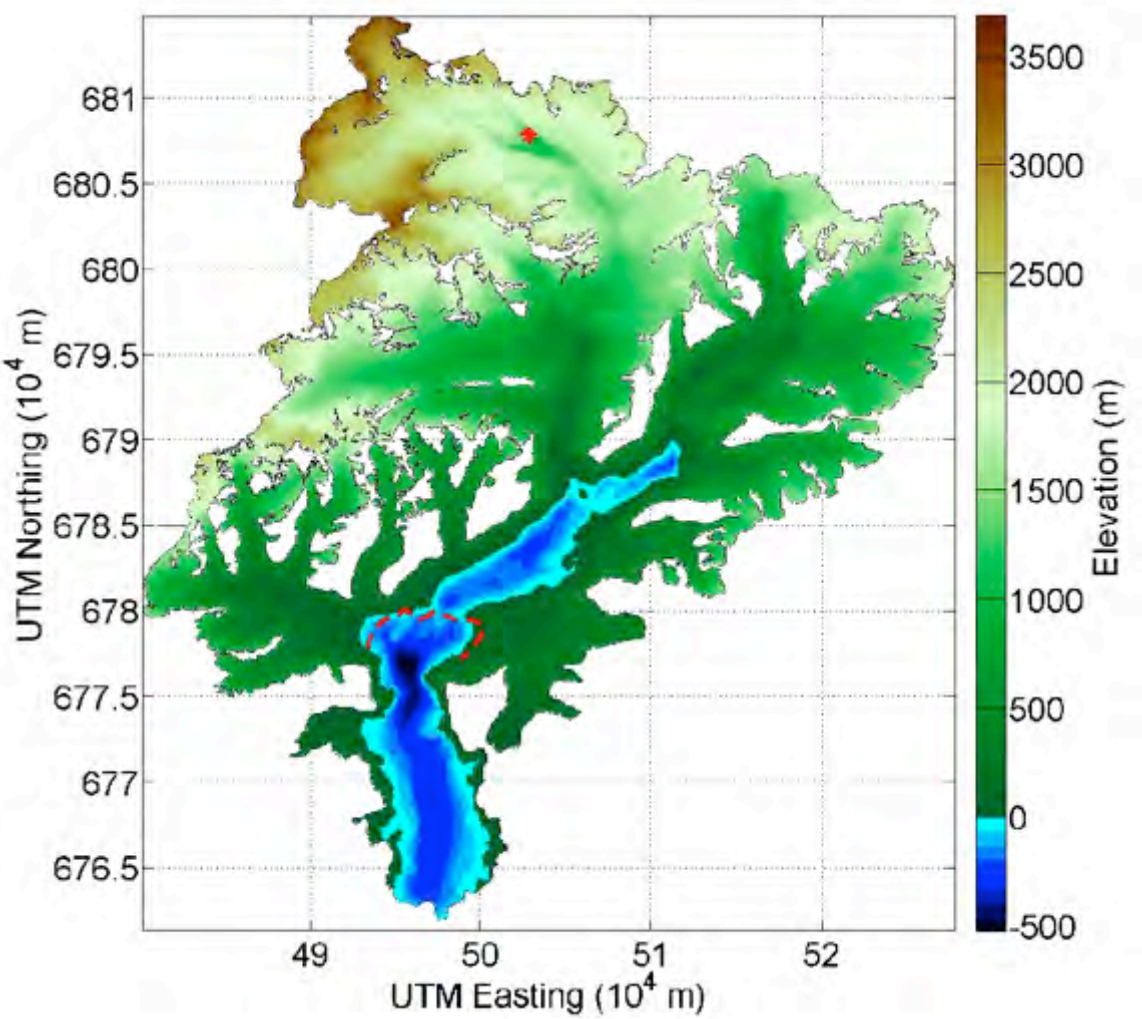

Figure 3: Fjord bed topography, combining NOAA survey data (Noll, 2005) and computed bathymetry (McNabb et al, 2012). The red dashed line shows the approximate position of the 2011-2012 terminus. *Source: Figure from McNabb et al, 2012.*

Subglacial bathymetry has been determined by three types of measurement: direct measurement of bathymetry in the open fjord below the terminus, computation of bathymetry above the terminus by ice flow modeling, and direct measurement of bathymetry above the terminus by ice-penetrating radar.

Sonar surveys: In the open fjord seaward of the glacier terminus, bathymetry can be measured directly by a variety of acoustic (sonar) techniques. Sonar surveys were conducted by the USGS research group periodically throughout the 1980s, but most of these were located in the immediate vicinity of the Heather Island moraine shoal because the forebay was almost continuously packed by calved ice. At certain times, however, the forebay was flushed clear of ice for days to years at a time. During the two-year period of ice-free conditions in 2004 and 2005, the NOAA ship Rainer

entered the forebay and made a complete survey of fjord bathymetry up to ca. Km. 52 (Figure 1b). This survey is the most detailed and comprehensive map of bathymetry made to date.

Bathymetry by computation: The bathymetry below the ice can be deduced computationally by analysis of detailed maps of velocities at the ice surface. The spatial resolution of the computed bathymetry is limited to length scales of approximately one ice thickness (between ca. 500 and 1500 m in most parts of the fjord), but is our only spatially complete source of bathymetry to date. Computed bathymetry in the outer forebay, calculated from observed ice flow from the 1980s when that region was occupied by ice, has been validated by comparison to the sonar surveys described above, and gives us confidence in the quality of our computed bathymetry in the regions still occupied by ice. Bathymetric computations, based on Rasmussen (1989), have been made by O'Neel et al (2005), Engel (unpublished MS thesis), and McNabb et al (2012). Digital Elevation Models (DEMs) are available from all of these sources.

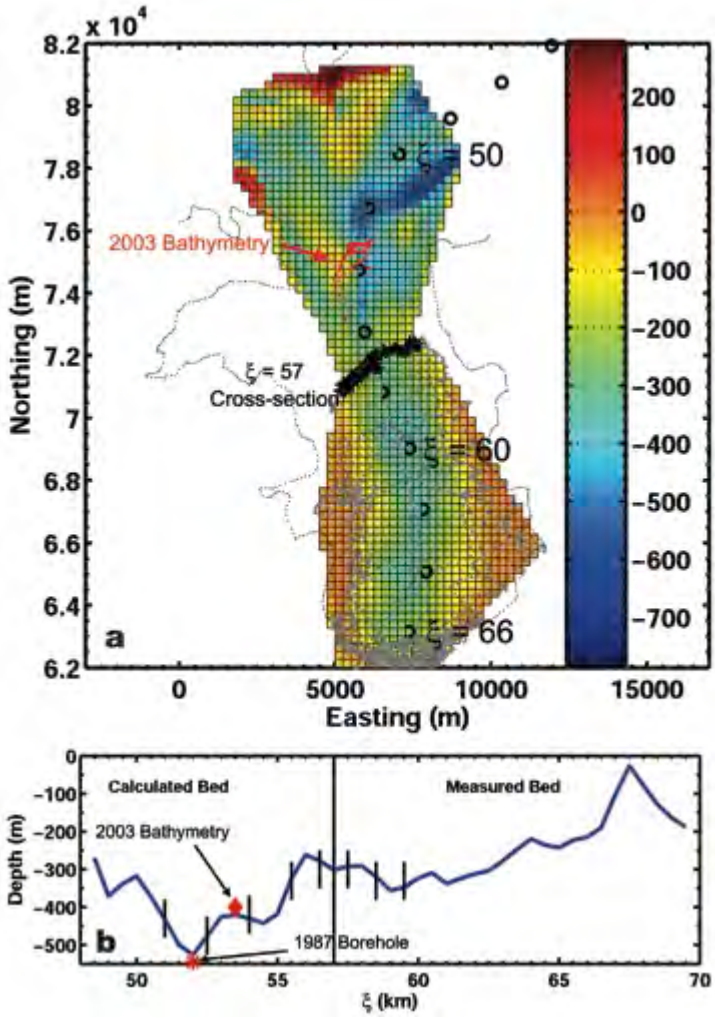

Figure 4a. Computed bathymetry from O'Neel et al, (2005).

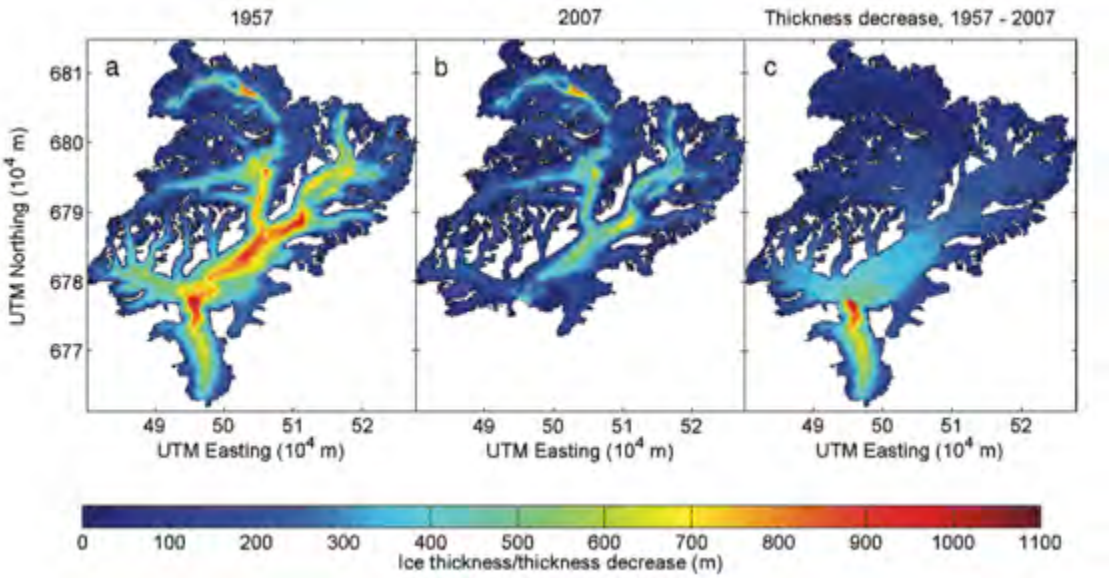

Figure 4b. Computed ice thickness (surface elevation – bed elevation) in 1957 (pre-retreat geometry) and 2007, from McNabb et al (2012). Their computed bed topography is shown in Figure 3b.

Ice penetrating radar: While widely used for depth sounding in polar ice, ice-penetrating radar has been difficult to adapt to temperate ice, where the presence of liquid water in the ice causes extensive scattering and attenuation of electromagnetic signals. Ground-based systems, where antennas laid on the surface are better coupled to the ice, are routinely used, but airborne systems have been much less successful, especially in thick, heavily crevassed ice typical of tidewater glaciers. Only in the past few years have airborne radar systems been developed that are capable of penetrating temperate glaciers as large and heavily crevassed as Columbia Glacier. Several airborne transects were flown successfully in 2010 (McNabb, et al, 2012) at Columbia Glacier. The soundings were profiles only (no grid surveys were flown), and their most immediate value for our purposes is as validation of the computed 2D bathymetry (Figure 5).

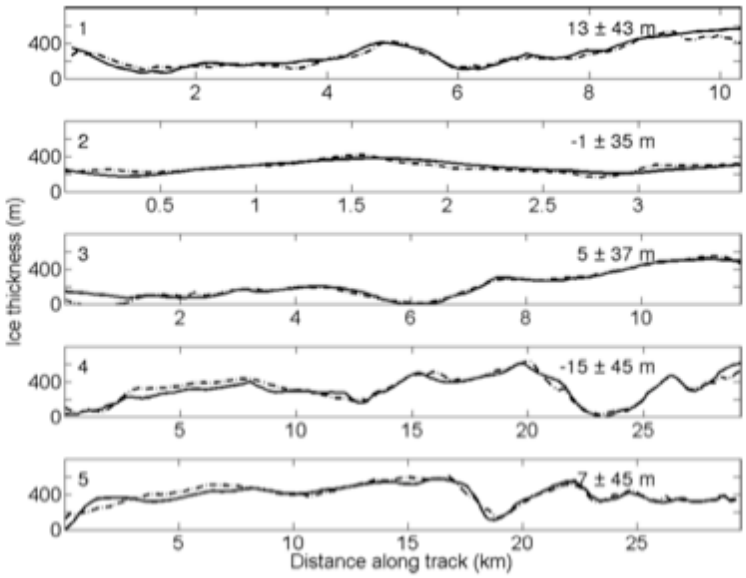

Figure 5: Computed (dash-dot line) compared to airborne radar soundings (solid line) for 5 different profiles at Columbia Glacier. The mean difference between computed and measured profiles is shown (in meters) on each panel. *From* McNabb et al, 2012; see the paper for location of profiles.

2b. Surface Topography

Over the three decades of retreat, the surface topography of the tidewater reach has been Columbia Glacier's most dramatically changing feature, and the documentation of that change is the most detailed record in the glacier archive. Sources of data include a pre-retreat (1957) USGS topographic map of the entire glacier (now digitized to a DEM), a full-glacier DEM derived from 2007 SPOT satellite imagery (Korona et al, 2009), periodic airborne laser profiles (Chris Larsen, UAF), a total of 135 vertical aerial photo missions covering 1974-2010, Worldview satellite and oblique aerial photo missions (and derived DEMs) starting in 2010, TerraSAR-X radar mapping at intervals starting in March 2011, and limited GPS and optical surveys of point locations throughout the project.

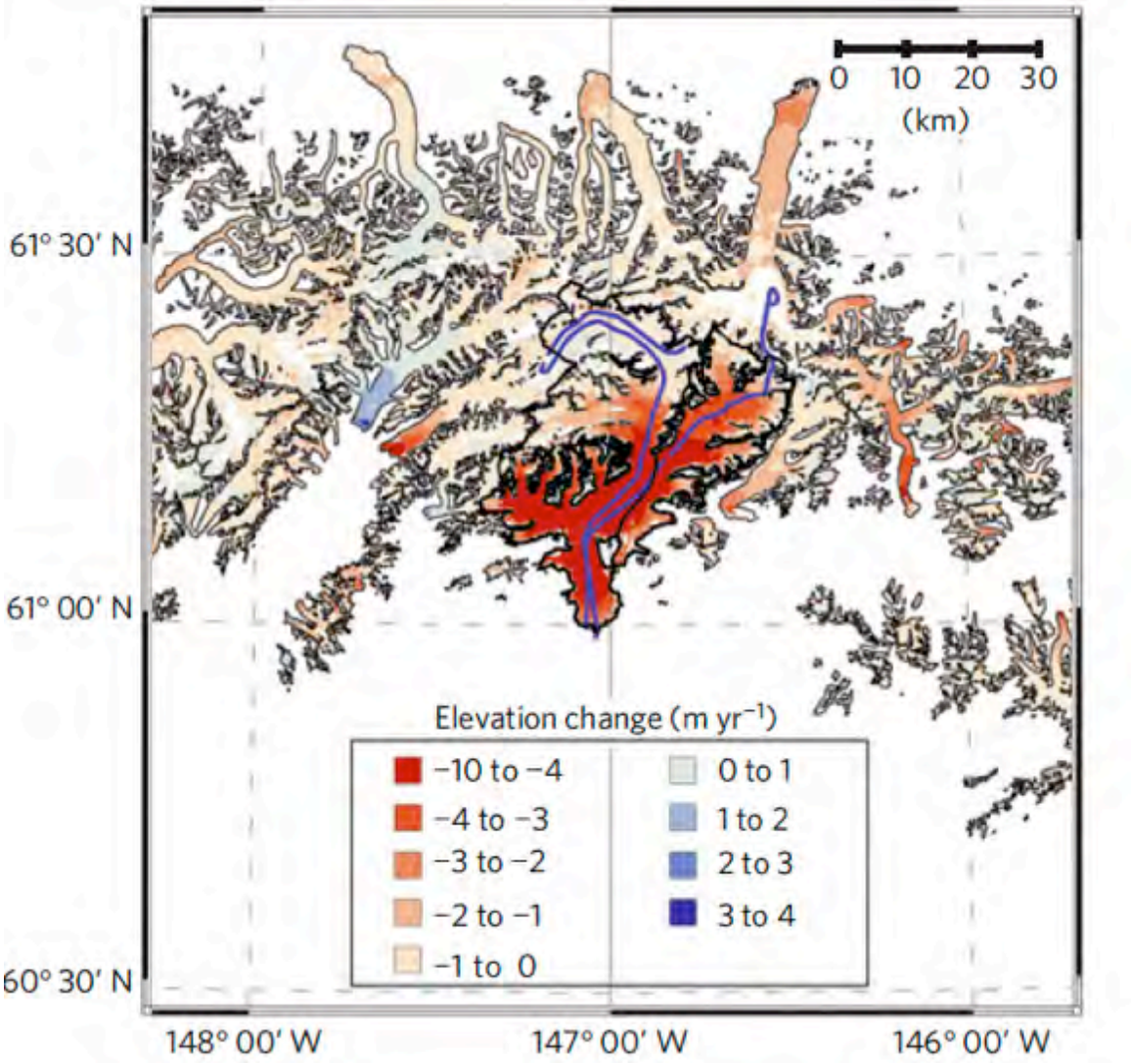

Figure 6a: Columbia Glacier elevation change, 1957-2007. Adapted from Berthier et al, 2010. Data sources are the 1957 USGS topographic map and 2007 SPOT5 Stereoscopic imagery (Korona, 2009).

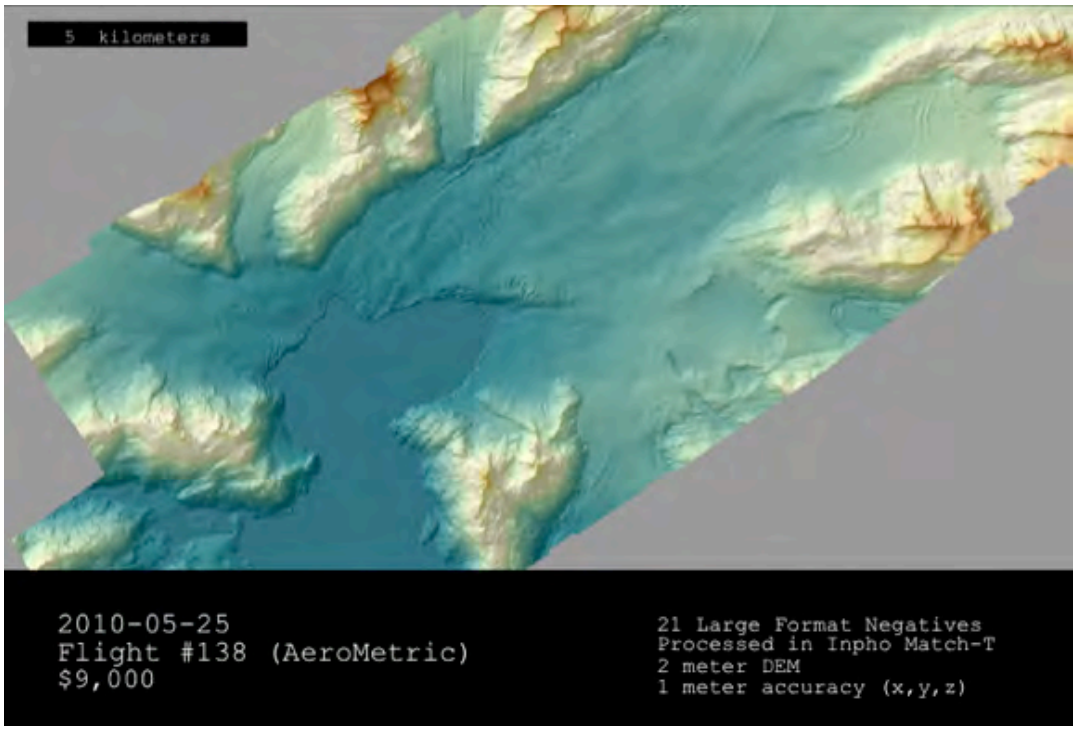

Figure 6b: DEM generated from vertical aerial photography and conventional photogrammetric analysis. Images acquired 25 May, 2010. Analysis: Aerometric Inc., and E. Z. Welty

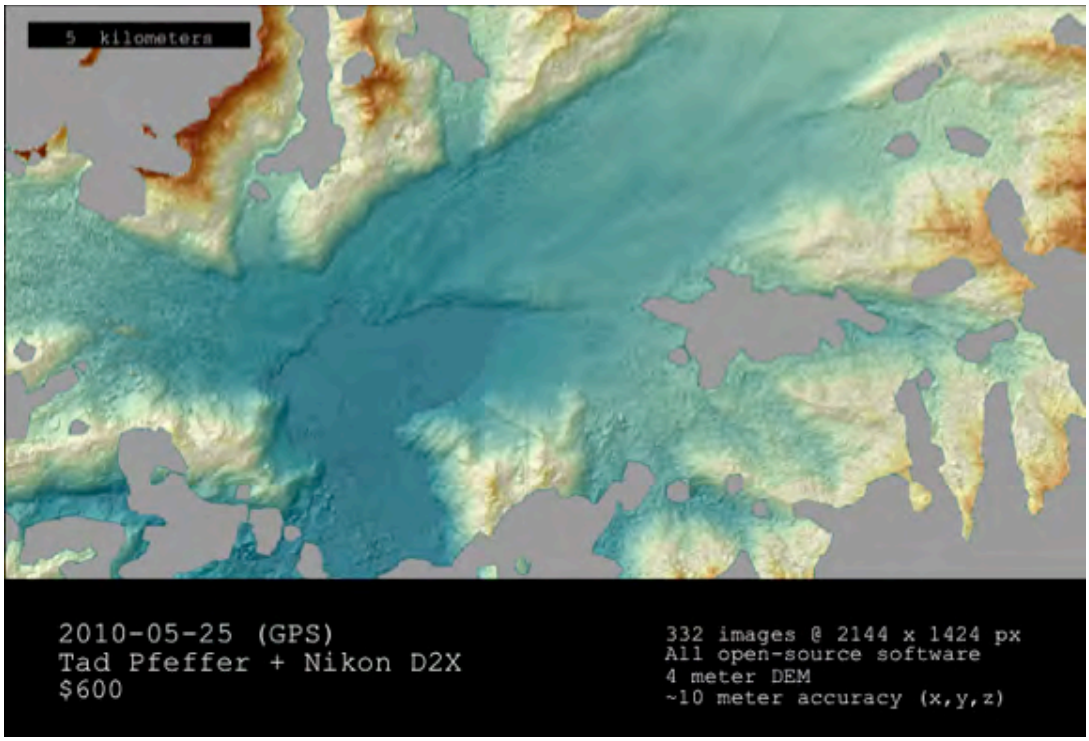

Figure 6c: DEM generated from oblique aerial photography and structure from motion (FM), images acquired 25 May, 2010. Analysis and plot: E. Z. Welty

Photogrammetric analyses by the USGS in the years up to 2001 were performed on analytical plotters, and feature tracking (for velocity determination) required manual point-by-point feature identification. As a result, topographic maps were made only on an as-needed basis (and most are unpublished) while velocity fields calculated during this time were generally very sparse, containing only a few hundred points. We have been working over the past several years to derive high resolution, digital maps of elevation and velocity using photogrammetric scans of the original film. This reanalysis has given us the opportunity to review and correct datum discrepancies (see section on ancillary data, below).

Most of the topographic analyses during the USGS Columbia Glacier project were focused on obtaining along-flow profiles of elevation change (Figure 6d), again because of the labor involved in making repeated topographic maps. Figure 6d shows an example of the evolution of glacier thinning and terminus retreat over the course of the retreat.

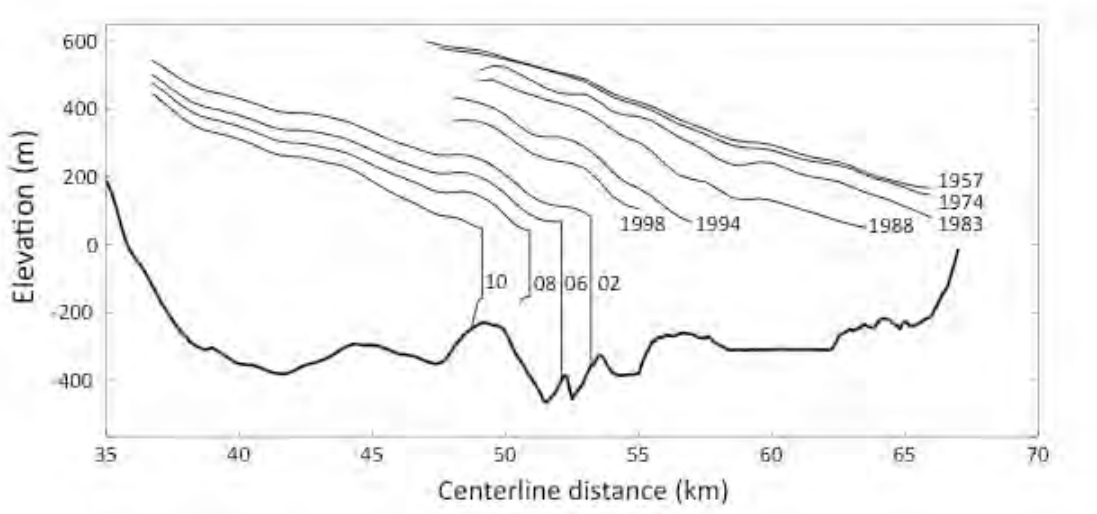

Figure 6d. Along-flow profile of surface elevation from pre-retreat (1957) to 2010. The profile follows the along-flow coordinate system shown in Figure 1b. The basal topographic profile is from McNabb et al, 2012. Plot: E. Z. Welty

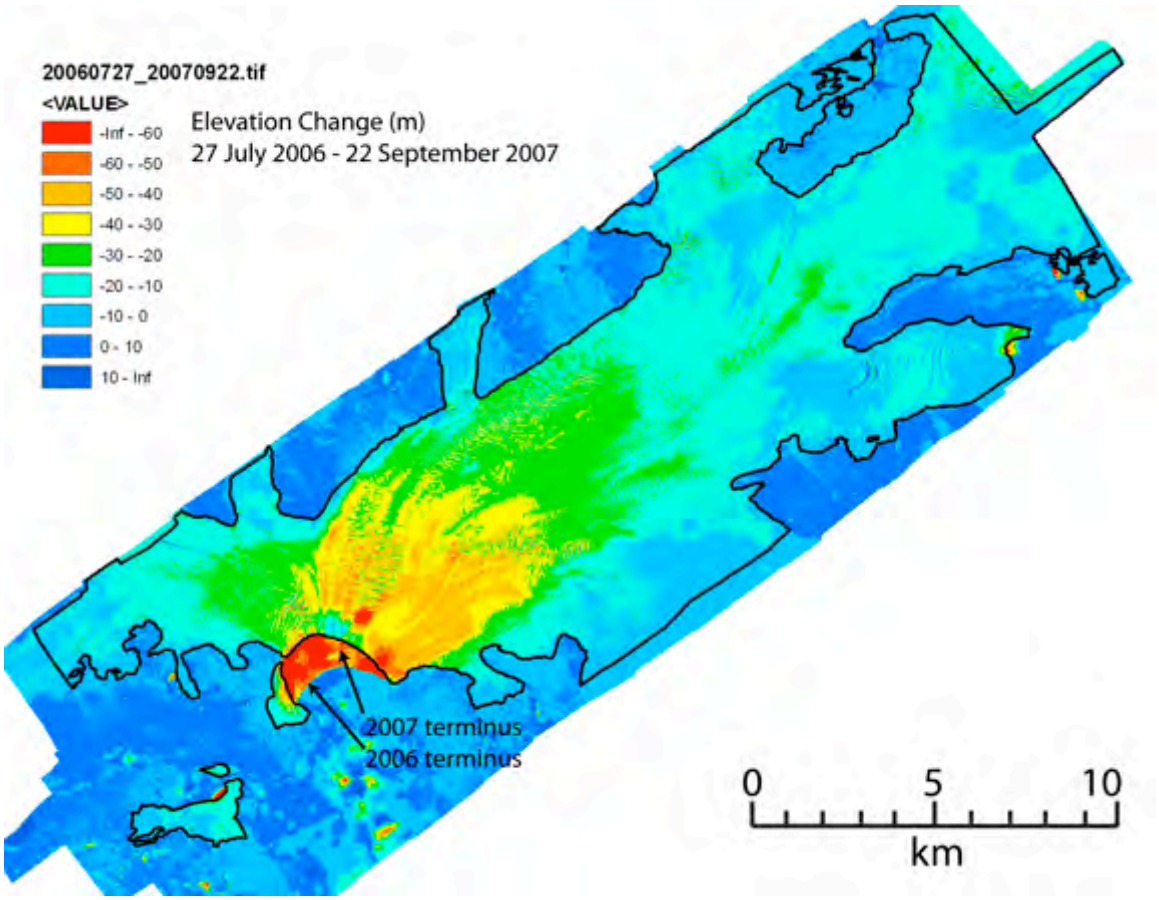

Figure 6e. DEM differencing from aerial photogrammetry obtained 27 July 2006 and 22 September 2007. Analysis: E. Z. Welty. The glacier is outlined in black; regions enclosed include the terminus, lowest part of the West Branch, and the Main Branch up to Divider Mountain. The thinning during this interval represents some of the maximum rates of observed change, when we observed a 5 x 5 km region that thinned in excess of 30 m in roughly 1 year.

2c. Terminus Retreat Rate

Terminus position has been measured over annual to seasonal time scales from vertical aerial and satellite photography, and on sub-seasonal to annual time scales using time-lapse photography. Assigning a single number to the terminus position (a glacier length) has been typically accomplished by averaging the position of the glacier terminus over a 1 km wide swath centered on the glacier flow centerline.

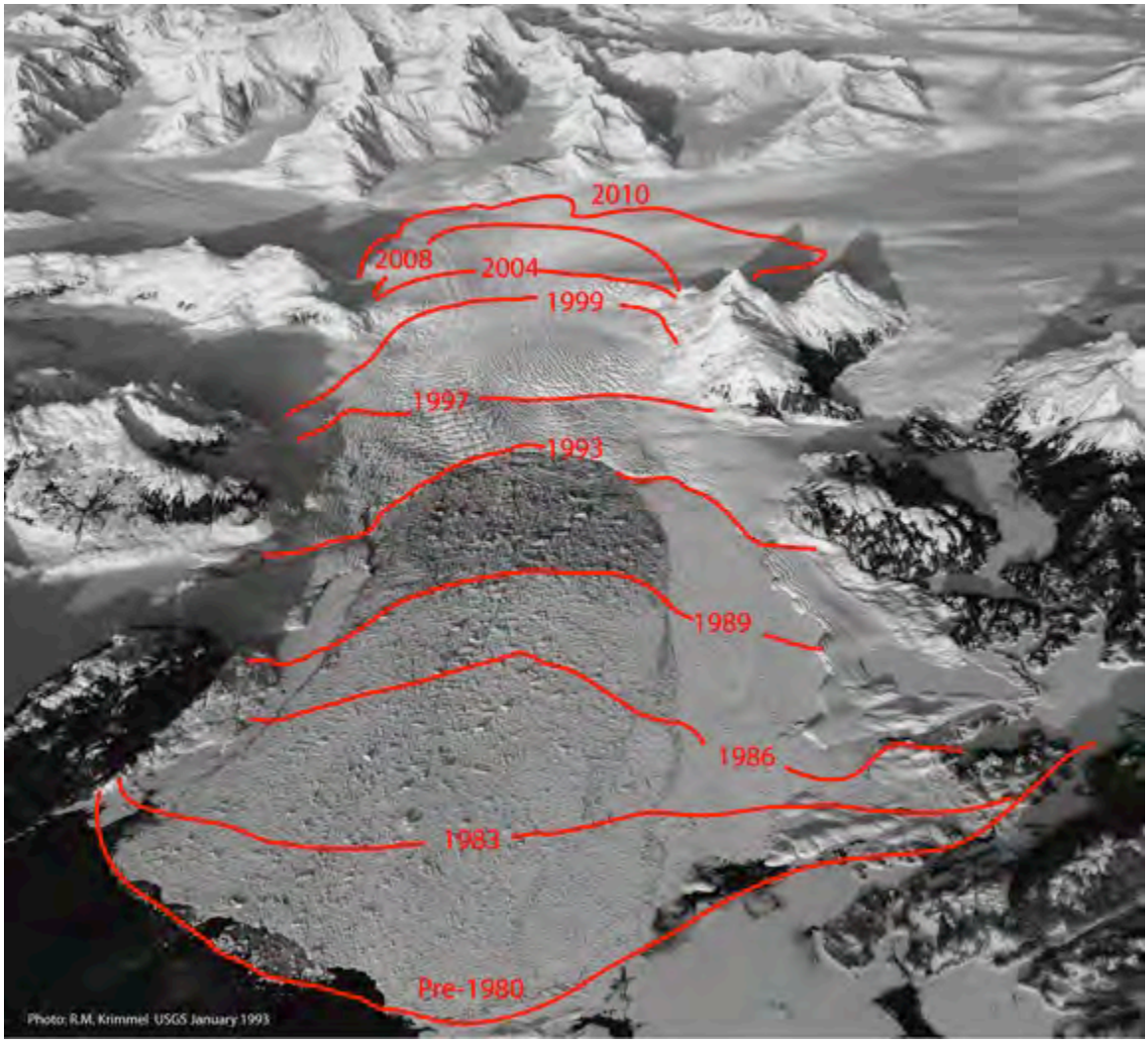

Figure 7a: Glacier terminus positions, pre-retreat to 2011. Photo: R.M. Krimmel, USGS

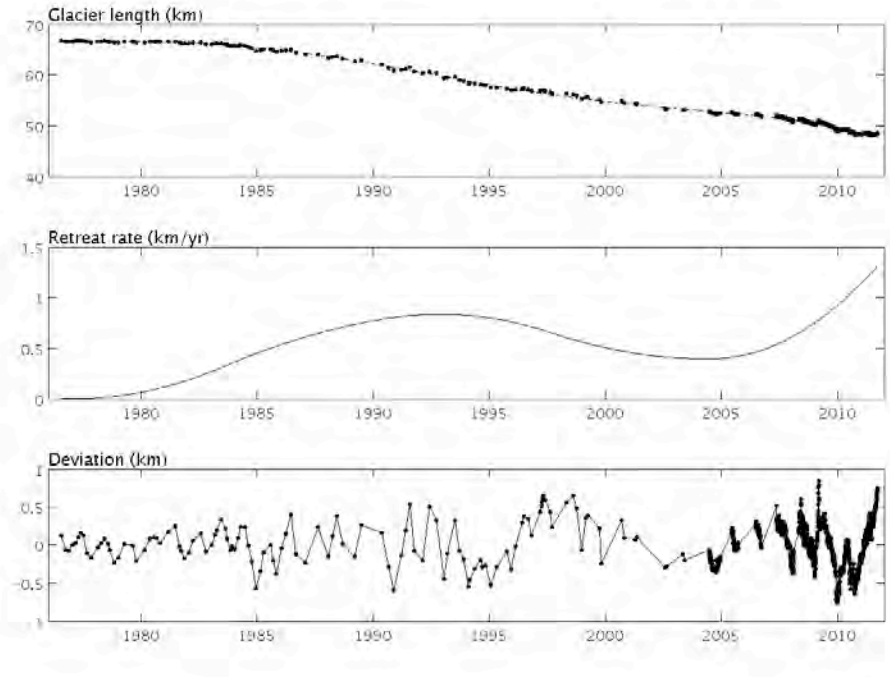

Figure 7b: Glacier length, terminus retreat rate, and deviation from local mean retreat rate. Analysis and Plot: E. Z. Welty

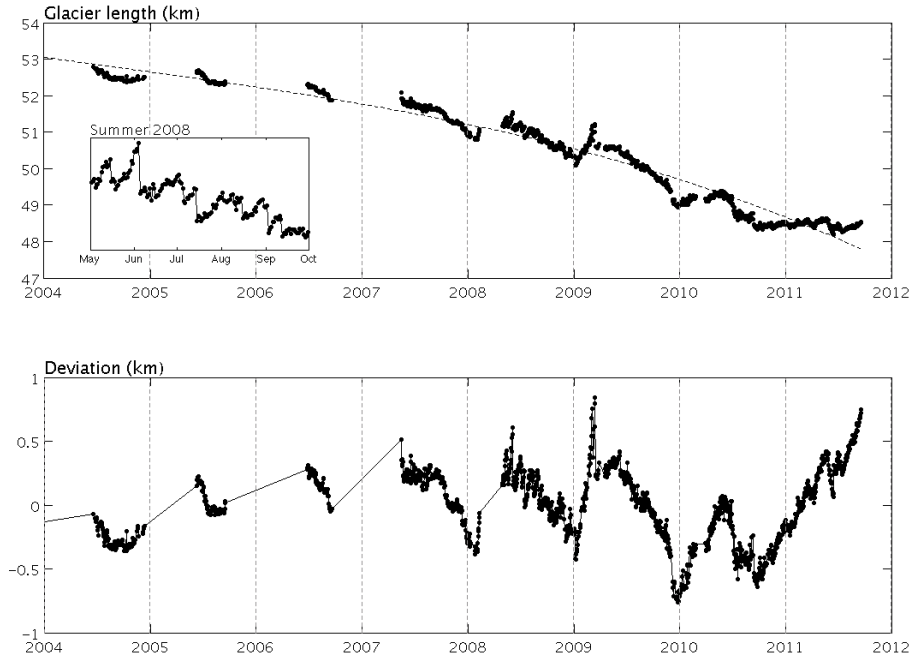

Figure 7c: Terminus position determined from time-lapse cameras, 2004-2012. Analysis and Plot: E. Z. Welty

2d. Ice Velocity

Measurements of ice surface velocity, together with thinning rate, provide the primary source of kinematic and dynamic information at Columbia Glacier. Velocity fields were calculated over the tidewater reach since the beginning of the USGS research program in the late 1970s, using manual point-by-point feature tracking. The coordinates of a distinctive feature visible in the first flight of a mission pair would be recorded and located again in the subsequent flight; the two 3D positions of the point divided by the time interval between the flights produces a 3D velocity vector for that period at that location. Manually identifying points was time consuming work, however, so velocities were measured for only a few hundred points in any given flight pair.

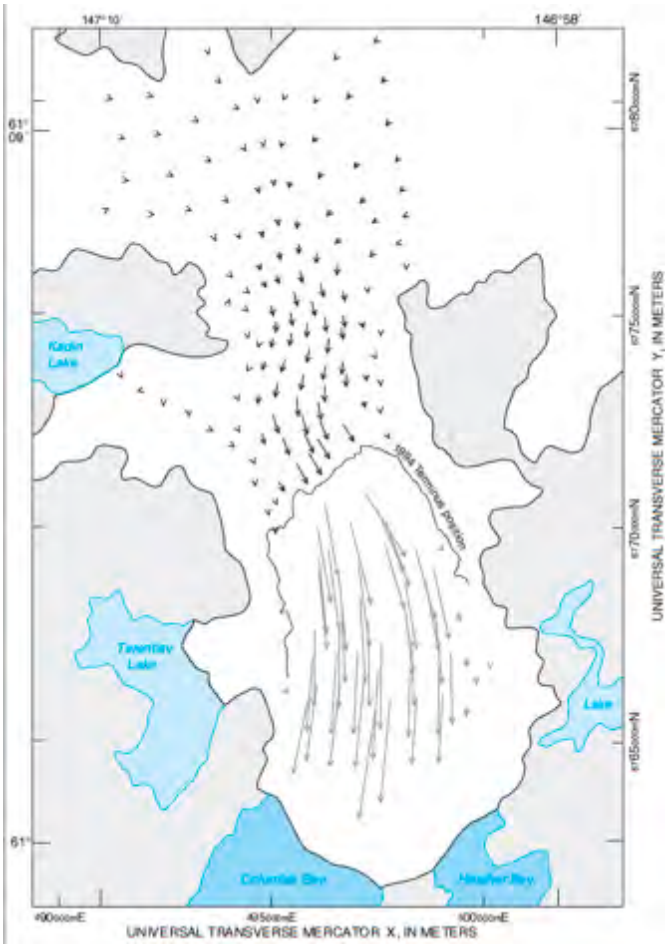

Figure 8a. Manually derived velocity field for the period August 13 – September 7, 1994. The velocity vectors are full scale: each connects the initial location of a feature to its final position 24 days later. Figure from Krimmel, 2001. Iceberg motion is shown in gray vectors.

After the conversion to digital photogrammetric analyses, it became feasible to use automated feature tracking, and the number of velocity vectors rose dramatically. Figure 8b shows a velocity map calculated using image processing and automated feature tracking.

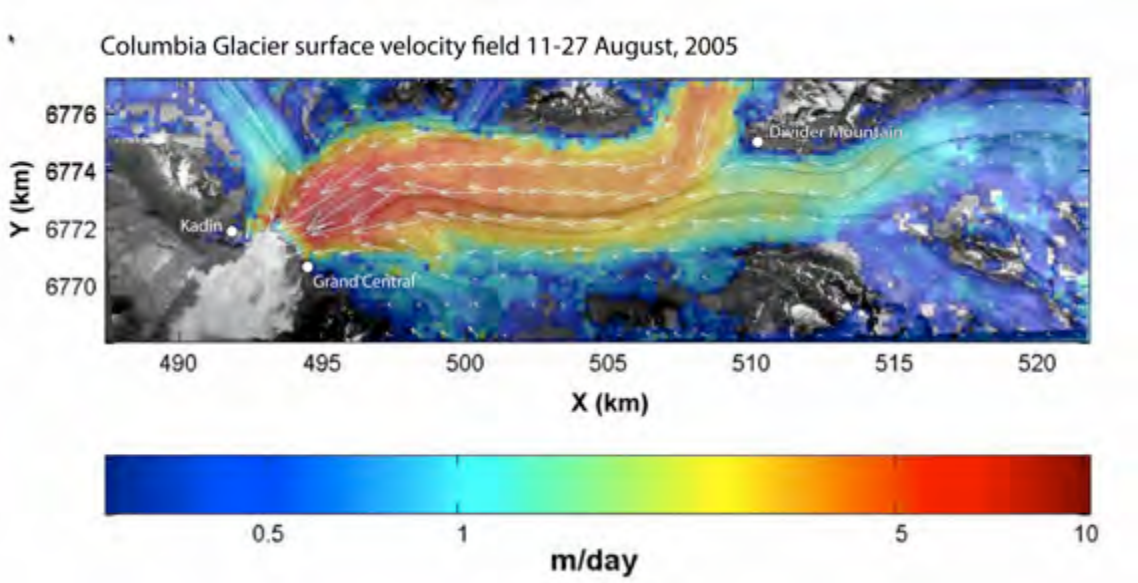

Figure 8b. Velocity field for 11-27 August, 2005, using automated feature tracking. Velocity points are determined on a 50x50 m grid. The entire field contains more than 120,000 velocity vectors. Analysis and image: Yushin Ahn.

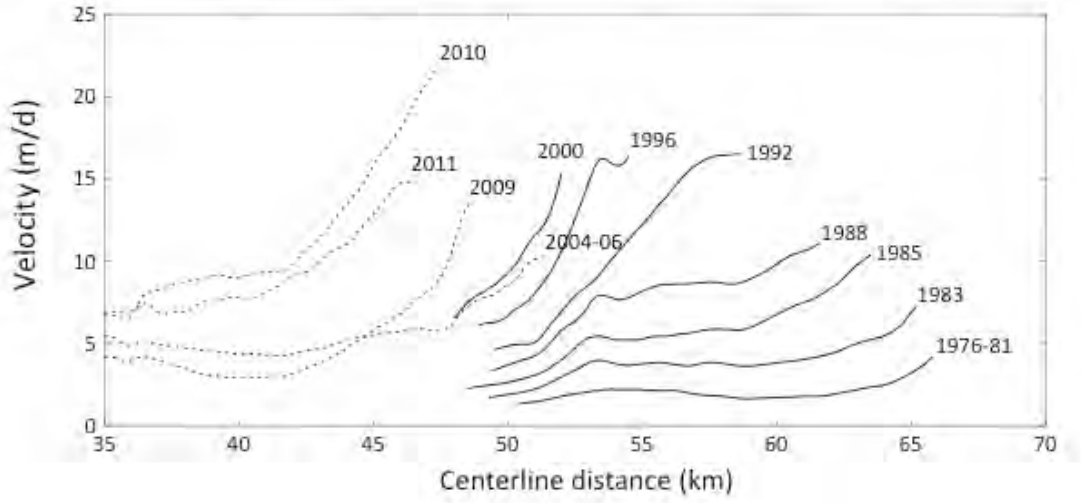

Figure 8c. Along-flow profile of surface velocity from pre-retreat (1957) to 2010. The profile follows the along-flow coordinate system shown in Figure 1b. Plot: E. Z. Welty.

Since the termination of aerial photogrammetric flights in 2010, we have obtained periodic high-resolution fields produced from TerraSAR-X radar imagery, courtesy

of Ian Joughin (APL, University of Washington). The radar imagery covers the entire glacier, and is available at 11-day intervals, which greatly increases the quantity of information available to us, although presently we are focusing our attention on velocity information extracted along a flowline starting above the TWL of the Main Branch and extending to the terminus. Figure 8d shows velocity profiles for the period 16 February to 26 July, 2011.

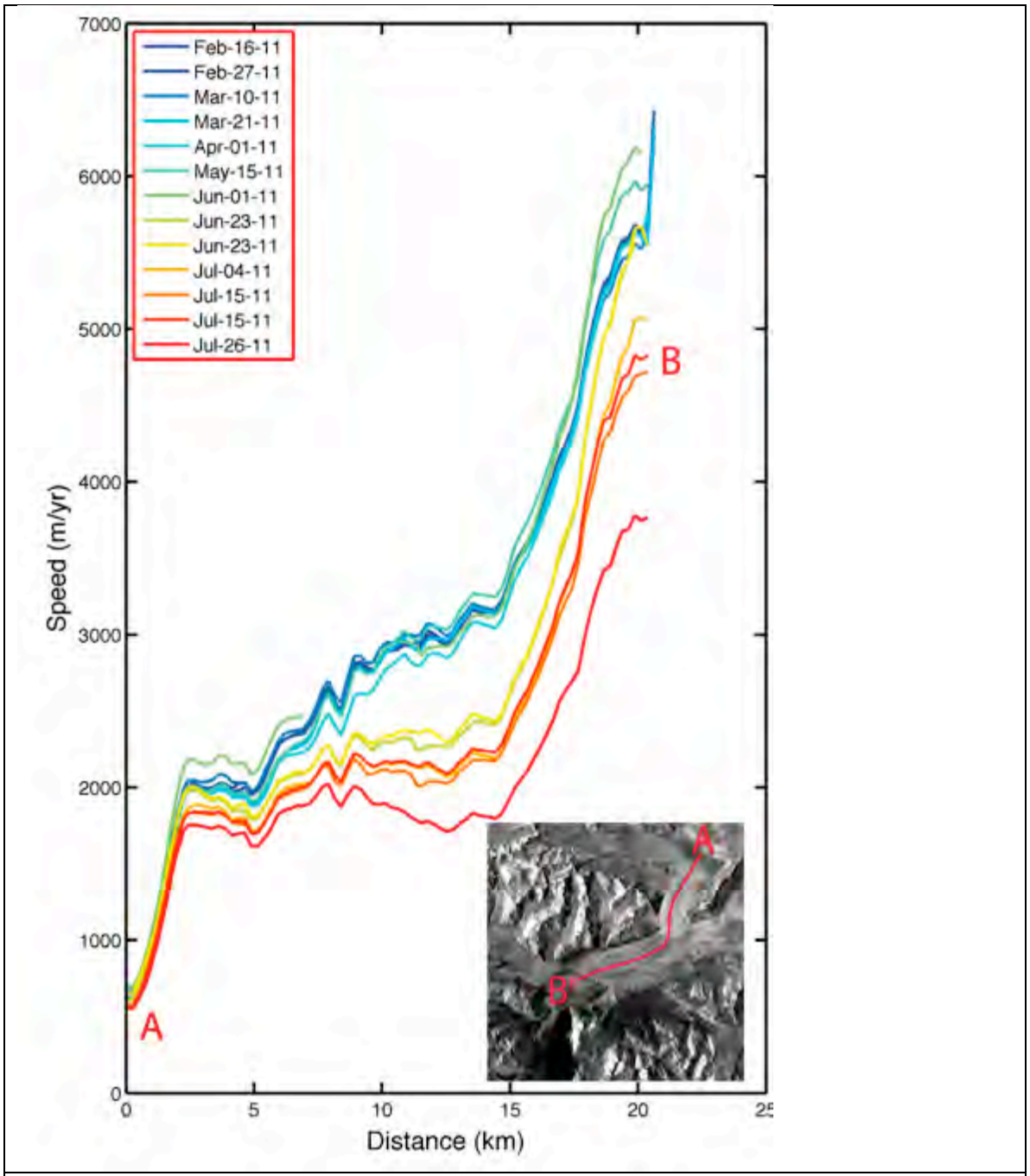

Figure 8d. Velocity profiles derived from TarraSAR-X radar data. Analysis and figure courtesy of Ian Joughin (APL, University of Washington)

2e. Calving

Calving flux – the volume (or mass) rate of ice leaving the glacier terminus as icebergs – is an easy quantity to define conceptually, but harder to quantify from measurements. If the glacier terminus is in steady state, neither retreating nor advancing, then the calving flux is simply the average terminus velocity times the full terminus cross sectional area. If the terminus is in motion, however, then the calving flux must be corrected for the amount of ice being consumed or lost in terminus advance or retreat, respectively. For this reason, calving flux requires measurements of both terminus (or near-terminus) velocity as well as the rate of terminus advance or retreat. Before continuous and reliable time-lapse cameras were in operation at Columbia Glacier, calving flux could only be determined for averaged rates over the intervals between flights. Since 2004, however, it has been possible to calculate calving flux on much shorter time scales. This is a useful source of information for analyzing short-term terminus dynamics; the analysis is ongoing.

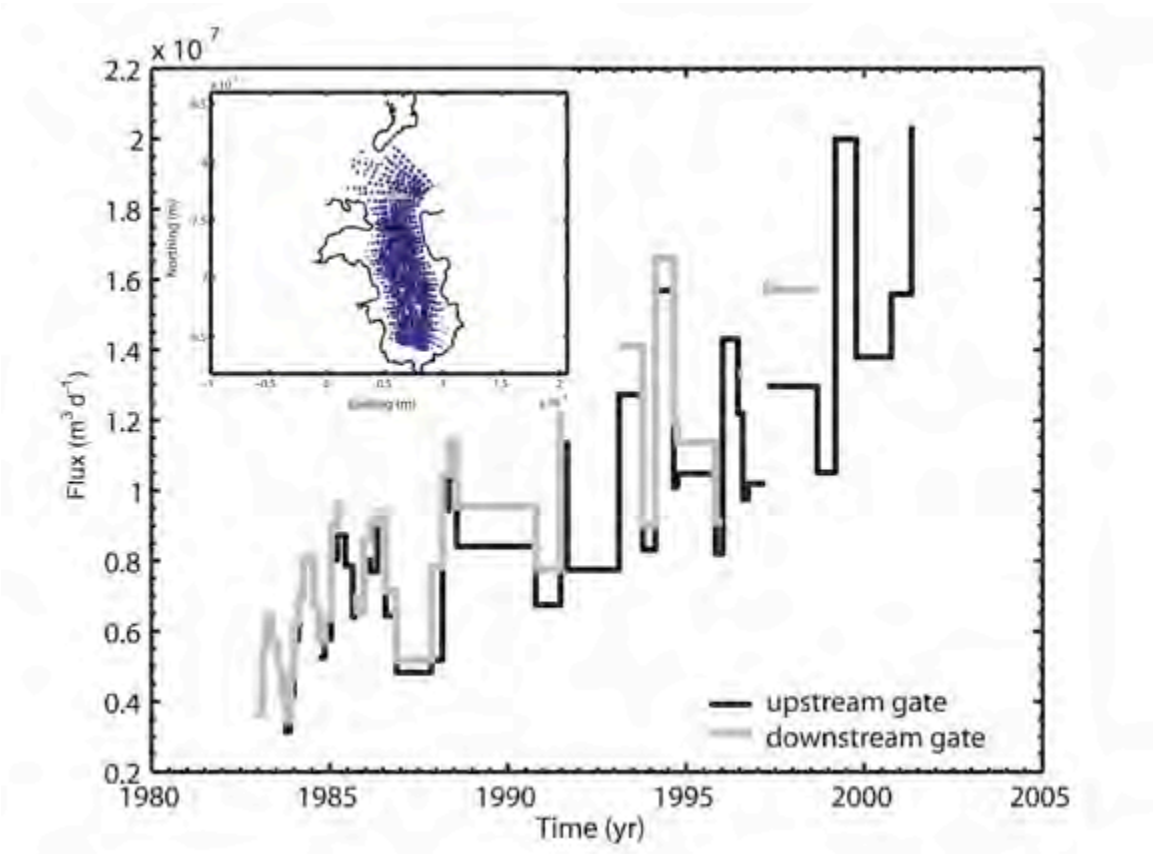

Figure 9a. Calving flux during Columbia Glacier's retreat up to 2003. From O'Neel et al, 2005.

2f. Mass Balance and meteorology

Measurements of glacier mass balance (the flux of mass into the glacier, primarily as snow, and flux out, primarily as iceberg calving and runoff of melt) require extensive and costly ground based measurements and regular surveys over long periods (years). The only mass balance data available for Columbia Glacier was obtaind during a comprehensive one-year survey in 1977-78, conducted by the USGS, and a much sparser survey, also conducted by the USGS (by Shad O'Neel) from 2010 to the present. This latter survey is ongoing. The results of these surveys are summarized in Figure 10.

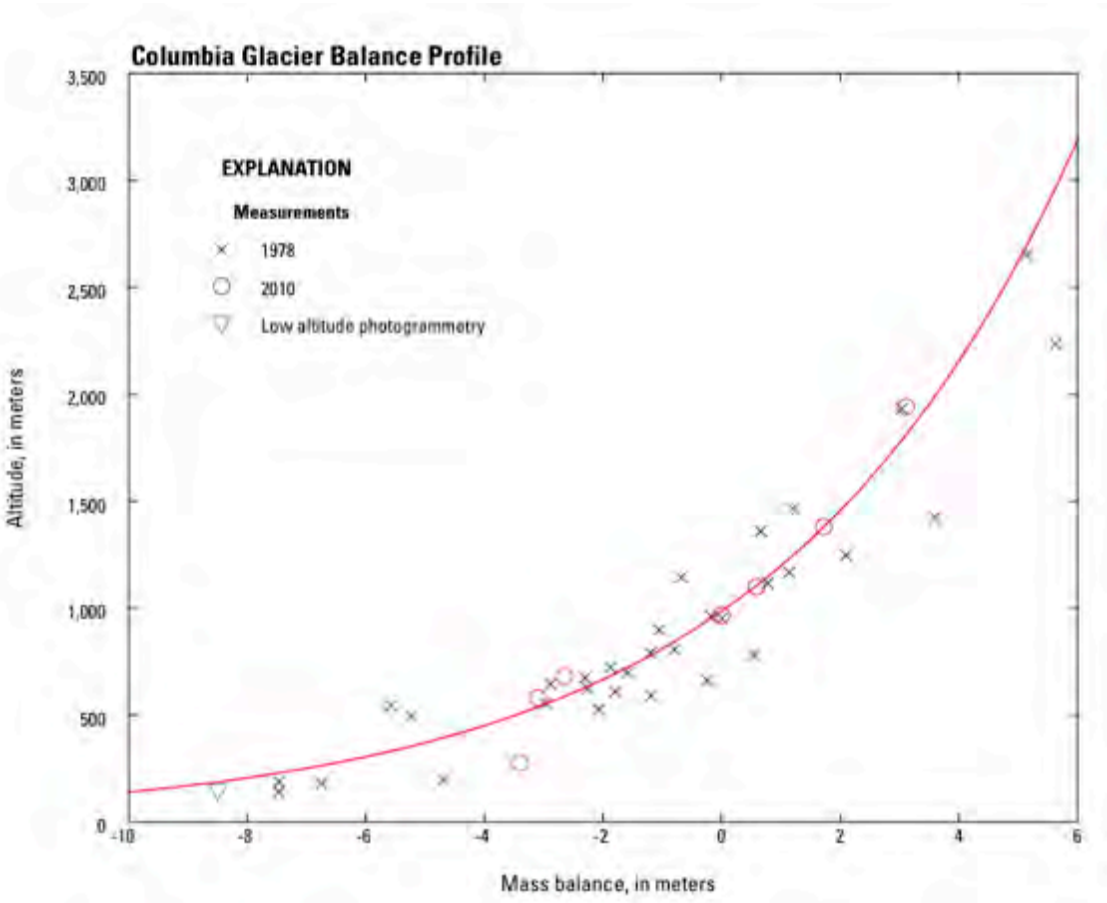

Figure 10. Mass balance, shown as the elevation distribution of net balance in meters^3 of water per m^2 per year (m yr^{-1}), for 1978 and 2010. *Source: O'Neel, 2012.*

Meteorological data is presently being recorded by an automated, telemetered weather station (operated by David Finnegan, USA CRREL) located at an elevation of 588 m (1929 ft.). Measured variables include air temperature, wind speed and direction, and barometric pressure. Seasonal mass balance measurements are conducted by Shad O'Neel. For the intervening period, calculated mass balance is provided by modeling, using regional meteorological observations, as described in

Rasmussen et al, 2011. Inferred mass balance for 1948-2007, in decadal periods, is shown in Figure 11.

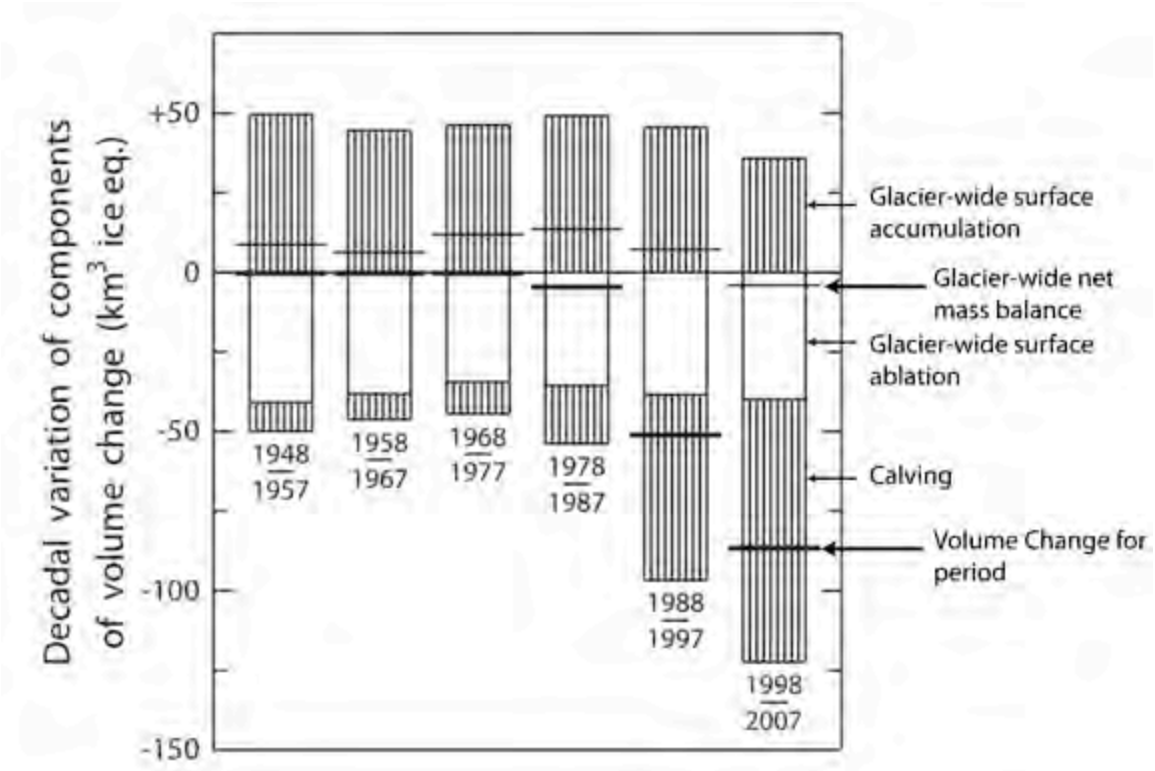

Figure 11. Decadal variation of mass balance components, from Rasmussen et al, 2011.

Time Line of Data Acquisition Figure 12a,b shows the distribution of the main observations conducted at Columbia Glacier between 1976 and the present, including the onset of retreat in the early 1980s .

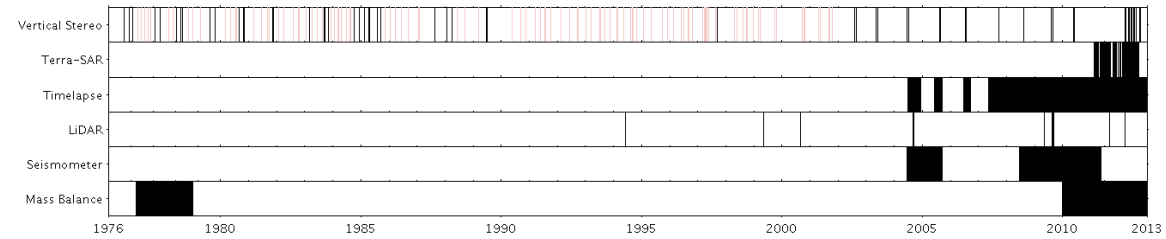

12a

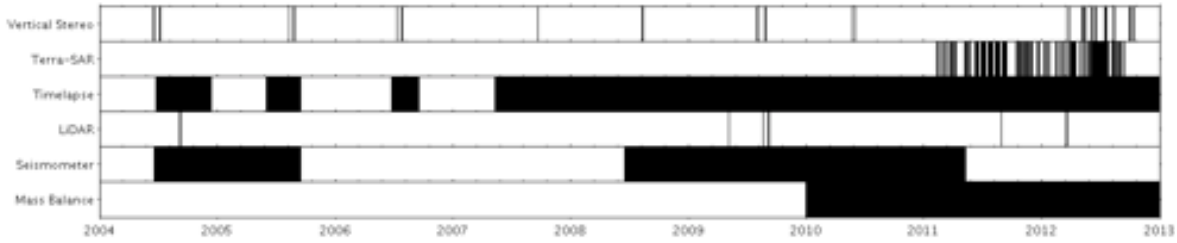

12b

Figure 12. Distribution of principal observational time series over the lifetime of Columbia Glacier observations. a) 1976-2012, b) expanded view of 2004-2012

2g. Ancillary Data

The following data is not directly a product of measurements on the glacier, but is required for processing and interpretation.

Camera time

All camera clocks have been calibrated to Coordinated Universal Time (UTC) using either environmental phenomena visible in the images (tides, solar angles, or large calving events identifiable in the seismic record) or, since August 2009, by comparison with reference UTC clock displays. The most contemporary sequences benefit from time adjustments that correct not only for a one-time offset, but also for linear clock drift as calculated from repeat comparisons to UTC.

Camera geometry

Photogrammetric analysis of the time-lapse imagery requires that both the position and orientation of the cameras be known. Position can be measured precisely with GPS, and once a camera is installed, its position is essentially constant. In contrast, orientation is both difficult to measure directly and can change substantially from image to image due to wind, snow drift, and settling of the ground or mounting hardware. So instead, orientation is calculated on an image-to-image basis using ground control, features of known 3D position that can be reliably identified in the oblique imagery.

Oblique ground control include points marked and surveyed in the field, natural features identified in the (2004-2010) orthoimagery and DEMs, and distant summits identified from USGS quadrangles. In the special cases that fixed control were insufficient, additional transient control were identified from same-day aerial-time-lapse pairs.

Columbia Glacier Time Lapse Camera External Orientations *data current 12/2011*

		UTM Coordinates			Camera Attitude				WGS84 Lat/Lon Pos	
Camera ID	Point Fixed(1)/ Variable(0) in solution	X_{wgs84}	Y_{WGS84}	Z_{HAE}	Azimuth deg from N + to E	Elevation deg from horizon Pos up	Roll deg about optic axis CW=+	Location Source	Lat	Lon
AK01	0	493221.97	6776736.40	463.26	60	-15	0	AK01b	61.1252	-147.1258
AK01b	1	493221.97	6776736.40	463.26	45	-15	0	GPS	61.1252	-147.1258
AK02	0	496804.14	6775877.21	88.62	-45	-5	0	GCP #3		
AK02b	0	496804.14	6775877.21	88.62	-10	-5	0	AK02		
AK03	1	497017.21	6776153.17	163.52	-45	-10	-2	AK03b	61.1200	-147.0554
AK03b	1	497017.21	6776153.17	163.52	-22.5	-5	3	GPS	61.1200	-147.0554
AK04	0	496703.89	6775902.28	86.57	-45	-5	0	GCP #1		
AK09	0	497331.58	6776358.62	235.44	-5	-15	0	AK09b		
AK09b	0	497331.58	6776358.62	235.44	30	-10	0	SfM		
AK10	1	499211.34	6783755.95	478.96	-165	-10	-4	GPS	61.1883	-147.0147
AK10b		499211.00	6783756.00	479.00				Handheld		
AK11	0				35	-15	0			
AK12										
AKJNC		494674.00	6780880.00	502.00						
AKH09	0				-10	-10	0			
AKHS1	0				-10	-20	0			
AKHS2	0				-10	-25	0			
AKHS3	0				-10	-20	0			
AKHS4	0				-15	-20	0			
AKST01A	1	496980.41	6776191.71	137.61	-10	-5	0	GPS	61.1203	-147.0560
AKST01B	1	496964.06	6776189.13	137.82	-5	-5	0	GPS	61.1203	-147.0563
AKST02A	0				10	-15	0			
AKST02B	0				5	-15	-3			
AKST03A	1	497415.25	6776328.42	270.83	0	-5	0	GPS	61.1216	-147.0480
AKST03B	1	497330.96	6776300.82	263.97	5	0	-4	GPS	61.1213	-147.0495
CG04	1	497294.99	6776046.32	266.15	-85	-5	-3	GPS	61.1190	-147.0502
CG05	1	496990.58	6776004.76	152.04	-65	0	0	CG06	61.1187	-147.0559
CG06	1	496990.58	6776004.76	152.04	-78	0	0	GPS	61.1187	-147.0559
CGBAY	0				-85	-10	0			
CGKDN	0	493222.00	6776736.40	463.30	120	-5	0	AK01b	61.1252	-147.1258
CGZM	0									
CG04	1	497294.53	6776046.63	268.47				BA		

Table 1: Columbia Glacier time lapse camera external orientation data

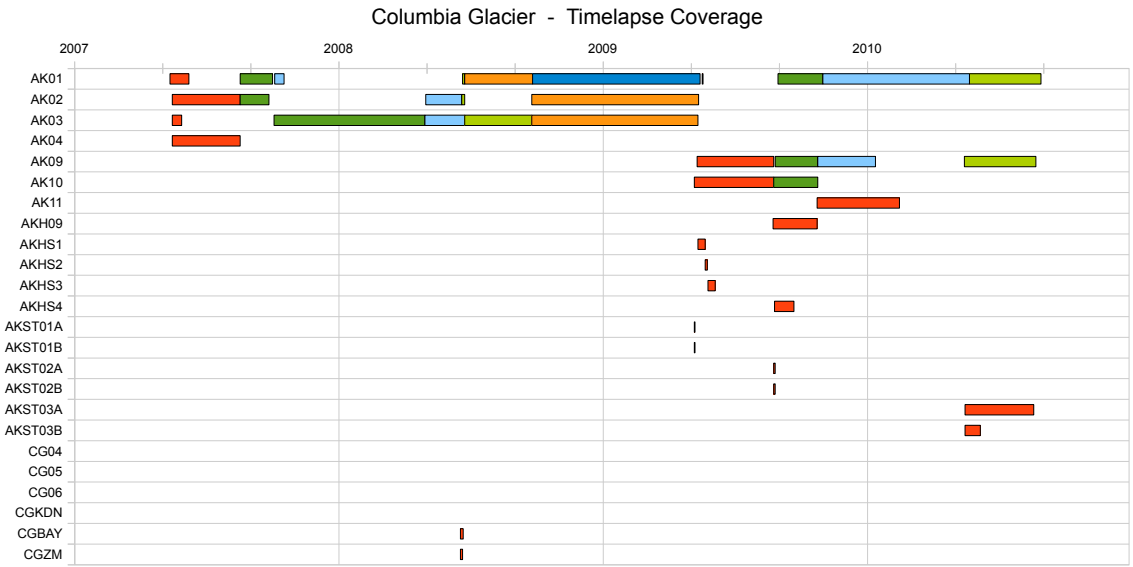

Table 2: Columbia Glacier time-lapse camera deployment intervals after start of the Extreme Ice Survey project. Time-lapse observations before 2007 are not shown.

Datum Convention

All data from 2002 to the present were produced directly in the reference datum WGS84. Horizontal coordinates (X and Y) are expressed as meters from the UTM Zone 6N origin, while elevations (Z) are expressed as height above the WGS84 ellipsoid (HAE).

In datasets reported through 2001, horizontal coordinates were referenced to the NAD27 datum, while elevations were referenced to the NGVD29 datum. These horizontal coordinates have been converted to our modern standard using the published transformation parameters for Alaska (excluding Aleutian Islands).

[Tx Ty Tz Rx Ry Rz s]= [-5 135 172 0 0 0 1]

The conversion from NGVD29 to WGS84 HAE is currently accomplished by an average +15 m adjustment, determined from GPS resurveying of historic USGS survey monuments at the Columbia Glacier.

Tides

Compiled hourly predicted and observed tides from the NOAA Station #9454240 in Valdez, Alaska (2000-2011), currently used for calculating the thickness of floating ice and determining terminus position with single-camera photogrammetry.

http://tidesandcurrents.noaa.gov/data_menu.shtml?stn=9454240%20Valdez,%20AK&type=Historic%20Tide%20Data

3. Data Sources

Forebay bathymetry

Mapping of the fjord bathymetry occurred in multiple campaigns over the past 30 years. At the very outset of the Columbia Glacier program, Post (1975) published preliminary soundings taken in the immediate vicinity of the glacier terminus in its pre-retreat position. Subsequent surveys were made during the 1980s, and although most of these results are unpublished, we have a number of plots in our library of materials that can be used if and when the need arises.

The 2001 Krimmel data report includes one generalized plot of bathymetry (shown here as Figure 2b).

The most recent and exhaustive effort occurred during 2005 by the NOAA ship *Rainier*. Their efforts (Noll, 2005) produced a 10 m gridded product that extends to within 2 km of the 2004-2006 terminus position. In addition to the Krimmel (2001)

bathymetric data set, there were earlier efforts to map the geometry of the submarine terminal moraine during and pre-dating IMP.

Digitizing these early bathymetric measurements in the region of the terminal moraine are central to our IMP-2 efforts, and will allow us to determine if the moraine has been substantially eroded.

Aerial Photogrammetry

The US Geological Survey maintained a program of vertical aerial photogrammetry (Krimmel, 2001) that provides the basis of our knowledge at Columbia glacier. This record consists of 123 photo flight missions spanning 1957-2001. Each mission pair has an associated manually derived velocity field, consisting of 10's to hundreds of vectors. Also included in this data set is a terminus position for each flight, and several measured profiles from which surface elevation change is calculated. Fjord bathymetry, as measured in 1994, is included in this report.

Since the publication of the Krimmel report, our group has performed a geodetic datum transformation to all the 2001 data, so that these products are directly comparable to more recent data collected in the WGS84 datum. Krimmel's work was all completed using manual analytical stereo-plotting techniques, and no full glacier surface elevation models were produced. A reanalysis effort produced 10 DEMs over the interval 1976-2003, plus 5 additional, higher quality DEMs over the more recent interval 2004-2010. Each of these products also includes dense velocity fields produced using automated feature tracking algorithms.

Surface Mass Balance

An extensive surface mass balance campaign was conducted by the USGS in 1977 (Mayo and others, 1978; O'Neel, 2012), that provided very detailed mass balance information in both space and time, but lasted for only one year. The data were reanalyzed by O'Neel (2012) and more limited data collection occurred from 2010-2012.

Two models have also been constructed for surface mass balance. Tangborn (1987) used low altitude meteorological observations to model accumulation and ablation, while more recently Rasmussen et al. (2011) used upper atmosphere observations to constrain a similar model.

Remotely Sensed Imagery

Remote sensing image quality is now sufficient to provide meaningful analysis tools at Columbia Glacier. Through collaborations with Ohio State University and USGS, we have obtained multiple images of the terminus region from which digital elevation models (DEMs) can be constructed. Ten DEMs covering the terminus region have been produced from imagery acquired since March, 2012. These products tie in to the aerial photogrammetric data to broaden the surface elevation dataset.

A separate effort (Dept. of Interior Climate Science Centers) has resulted in collection of radar images from the TerraSAR-X satellite. Acquisition spans March 2011 to the present at nominal 11-day interval. Radar speckle tracking (Ian Joughin, U Washington) produces nearly full glacier velocity fields at 100 m spacing.

Airborne Lidar

Beginning in the mid-1990s, and ongoing at variable intervals since, the glaciology group at University of Alaska Fairbanks has measured surface elevation profiles of the glacier. Since approximately 2005 the profiling system has been upgraded to a 500 m swath LiDAR and measurements have occurred nearly seasonally. Chris Larsen (UAF) now operates this program with support from NASA.

GPS/optical surveys

A semi-permanent GPS station was deployed approximately 7 km from the 2004 calving front and recorded data for 100 days. (Data archived with UNAVCO) During summers 2009 and 2010 experimental GPS rovers were deployed onto the glacier surface and recorded position information for days to weeks. (Ian Howat; Ohio State)

We conducted optical surveys of markers placed in close proximity to the calving front for intervals of days to weeks in 2004-06, and in 2008. This data is unpublished but in our possession.

David Finnegan (CRREL, Hanover, NH) conducted a ground-based LiDAR survey of the calving front in 2010. This data is available to us.

Passive Seismology

During 2004-2005 a 12-sensor passive seismology network was installed around the lower glacier to study the mechanics of iceberg calving. After 2005, a single station remained, and has operated intermittently to present. All 2004-09 data are archived at the IRIS Data Management Center in Washington DC, using the network codes YM (04-05) and XL (08-09).

Oceanography

We collected oceanographic measurements to characterize fjord conditions during 2005 and 2006. The cast data, which provide profiles of conductivity (salinity) and temperature as functions of depth, showed that thermal conditions in the deep water favor strong melting of the submarine terminus and icebergs. These records are unpublished but are in our possession.

Meteorology

In collaboration with Army Corps of Engineers, Cold Regions Research Laboratories (CRREL) we installed a high-elevation weather station (1000m) that measures temperature, wind, barometric pressure, and solar radiation. A near-real time camera was

installed near the glacier terminus, and transmits images every 4 hours during daylight hours. The initial installation was done in 2010, but hardware and transmission problems caused a variety of failures; the system was replaced in 2012 and is now performing reliably. Data can be viewed at glacierresearch.com and is archived on a CRREL server in Hanover NH.

Time-Lapse Imagery

To fill the need for direct observation of short-term glacier dynamics, time-lapse cameras have been deployed at the Columbia Glacier nearly continuously since 2004, photographing the near-terminus every 4 hours to 45 seconds. The result is a vast database of over 163,000 images documenting the retreat of a tidewater glacier in unprecedented detail. The imagery is archived by the National Snow and Ice Data Center at the following locations:

NSIDC Archive
Original Full Resolution Time-lapse Images for Columbia Glacier
Time-corrected High Resolution Time-lapse Images for Columbia Glacier
Time-corrected Low Resolution Time-lapse Images for Columbia Glacier
Time-corrected Low Resolution Time-lapse Movies for Columbia Glacier

Products Derived from Time-Lapse Imagery

Forebay Ice

The coverage of loose ice in the Columbia Glacier forebay was assessed visually from the time-lapse images (2004-2011) and rated on the following scale:

clear	0	forebay clear, or very lightly salt and peppered with ice
sparse	1	ice very loosely fills part of the forebay against the terminus
thin	2	ice mostly fills the forebay or upwelling visible at terminus
thick	3	ice fills the forebay and upwelling not visible
choked	4	ice fills the forebay and difficult to distinguish glacier terminus

The derived time series is shown in Figure 13.

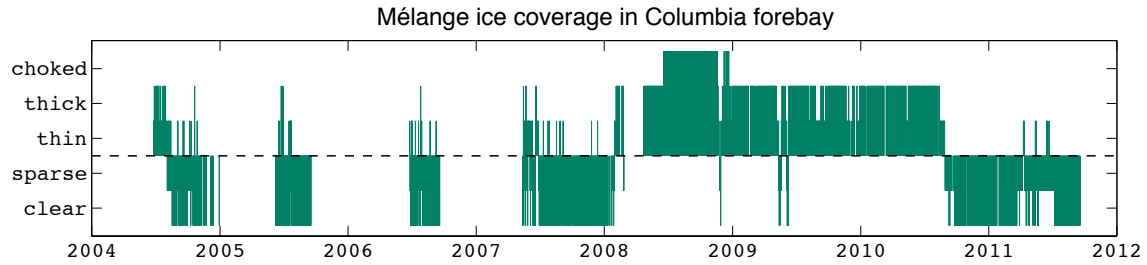

Figure 13: Ice coverage in Columbia Glacier forebay 2004-2012.

Terminus Position

The daily position of the glacier terminus was mapped for all 1,680 days from 2004 through 2011 during which a time-lapse camera was operating. These have been merged with the terminus positions reported in the Krimmel report (aerial photogrammetry, 1957-2001) and traced from modern orthoimagery (2002-2010).

Ice Cliff Height

Heights of the terminus ice cliff have so far only been compiled in the Krimmel report (aerial photogrammetry), and only for years 1978-1998.

Aerial Photographs from Columbia Glacier, 1976-2010
Digital Elevation Models for Aerial Stereographic Flights, 2002-2010
Hillshade Rasters for Digital Elevation Models, 2002-2010http://data.eol.ucar.edu/codiac/dss/id=106.376
Orthorectified Mosaics for Aerial Stereographic Flights, 2002-2009http://data.eol.ucar.edu/codiac/dss/id=106.382
Glacier Surface Velocity Fields from Columbia Glacier, 2004-2010
http://data.eol.ucar.edu/codiac/dss/id=106.379

References ***(Note: these are references cited in this report. See General Bibliography for comprehensive list of publications on Columbia Glacier)***

Berthier E, Schiefer E, Clarke GKC, Menounos B and Re´my F (2010) Contribution of Alaskan glaciers to sea-level rise derived from satellite imagery. Nature Geosci., 3(2), 92–95 (doi: 10.1038/ngeo737)

Korona J, Berthier E, Bernard M, Re´my F and Thouvenot E (2009) SPIRIT. SPOT 5 stereoscopic survey of polar ice: reference images and topographies during the fourth International Polar Year (2007–2009). ISPRS J. Photogramm. Remote Sens., 64(2), 204– 212 (doi: 10.1016/j.isprsjprs.2008.10.005)

Krimmel, R.M. (2001), Photogrammetric data set, 1957-2000, and bathymetric measurements for Columbia Glacier, Alaska, *USGS Water-Res. Inv. Rpt. 01-4089*, 40 pp.

Larsen, Chris (2010.) *IceBridge UAF Lidar Profiler L1B Geolocated Surface Elevation Triplets*. Version 1. [indicate subset used]. Boulder, Colorado USA: NASA DAAC at NSIDC.

Mayo, L.R., Trabant, D.C., March, R., and Haeberli, W., (1979) Columbia Glacier stake location, mass balance, glacier surface altitude, and ice radar data 1978 measurement year: U. S. Geological Survey Open File Report 79-1168, 72 p.

Noll, G. T. (2005). Report of Equipment and Methods to Accompany Data from Project OPR-P132-RA-05, Eastern Prince William Sound, AK, Columbia Bay Hydrographic Survey Sheets H11493 & H11494, Tech. rep., National Oceanographic and Atmospheric Administration.

O'Neel, S. (2012) Surface mass balance of Columbia Glacier, Alaska, 1978 and 2010 balance years. U.S. Geological Survey Data Series 676, 8 p.

O'Neel, S., H. Marshall, D. McNamara, and W. T. Pfeffer (2007), Seismic detection and analysis of icequakes at Columbia Glacier, Alaska, J. Geophys. Res., 112, F03S23, doi:10.1029/2006JF000595.

Rasmussen, A. L. (1989), Surface velocity variations of the lower part of Columbia Glacier, Alaska, 1977–1981, U.S. Geol. Surv. Prof. Pap., 1258-H, 52 pp.

Rasmussen, L. A., H. Conway, R. M. Krimmel and R. Hock (2011). Surface mass balance, thinning and iceberg production, Columbia Glacier, Alaska, 1948-2007, Journal of Glaciology, 57(203).

Welty, E., T. C. Bartholomaus, S. O'Neel and W. T. Pfeffer (in review). Cameras as clocks. Submitted to Journal of Glaciology.

Welty, E., S. O'Neel, W. T. Pfeffer, J. Balog and A. LeWinter (2012). Time-corrected High Resolution Timelapse Images for Columbia Glacier. UCAR/NCAR - Earth Observing Laboratory, Digital media.
(http://data.eol.ucar.edu/codiac/dss/id=106.377)

Part II: First Order Estimates of Future Discharge

A complete iceberg delivery projection includes the following stages:
1) Project future retreat rate, velocity, upstream reservoir drainage, and time to stabilzation.
2) Analyze down-fjord iceberg transport.
3) Analyze transport across moraine.
4) Estimate iceberg size distribution and numbers leaving forebay.

Here we focus on the first of these objectives, and give three estimates of time to stabilization of the retreat of Columbia Glacier, iceberg discharge from the glacier during retreat, and net ice loss over the lifetime of the retreat.

Summary Results:
Time to stabilization: Approximately 17 to 24 years (2029-2036)
Typical iceberg flux during retreat: Approximately 3×10^9 tons year^{-1} (ca. 8.2×10^6 tons day$^{-1)}$
Net loss over lifetime of retreat: $5.7 - 7.2 \times 10^{10}$ tons

---

1) First Order Model of remaining retreat and iceberg flux.

Note: Magnitudes of mass, length, speed, flux, etc are given in the discussion in mks units (e.g. km^3 of ice); summary quantities will be also given in English units (e.g. tons of ice) in Table 1.

While most aspects of iceberg calving and glacier dynamics relevant to the retreat of ocean-ending glaciers are understood in broad or conceptual terms, no validated, comprehensive numerical model exists to make reliable simulations of the retreat of glaciers like Columbia Glacier, and no precise, quantitative projection of the future retreat of Columbia Glacier (or any other glacier) is possible at this time. Despite this absence of a complete, model-based understanding of ocean-ending glacier dynamics, certain constraints can be placed on Columbia's future behavior. Some of these simplified approaches are demonstrated here, and the results provide us with a first-order estimate of the remaing years of Columbia Glacier's retreat. These estimates are based on the well-founded assumption that the rapid retreat of Columbia Glacier will cease when the terminus has receded to a point where the glacier bed rises above sea level (i.e. the tidewater limit, marked as "TWL" on Figure 1b), or to a point where both the calving flux and thinning rate can be matched by ice flow arriving from upstream. Here we present three analyses, based on different methods of projecting future retreat, including the monte carlo model recently published in the Cryosphere (Colgan et al, 2012), on which WTP is a coauthor. We compare the results of these analyses, and consider the spread of the results to be a first-order measure of our uncertainty. This uncertainty can be expressed quntitatively, but is nevertheless has a qualitative aspect since we cannot be sure at this stage that the methods bound the actual range of outcomes.

1a. Projection of extrapolation of observed retreat characteristics.

The simplest way to project Columbia Glacier's future retreat rate and calving flux is to project historically observed rates forward in time. This approach assumes that the processes governing retreat so far will continue to operate in the same way in the future. This approach can be refined later by modifying various controlling processes to reflect changing conditions as the retreat continues.

We consider the following observed characteristics:

1a.1 A further ~ 10 km separates the current terminus position from the TWL at the head of the fjord where the bed of the glacier rises above sea level.

1a.2 The long-term retreat rate of the glacier over the 29-year lifetime of the retreat to date has been approximately 0.6 km year^{-1}.

1a.3 The flux of ice crossing the TWL, evaluated at the the Main Branch at Divider Mountain (referred to as the "Divider Gate") during this period from the upper glacier into the tidewater reach of the glacier is estimated to decline from its present-day value of ca. 2.6 km^3 yr^{-1} to approximately 2 km^3 yr^{-1}, its pretreat value.

The rapid, dynamically controlled retreat that has characterized Columbia Glacier since 1983 requires that the glacier be resting in water of sufficient depth for buoyancy forces to influence the balance of forces acting on the terminus (see Pfeffer, 2007). Thus, if the rapid dynamic behavior (including, notably, high rates of iceberg calving) of Columbia Glacier will end after another 10 km of retreat. We estimate calving flux and total ice calved by adding the volume of ice evacuated from the remaining tidewater reach of the glacier (i.e. the glacier volume from the TWL to the present terminus, see Figure 1) to the ice advected through the Divider Gate into the tidewater reach. For the present we neglect the added flux from the East Branch and calving from the West Branch. While probably not negligible, these additional sources are presently a small fraction of the total present-day mass loss, and we expect that relationship to continue.

We estimate the volume of ice to be evacuated from the Tidewater Reach during at 12.77 km^3, using data from McNabb et al (2012) and our own ice geometry data. The ice advected into the Tidewater Reach through the Divider Gate is estimated by multiplying the estimated gate cross sectional area times the declining ice velocity, and integrating the flux rate over the period of retreat.

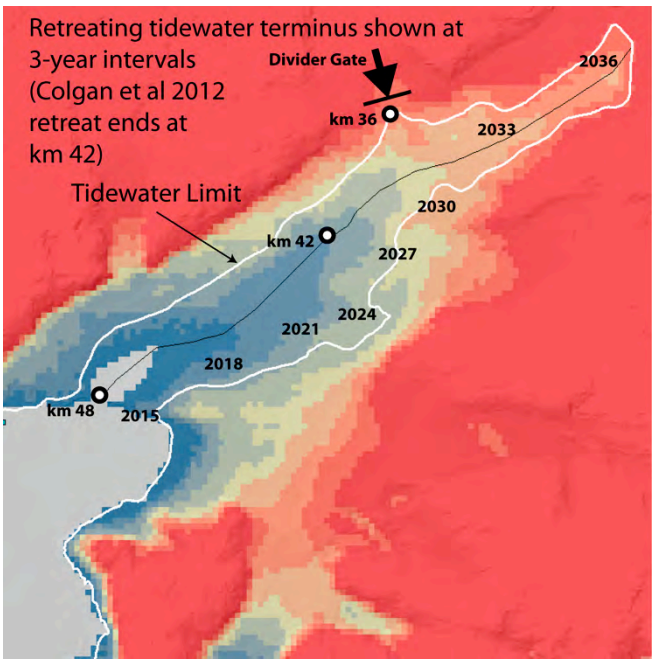

Figure 1: Map of remaining ice in Tidewater Reach, from ca. km 36 upstream to ca. km 48 downstream. The color-coded contours show the position of the terminus at three-year intervals as determined by the $H_{ice} = 3/2H_{water}$ discussed in the text.

Linear Retreat Rate: If we assume that the observed rate of terminus retreat (0.6 km yr^{-1}) continues unaltered into the future, then the retreat will continue for 17 years, ending in 2029. Evacuating the 12.77 km^3 of ice in the tidewater reach over 17 years gives a constant flux of 0.75 km^3 yr^{-1}. Ramping the Divider Gate flux down from 2.6 to 2.0 km^3 yr^{-1} over 17 years provides another 29 km^3. Since some fraction of the mass loss occurs by melt and runoff, as opposed to iceberg calving, we reduce the calving flux by 4 m yr^{-1} times the declining area in the tidewater reach, equal in magnitude to 5% of the projected thinning rate of 20 m yr^{-1}. The declining calving flux vs time is shown in Figure 2 ("Linear Retreat"); the net mass loss over the 17 year retreat is 52.9 km^3.

Dynamically-Controlled Retreat Rate: The assumption that terminus retreat will continue at the long-term average rate of 0.6 km yr^{-1} is probably the weakest assumption in the linear retreat rate model. Here we replace this assumption by a calculation of the migration of a boundary of dynamic instability, driven by long-term thinning rate. In doing this we are trading the assumption of constant retreat rate by constant thinning rate, but the observed near-terminus thinning rate is observed to be less variable over the history of the retreat than retreat rate. An analysis of instability of a tidewater terminus is presented in Pfeffer (2007), where ice thickness relative to water depth determines a critical ice thickness, equal to 3/2 times the water depth (or, equivalently 4/3 times the ice floation thickness) below which further thinning leads to acceleration and an unrecoverable feedback. We simulated a instability-forced terminus retreat rate by thinning ice in the Tidewater Reach at a uniform 20 m yr^{-1} and following the progression of the boundary marking the position of $H_{ice} = 3/2*H_{water}$. This produces a non-uniform terminus retreat because the bathymetry of the tidewater (i.e. H_{water}) reach is non-uniform. The retreat to the TWL using this model is 24 years instead of 17. The declining calving

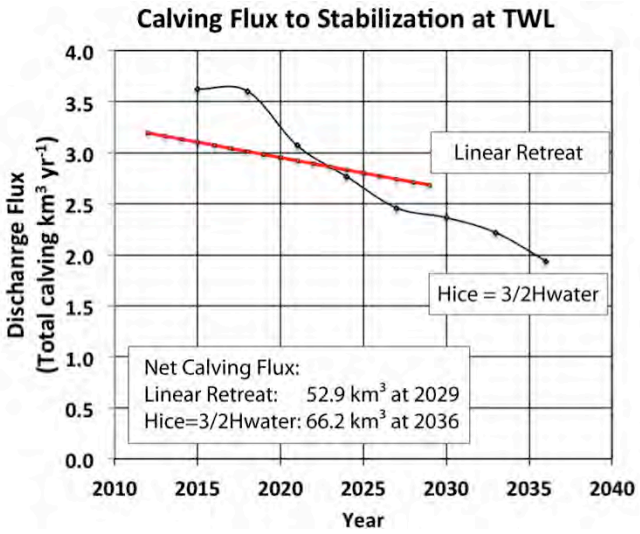

Figure 2: Calculated time series of calving flux from Columbia Glacier from 2012 to stabilization at the Tidewater Limit (TWL) for two models of terminus retreat. Both projections start in 2012; the non-linear "$Hi_{ce} = 3/2\ H_{water}$" model reports net flux in 3-year intervals, so the first point plotted represents 2012-2015.

flux vs time for this model is shown in Figure 2 ("$H_{ice} = 3/2H_{water}$"); the net mass loss over the 24 year retreat is 66.2 km^3. Note that the larger net loss in this case is due to the longer duration of the retreat; the volume of ice evacuated from the Tidewater Reach is unchanged.

Monte Carlo Model from Colgan et al (2012): Using fundamentally different procedures, including a 1D flow line model that takes account of the centerline bathymetric profile of the Tidewater Reach but not the full 2D bathymetry, Colgan et al (2012) project only 8 km further retreat, which will be complete by 2020 and will involve a loss of only 16 km^3 of ice. This retreat occurs at the same rate as the 0.6 km yr^{-1} used for the linear retreat case, and is complete after a shorter period only because Colgan et al's model find a more extended steady position for the terminus (at km 42) that used in either of the cases described above (km 36). The total calving loss is significantly less than the linear or non-linear models, however. This discrepancy appears to be due to two main factors; first, the volume of ice to be exavuated from the Tidewater Reach is determined in Colgan et al's case by intergrating a width function *w(x)* over the 8 km retreat distance, which produced a different (and probably less accurate) volume measure. Second, and more significant, is the fact that the Colgan et al model underestimates the flux entering the Tidewater Reach through the Divider Gate. This is discussed in their paper (in Section 3: Results) but not quantified.

The non-linear ($Hi_{ce} = 3/2\ H_{water}$) model can be adjusted to match the conditions of the Colgan et al model more closely, and the results can be compared more directly.

If the non-linear retreat model is run back only to km 42 and assumed to stabilize there, then the retreat ends eight years sooner, in 2021, essentially the same time that the Colgan model predicts. The volume of ice evacuated from the Tidewater Reach is also reduced, from 12.77 km^3, to 8.74 km^3. If the Divider Gate flux is then reduced to 30% of the value used in the non-linear model, the net non-linear model mass loss matches Colgan et al's result of 16 km^3. Thus, the differences between the models presented here and Colgan et al's model reduce to a different point of stabilization, and an anomalously low Divider Gate flux, already suggested by Colgan et al, to 30% of the value presently observed.

Year	Linear Model		Nonlinear Model*	
	$km^3\ yr^{-1}$	tons yr^{-1}	$km^3\ yr^{-1}$	tons yr^{-1}
2012	3.19	3.48E+09	* flux units are yr^{-1} but	
2013	3.16	3.45E+09	reported every third year	
2014	3.13	3.41E+09		
2015	3.10	3.38E+09	3.63	3.96E+09
2016	3.07	3.35E+09		
2017	3.04	3.32E+09		
2018	3.01	3.28E+09	3.60	3.92E+09
2019	2.98	3.25E+09		
2020	2.95	3.22E+09		
2021	2.92	3.19E+09	3.07	3.35E+09
2022	2.89	3.15E+09		
2023	2.86	3.12E+09		
2024	2.83	3.09E+09	2.76	3.01E+09
2025	2.81	3.06E+09		
2026	2.78	3.03E+09		
2027	2.75	2.99E+09	2.46	2.68E+09
2028	2.72	2.96E+09		
2029	2.69	2.93E+09		
2030	End		2.36	2.57E+09
2031				
2032				
2033			2.22	2.42E+09
2034				
2035				
2036			1.94	2.11E+09
Total mass loss over retreat:	52.90 km^3	5.77E+10 tons	66.20 km^3	7.22E+10 tons

Table 1: Calving rates, over time and cumulatively, for two models of future Columbia Glacier retreat.

These three calculations are approximate estimates, and depend principally on assumptions about the speed of terminus retreat and the magnitude of ice flux devlivered to the Tidewater Reach through the Divider Gate. Both of these factors could be developed further, and these results could be refined. There is also another presently unquantified possibility that the future retreat and loss rate of the glacier may be significantly smaller and shorter lived than these estimates suggest. In a brief analysis in McNabb et all (2011), the instability theory developed by Pfeffer (2007) is applied to the Columbia Glacier's terminus geometry in its present configuration and the author's conclusion is that the glacier may be leaving the state of dynamic instability that has been driving its rapid retreat since the early 1980s. If so, the calving discharge from the glacier may soon drop dramatically.

All of the foregoing refers only to instability and projected loss rates from the glacier. Beyond these questions are the additional problems that must be addressed to make estimates of iceberg fluxes out of Columbia Bay into Prince William Sound. These include problems of iceberg transport down the lengthening fjord, melt and mechanical damage to bergs during their passage to the moraine shoal, and finally the problem of trapping by the moraine shoal. None of these have been studied as a regular part of past Columbia Glacier research projects, but they were a part of Austin Post's and Wendell Tangborn's IMP project, and an extensive literature exists on iceberg drift and melt. We will make full use of the existing literature, although we believe that some aspects of the problem may present some entirely new challenges.

2) Model Strategy for Improved Estimates

1. Calving discharge. Refinements can be made to iceberg discharge by process-based modeling of calving and flow dynamics. Calving mechanics models are not highly developed, however, and it is not clear that such refinements to our method of projection will actually reduce the uncertainty in range of projected outcomes. We will evaluate some model possibilites and consider whether sufficient gains in confidence in our projections can be achieved to justify this effort. We will also continue to refine the types of projections descrtibed here, and explore variations of these, to develop our confidence in the range of projections by comparing a variety of approximate methods.

2. Iceberg generation and transport. The evolution of size distributions as icebergs are carried away from the terminus and toward the moraine shoal is influence by both melt and fracture into smaller bergs. Our modern time-lapse records of the terminus provide us with observations of iceberg formation at the terminus over the past ca. 8 years. In addition to these images, Austin Post, Robert Krimmel, and other USGS personnel, operated time-lapse cameras at Columbia Glacier as early as 1978, so we also have records of calving from early in the retreat. Finally, the cameras now in operation will continue to operate for the forseeable future.

A substantial body of literature on iceberg drift and transport exists in the marine geology literature, and there are a number of experts in this area available at CU/INSTAAR for guidance and discussions. While extensive modeling of iceberg transport is beyond the scope of this project, we can investigate how to select the relevant processes to concentrate on and develop methods to constrain their probable influence.

3. Transport over the moraine shoal. The Heather Island moraine shoal is a major obstacle to free passage of Columbia Glacier icebergs into outer Columia Bay and Prince William Sound. Icebergs are generally trapped very effectively by the moraine shoal, but periodic "flushing" events occur when all of the grounded bergs at the shoal are swept over the moraine by some combination of currents and tides. We do not know the primary causes of these flushing events, but the time-lapse camera we will install at Heather Island will give us an opportunity to obeserve flushing events and match tidal and meteorological conditions to them.

The depth of the moraine crest is also a critically important factor in iceberg trapping. The shoal bathymetry has been carefully mapped on various occasions in the past, but there has been no organized survey done since 2005 when the NOAA survey ship *Rainier* made its complete bathymetric survey. We are very interested in whether erosion of the shoal has occurred since 2005 and plan to do some bathymetric profiling in Summer 2013, using on of the local charter vessels.

Finally, all of these pieces must be tied together into a single transport model that tracks ice flux from the glacier through the calving front, down the fjord, and over the moraine. This model will produce iceberg discharge scenarios that depend on a range of parameters and constraints that must wherever possible be tied to quantities that can be constrained, either by observation or calculation. This model will give us a tool to explore which input variables are the most significant controls on the end product of iceberg delivery into Prince William Sound, and allow us to focus our efforts on the most important of these.

General Bibliography : Columbia Glacier literature

Arendt,.A. A., K. A. Echelmeyer, W. D. Harrison, C. S. Lingle, V. B. Valentine (2002), "Rapid Wastage of Alaska Glaciers and Their Contribution to Rising Sea Level." *Science* 19 July, Vol. 297. no. 5580, pp. 382 – 386. DOI: 10.1126/science.1072497

Berthier E, Schiefer E, Clarke GKC, Menounos B and Re´my F (2010) Contribution of Alaskan glaciers to sea-level rise derived from satellite imagery. Nature Geosci., 3(2), 92–95 (doi: 10.1038/ngeo737)

Korona J, Berthier E, Bernard M, Re´my F and Thouvenot E (2009) SPIRIT. SPOT 5 stereoscopic survey of polar ice: reference images and topographies during the fourth International Polar Year (2007–2009). ISPRS J. Photogramm. Remote Sens., 64(2), 204– 212 (doi: 10.1016/j.isprsjprs.2008.10.005)

Bindschadler, R.A., and Rasmussen, L.A. (1983), "Finite-difference model predictions of the drastic retreat of Columbia Glacier, Alaska." U.S. Geological Survey Professional Paper 1258-D, 17 p.

Brown, C.S., Meier, M.F., and Post, Austin (1983), "Calving speed of Alaska tidewater glaciers, with application to Columbia Glacier." U.S. Geological Survey Professional Paper 1258-C, pp. C1-C13.

Brown, C.S., Rasmussen, L.A., and Meier, M.F. (1986), "Bed topography inferred from airborne radio-echo sounding of Columbia Glacier, Alaska." U.S. Geological Survey Professional Paper 1258-G, pp. G1-G26.

Calkin, P.E, G.C. Wiles, and D.J. Barclay (2000), "Holocene coastal glaciation of Alaska." *Quaternary Sci. Rev.* 20, pp. 449-461

Fountain, A.G. (1983), "Columbia Glacier photogrammetric altitude and velocity; Data set (1975 to 1981)." U.S. Geological Survey Open-File Report 82-756, pp. 229

Field, W.O. (1937), "Observations on Alaska Coastal Glaciers in 1935." *Geogr.l Rev.*, Vol. 27, No. 1, pp. 63-81.

Friedman, K. S., Clemente-Colon, P., Pichel, W. G., and Li, X. F. (1999), "Routine monitoring of changes in the Columbia Glacier, Alaska, with synthetic aperture radar." *Remote Sens. Environ.,* 70(3), pp. 257-264.

Grant, U.S., and Higgins, D.F. (1913), "Coastal Glaciers of Prince William Sound and the Kenai Peninsula."U.S. Geological Survey Bulletin 526, 75 pgs.

Grant, U.S. and Higgins, D.F.(1910), "Glaciers of the northern part of Prince William Sound." *Bull. Amer. Geog. Soc*. Vol. 52, pp. 727-735.

Gilbert, G.K. (1910), *Volume III, Glaciers and Glaciation*, pg. 109. Harriman Alaska Expedition, Smithsonian Institution

Haeberli, W. (1981). "Columbia Glacier and the Trans-Alaska Pipeline [Der Columbiagletscher und die Alaska-Pipeline]." *Wasser, Energie, Luft—Eau, énergie, air,* 72(5/6), pp. 111-117.

Hannon, L. J. (1978)."Parameters influencing drift of ice from Columbia Glacier, Alaska, into Valdez Arm and Prince William Sound." *Trans. Am. Geophys. Union.*

Hart, J. K., and Smith, B. (1997). "Subglacial deformation associated with fast ice flow, from the Columbia Glacier, Alaska: Subglacial environment." *Sediment. Geol.,* 111(1-4), pp. 177-197.

Humphrey, N., Kamb, B., Fahnestock, M., and Engelhardt, H. (1993). „Characteristics of the bed of the lower Columbia Glacier, Alaska." *J. Geophys. Res.,* 98(B1), pp. 837-846.

Kamb, B., M.F. Meier, H. Engelhardt, M. Fahnestock, N. Humphrey, D. Stone (1994). "Mechanical and hydrologic basis for the rapid motion of a large tidewater glacier. 2, Interpretation." *J. Geophyis.Res.*, **99**(B8), pp. 15,231-15,244.

Krimmel, R.M. (1987), "Columbia Glacier, Alaska---Photogrammetry data set 1981-82 and 1984-85." U.S. Geological Survey Open-File Report 87-219, 104 p.

Krimmel, R.M.(1987), "Columbia Glacier in 1986---800 meter retreat." U.S. Geological Survey Open-File Report 87-207, 7 p.

Krimmel, R.M. (1996), "Columbia Glacier Alaska--Research on tidewater glaciers." U.S. Geological Survey Fact Sheet FS-091-96, 4 p.

Krimmel, R.M. (2001), "Photogrammetric Data Set, 1957-2000, and Bathymetric Measurements for Columbia Glacier, Alaska." U.S. Geological Survey Water-Resources Investigations Report 01-4089, 40 p. + CDROM.

Krimmel, R. M. (1997), "Documentation of the retreat of Columbia Glacier, Alaska." In, *Calving Glaciers.* Edited by C.J. Van der Veen; Ohio State University. Byrd Polar Research Center. BPRC report, No. 15, 105-108.

Krimmel, R. M., Rasmussen, L. A., *et al.* (1986), "Using sequential photography to estimate ice velocity at the terminus of Columbia Glacier, Alaska." *Ann. Glaciol.,* 8, pp. 117-123.

Krimmel, R. M., & Vaughn, B. H. (1987), „Columbia Glacier, Alaska: changes in velocity 1977-1986." *J. Geophys. Res.,* 92(B9), pp. 8961-8968.

Larsen, Chris (2010.) *IceBridge UAF Lidar Profiler L1B Geolocated Surface Elevation Triplets*. Version 1. [indicate subset used]. Boulder, Colorado USA: NASA DAAC at NSIDC.

Mayo, L.R., Trabant, D.C., March, Rod, and Haeberli, Wilfried (1979), "Columbia Glacier stake location, mass balance, glacier surface altitude, and ice radar data - 1978 measurement year." U.S. Geological Survey Open-File Report 79-1168, 79 p.

McNabb, R. W., Hock, R., & O'Neel, S. (2012). Using surface velocities to calculate ice thickness and bed topography: a case study at Columbia Glacier, Alaska, USA. *Jour. Glaciol. V. 58 No. 212, doi: 10.3189/2012JoG11j249.*

Meier, M. F. (1979), "Variations in time and space of the velocity of the lower Columbia Glacier, Alaska." *J. Glaciol.,* 23(89), 408.

Meier, M. F. (1993), "Columbia Glacier during rapid retreat: Interactions between glacier flow and iceberg calving dynamics." In, *Workshop on the Calving Rate of West Greenland Glaciers in Response to Climate Change,* Copenhagen, Denmark, Sep. 13-15, 1993. Edited by N. Reeh, 63-83. Copenhagen, Denmark: Danish Polar Center.

Meier, M. F. (1997), "Iceberg discharge process: Observations and inferences drawn from the study of Columbia Glacier." In, *Calving Glaciers.* Edited by C.J. Van der Veen; Ohio State University. Byrd Polar Research Center. BPRC report, No. 15, pp. 109-114.

Meier, M.F., and others (1980), "Retreat of Columbia Glacier---A preliminary prediction." U.S. Geological Survey Open-File Report 80-10, 12 p.

Meier, M.F., and others (1980), "Predicted timing of the disintegration of the lower reach of Columbia Glacier, Alaska." U.S. Geological Survey Open-File Report 80-582, 58 p.

Meier, M.F., and others (1984), "The 1983 recession of Columbia Glacier." U.S. Geological Survey Open-File Report 84-59, 12 p.

Meier, M.F., and others (1985), "Photogrammetric determination of surface altitude, terminus position and ice velocity of Columbia Glacier, Alaska." U.S. Geological Survey Professional Paper 1258-F, p. F1-F41.

Meier, M.F., Rasmussen, L.A., and Miller, D.S. (1985), "Columbia Glacier in 1984 - disintegration underway." U.S. Geological Survey Open-File Report 85-81, 21 p.

Meier, M.F. and A. Post (1987), "Fast tidewater glaciers." *J. Geophys. Res.,* Vol. 92, No B9, pg. pp. 9051-9058.

Meier, M.F, S. Lundstrom, D. Stone, B. Kamb, H. Engelhardt, N. Humphrey, W.W. Dunlap, M. Fahnestock, R.M. Krimmel, and R. Walters (1994), "Mechanical and hydrologic basis for the rapid motion of a large tidewater glacier. 1. Observations." *J. Geophys. Res.*, 99(B8), pp. 15,219-15,229.

Meier, M.F., and M.B. Dyurgerov (2002), "How Alaska Affects the World." *Science*, 19 July, Vol. 297, No. 5580, pp. 350-351, DOI: 10.1126/science.1073591

Nick, F. M., C. J. van der Veen, and J. Oerlemans (2007), "Controls on advance of tidewater glaciers: Results from numerical modeling applied to Columbia Glacier." *J. Geophys. Res.*, 112, F03S24, doi:10.1029/2006JF000551.

Nature (2003). "Columbia Glacier rides the tide." *Nature,* 426(6967), 602.

Nielsen, L. E. (1963), "A glaciological reconnaissance of the Columbia Glacier. Alaska." *Arctic,* 16(2), 134-142.

O'Neel, S. (2012) Surface mass balance of Columbia Glacier, Alaska, 1978 and 2010 balance years. U.S. Geological Survey Data Series 676, 8 p.

O'Neel S. and W.T. Pfeffer (2007) Source mechanics for monochromatic icequakes produced during iceberg calving at Columbia Glacier, AK, *Geophys. Res. Let.* V. 34, L22502, doi:10.1029/2007GL031370.

O'Neel, S., Pfeffer, W. T., Krimmel, R., and Meier, M. F. (2005), „Evolving force balance at Columbia Glacier, Alaska, during its rapid retreat." *J. Geophys. Res.,* V. 110, F03012, doi: 10.1029/2005JF000292, 2005

O'Neel, S., H. P. Marshall, D. E. McNamara, and W. T. Pfeffer (2007), "Seismic detection and analysis of icequakes at Columbia Glacier, Alaska." *J. Geophys. Res.*, 112, F03S23, doi:10.1029/2006JF000595.

Post, Austin (1975), "Preliminary hydrography and historic terminal changes of Columbia Glacier, Alaska." U.S. Geological Survey Hydrologic Investigations Atlas HA-559 [1976], 3 sheets.

Post, Austin (1977), "Reported observations of icebergs from Columbia Glacier in Valdez Arm and Columbia Bay, Alaska, during the summer of 1976." U.S. Geological Survey Open-File Report 77-235, 3 p.

Post, Austin (1978), "Interim bathymetry of Columbia Glacier and approaches, Alaska." U.S. Geological Survey Open-File Report 78-449, 1 pl.

Pfeffer, W. T. (2007), "A simple mechanism for irreversible tidewater glacier retreat." *J. Geophys. Res.*, 112, F03S25, doi:10.1029/2006JF000590.

Pfeffer, W.T., J. Cohn, M.F. Meier, and R.M. Krimmel (2000), Alaskan glacier beats a rapid retreat. *EOS* V. 81 No. 48.

Qamar, A. (1988), Calving icebergs: a source of low-frequency seismic signals from Columbia Glacier, Alaska. *J. Geophys. Res.,* 93(B6), 6615-6623.

Rasmussen, L. A., H. Conway, R. M. Krimmel and R. Hock (2011). Surface mass balance, thinning and iceberg production, Columbia Glacier, Alaska, 1948-2007, Journal of Glaciology, 57(203).

Rasmussen, L.A., and Meier, M.F. (1982), "Continuity equation model of the predicted drastic retreat of Columbia Glacier, Alaska." U.S. Geological Survey Professional Paper 1258-A, pp. A1-A23.

Rasmussen, L.A., and Meier, M.F., (1985), "Surface topography of the lower part of Columbia Glacier, Alaska, 1974-81." U.S. Geological Survey Professional Paper 1258-E, pp. E1-E63.

Rasmussen, L. A. (1986), "Estimating atmospheric refraction over Columbia Glacier." *Zeitschrift für Gletscherkunde und Glazialgeologie,* 22(1), pp. 61-72.

Rasmussen, L. A. (1988), "Bed topography and mass-balance distribution of Columbia Glacier, Alaska, U.S.A., determined from sequential aerial photography." *J.Glaciology,* 34(117), pp. 208-216.

Rasmussen, L.A. (1989), "Surface velocity variations of the lower part of Columbia Glacier, Alaska, 1977-1981." U.S. Geological Survey Professional Paper 1258-H, pp. H1-H52.

H.F. Reid (1909), "Variations of glaciers." *J. Geol.*, Vol. XIV, 1906, pp. 406-7; Vol. 27, pp. 71-81

Sikonia, W.G. (1982), "Finite element glacier dynamics model applied to Columbia Glacier, Alaska." U.S. Geological Survey Professional Paper 1258-B, pp. B1-B74.

Sikonia, W.G., and Post, A. (1980), "Columbia Glacier, Alaska: Recent ice loss and its relationship to seasonal terminal embayments, thinning, and glacial flow.".S. Geological Survey Hydrologic Investigations Atlas HA-619, 3 sheets

Tangborn, W. V. (1997), "Using low-altitude meteorological observations to calculate the mass balance of Alaska's Columbia Glacier and relate it to calving and speed." In, *Calving glaciers.* Edited by C.J. Van der Veen; Ohio State University. Byrd Polar Research Center. BPRC report, No. 15, pp. 141-161.

Tarr, R. S., and L. Martin (1914), Chap. 10, *Alaskan Glacier Studies*, National Geographic Society.

van der Veen, C. J. (1995), "Controls on calving rate and basal sliding: Observations from Columbia Glacier, Alaska, prior to and during its rapid retreat, 1976-1993." Ohio State University. Byrd Polar Research Center. BPRC report, No.11, 72 p.

van der Veen, C. J., and Whillans, I. M. (1993), "Location of mechanical controls on Columbia Glacier, Alaska, U.S.A., prior to its rapid retreat." *Arctic Alpine Res.,* 25(2), pp. 99-105.

van der Veen, C.J. (1996), "Tidewater calving." *J. Glaciol.,* Vol. 42, No. 141, pp. 375-385.

van der Veen, C.J., E. Venteris and I. Whillans (1996), "Flow of Columbia Glacier, Alaska." *Ice*, 110, 10.

van der Veen, C.J., "Controls on the position of iceberg-calving fronts." In: *Calving Glaciers: Report of a Workshop, February 28 - March 2, 1997 (ed. C.J. van der Veen).* BPRC Report No. 15, Byrd Polar Research Center, The Ohio State University, Columbus, Ohio, 163-172.

van der Veen, C.J. (2000), "Controls on the position of iceberg calving fronts." *EOS*, V. 81, H51E-10,.

van der Veen, C.J. (2002), "Calving Glaciers." *Prog.Phys. Geog.*, 26(1), pp. 96-122,

Vaughn, B.H. (1985), "Short-term velocity measurements at Columbia Glacier, Alaska, August to September 1984." U.S. Geological Survey Open-File Report 85-487, 29 p.

Venteris, E. R. (1997), "Evidence for bottom crevasse formation on Columbia Glacier, Alaska, U.S.A." In, *Calving glaciers.* Edited by C.J. Van der Veen; Ohio State University. Byrd Polar Research Center. BPRC report, No. 15, pp. 181-185.

Venteris, E. R. (1999), "Rapid tidewater glacier retreat: A comparison between Columbia Glacier, Alaska and Patagonian calving glaciers: Glaciers of the Southern Hemisphere." *Global Planet. Change,* 22(1-4), pp. 131-138.

Venteris, E. R., Whillans, I. M., and van der Veen, C. J. (1997). "Effect of extension rate on terminus position, Columbia Glacier, Alaska, U.S.A." *Ann. Glaciol.,* 24, pp. 49-53.

Vieli, A., M. Funk, and H. Blatter (2001), "Flow dynamics of tidewater glaciers: a numerical modeling approach." *J. Glaciol.*, 47(159), pp. 595-606.

Walter, F.; S. O'Neel, D. McNamara, W.T. Pfeffer; J. Bassis, H.A. Fricker, (2010) Iceberg Calving During Transition from Grounded to Floating Ice, Columbia Glacier, Alaska, *Geophys. Res. Let.*, Vol. 37, L15501, doi:10.1029/2010GL043201

Walters, R. A., and Dunlap, W. W. (1987), "Analysis of time series of glacier speed: Columbia Glacier, Alaska." *J. Geophys. Res.,* 92(B9), pp. 8969-8975.

Walters, Roy A., Josberger, E. G., and Driedger, C. L. (1988), "Columbia Bay, Alaska: An 'upside down' estuary." *Estuar., Coast. Shelf S.,* 26(6), pp. 607-617.

Weisburd, Stefi (1985), Columbia Glacier: "The retreat is real." *Sci. News,* 127, 101.

Whillans, I. M., and Venteris, E. R. (1997), "Backstress on Columbia Glacier." In, *Calving glaciers.* Edited by C.J. Van der Veen; Ohio State University. Byrd Polar Research Center. BPRC report, No. 15, pp. 187-194.

Whillans, I.M. and C.J. van der Veen (1994), "Stress maps for Columbia Glacier, Alaska." *EOS*, V. 75, No. 222

Wood, Larry (1986), "Columbia: Glacier in retreat." *Sea Frontiers,* 32, 244-252.

13 June 2013

Report to Prince William Sound Citizen's Regional Advisory Council:
Future Iceberg Discharge from Columbia Glacier, Alaska

Reference PWSRCAC Project #8551
Contractor: W. T. Pfeffer Geophysical Consultants, Nederland, Colorado

Report #2

1. Recovery and Inventory of Historic Materials

Time-Lapse Films. Long before the digital time-lapse program was initiated in 2004, film cameras were being used to monitor the glacier's rapid retreat. In 1978-1985, a 16mm film camera maintained by the U.S. Geological Survey (under the direction of Robert M. Krimmel) photographed the glacier front at least once per day uninterrupted for seven years (Krimmel and others, 1985). Then, in 1996-1997, Austin Post and Wendell Tangborn (Hydromet, Inc. of Seattle, Washington) maintained three 35mm film cameras which photographed the glacier terminus, moraine shoal, and Columbia Bay every ten minutes for 16 months as part of the Iceberg Monitoring Project (IMP) research program (Post and others, 1997).

Until recently, the only copies available were low-quality transfers to Video Home System (VHS) tapes, a format with an effective resolution of 0.15 megapixels. Late-production 16mm film copies of the USGS time-lapse sequence have since been recovered from the USGS Washington Water Science Center in Tacoma, and additional 16mm film reels, presumably the camera originals, are currently in the custody of Video Producer Don Becker at the USGS Federal Center in Denver, Colorado. Three 35mm film reels presumed to be the IMP camera originals are currently held by the Valdez Museum. Negotiations are underway with both custodians to produce high quality digital and analog reproductions of the film originals for photogrammetric analysis and scientific archival.

Iceberg Monitoring Project (IMP). The IMP research program (Tangborn, et al, 2000) culminated in a plastic binder with a bound printed report, a series of fourteen Open File Reports (OFR), and a floppy disk with meteorological data (Tangborn and others, 2000). Four complete copies are known to exist - one at the Valdez Museum, one at RCAC's Valdez office, one with Shad O'Neel at the USGS Alaska Science Center, and one with Ethan Welty and W. Tad Pfeffer at the Institute of Arctic and Alpine Research. Digital copies of all available IMP materials will be archived and delivered to the RCAC upon the completion of the current study.

To facilitate frame-by-frame analysis of iceberg drift, the 35mm time-lapse sequences were transferred to 16 inch laserdiscs, a digital format far superior to VHS wherein each frame is stored as a 0.27 megapixel image. Wendell Tangborn recalls sending the laserdiscs to RCAC. If the film

reels held by the Valdez Museum are discovered to be incomplete, finding these missing laserdiscs should be made a high priority.

Finally, iceberg trajectories were derived from the time-lapse photographs using the laser disc reader "by plotting iceberg positions on a 1-km grid overlain directly onto the monitor" (Tangborn and others, 2000, p. 3). However, neither the large notebook that once contained these observations, nor any digital copy of this data, has yet been found.

Additional Materials. A formal agreement was recently struck approving the transfer of Alaskan glacier materials from the USGS Washington Water Science Center to Shad O'Neel at the USGS Alaska Science Center. Among these are the vast majority of film aerial photographs acquired over the Columbia Glacier by the USGS in 1976-2001.

The scanning and processing of these historical stereo photographs can yield information about terminus position, ice surface elevation, and flow velocity, three physically observable quantities that together best describe a tidewater glacier's geometry and behavior. To further our understanding of the phenomena triggering and regulating Columbia Glacier's retreat, understanding critical to projections of future behavior, we are making a deliberate effort to assemble this information from all available sources. This includes vertical stereo photographs, oblique time-lapse photographs, LiDAR scans, and TerraSAR-X radar images, described in the previous report, as well as terminus positions gleaned from newly discovered analog maps (Post, 1975; Post, 1982; Post, 1983; Sikonia and Post, 1980).

Our ongoing efforts to assemble time-series of terminus position, ice thickness, and velocity over the full history of the glacier's retreat are documented in a Google Spreadsheet.

2. Bathymetric Observations

History of Bathymetric Surveys in Columbia Bay. To our knowledge, four rounds of bathymetric measurements have been carried out at or near the Columbia Glacier moraine shoal, from the onset of the USGS research program in 1977 to the hydrographic survey by NOAA Ship Rainier in 2005. Each are described below, followed by a discussion of opportunistic data either known to exist or freshly acquired.

1977-1983
USGS R/V Growler and Bergy Bit
Columbia Bay, moraine shoal, forebay to 1983 terminus

Soundings were collected throughout Columbia Bay and approaches during the summer and fall of 1997 by the U.S. Geological Survey R/V Growler and the radio-controlled Bergy Bit. Taking advantage of a large embayment in the glacier terminus in August - September of that year, soundings were collected outside, along, and just within the moraine shoal. This is the earliest bathymetry on file, but the accuracy of the data is poorly constrained. As Austin Post (1978)

explains, "tidal adjustments to approximate mean lower low water were made utilizing predicted Cordova tides; spot checks from temporary tide recorders in Columbia Bay indicated these data to be accurate within about 3 feet of measured tides."

Additional soundings were collected in later years in the expanding forebay with the same boat and presumably similar methods. As explained in the Iceberg Monitoring Project (IMP) Open File Report (OFR) 4B by Post and others (1998b), "a preliminary survey of the [forebay] between Heather Island and Tropic Isle was surveyed by the U.S. Geological Survey R/V Growler 1977-1983." A larger scale chart of the moraine shoal bathymetry is provided in IMP OFR 5 (Post and others, 1998a), again citing years 1977-1983 for the earliest soundings in the forebay.

Finally, file BATH in the Krimmel (2001) data report contains "all the bathymetric measurements from Columbia forebay." The soundings are dated either "pre-1985" (presumably the soundings discussed above) or one of 1995-11-26, 1996-09-13, and 1997-10-17 (the soundings discussed below).

1995-1997
Stan Stephens Charters
Forebay to 1997 terminus (partial)

"Stan Stephens Charters, assisted by the USGS in 1995 and by IMP in 1996-1997, obtained water depths in the forebay north of the moraine" (Post and others, 1998a). While R/V Growler surveyed Heather Island to Tropic Isle (the eastern forebay) in 1977-1983, "the remainder of the forebay was surveyed by the Stan Stephens Charters" (Post and others, 1998b). These soundings make up the majority of the BATH file in the Krimmel (2001) data report.

September 5-29, 1994
NOAA Ship Rainier
Columbia and Heather Bays, moraine shoal

National Oceanic and Atmospheric Administration (NOAA) Ship Rainier performed a hydrographic survey of Columbia and Heather Bays up to and including the moraine shoal. The data was published as Hydrographic Survey Sheet H-10567 (NOAA, 1994).

September 1 - October 3, 2005
NOAA Ship Rainier
Moraine shoal, forebay to 2005 terminus

NOAA Ship Rainier returned in 2005 to perform a hydrographic survey of the moraine shoal and forebay up to the glacier terminus. The data was published as Hydrographic Survey Sheets H-11493 and H-11494 (NOAA, 2005).

New and possible acquisitions

Rob Campbell (Prince William Sound Science Center) performs bimonthly conductivity, temperature, and depth (CTD) surveys of the Sound. He has generously provided us with depth soundings acquired on 7 May, 2013 in Columbia Bay and along the moraine shoal, and volunteered himself and his boat for a more rigorous and complete survey of the moraine shoal sometime later this summer.

Bernard Hallet (Professor at University of Washington Earth and Space Sciences) is known to have carried out oceanography in Columbia Bay as recently as 2011, but none of his data has been made available to us.

Next 3 pages: *Figure 2-1: Bathymetric surveys, 1977-201; spatial coverage in map view*

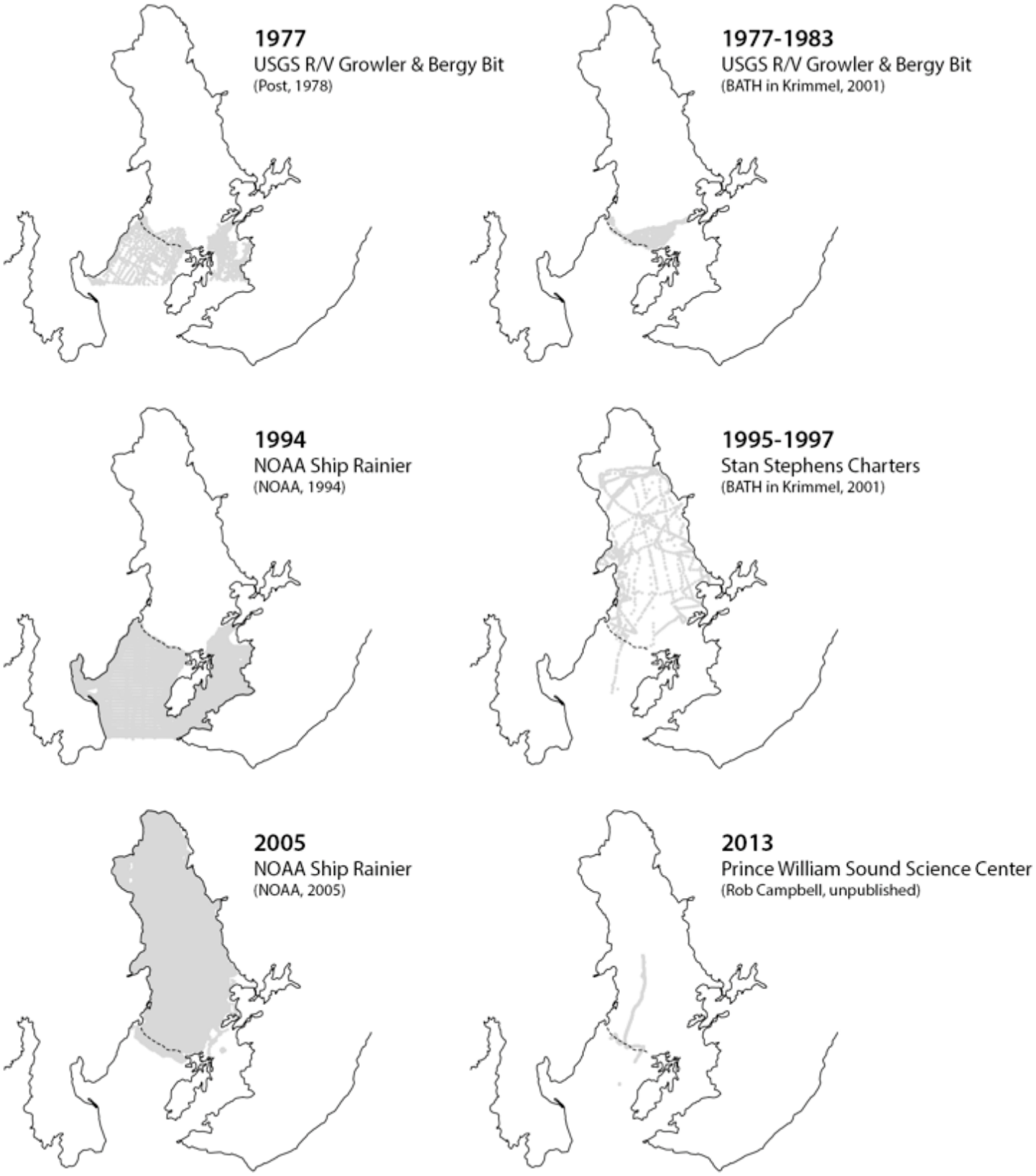

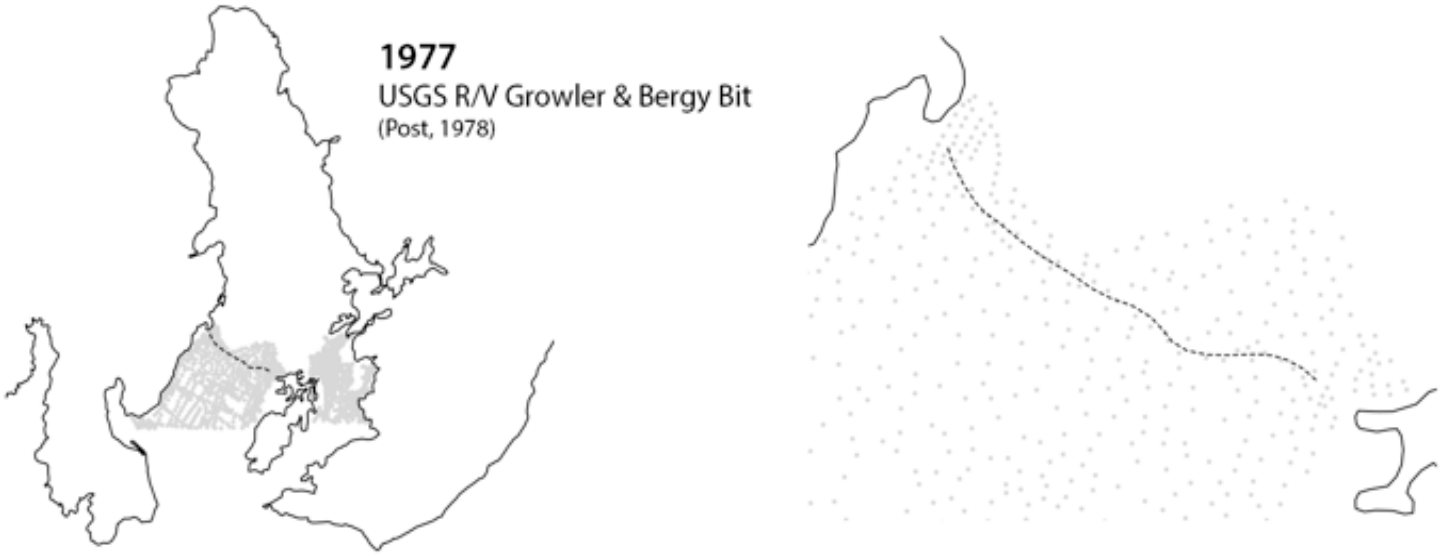
1977
USGS R/V Growler & Bergy Bit
(Post, 1978)

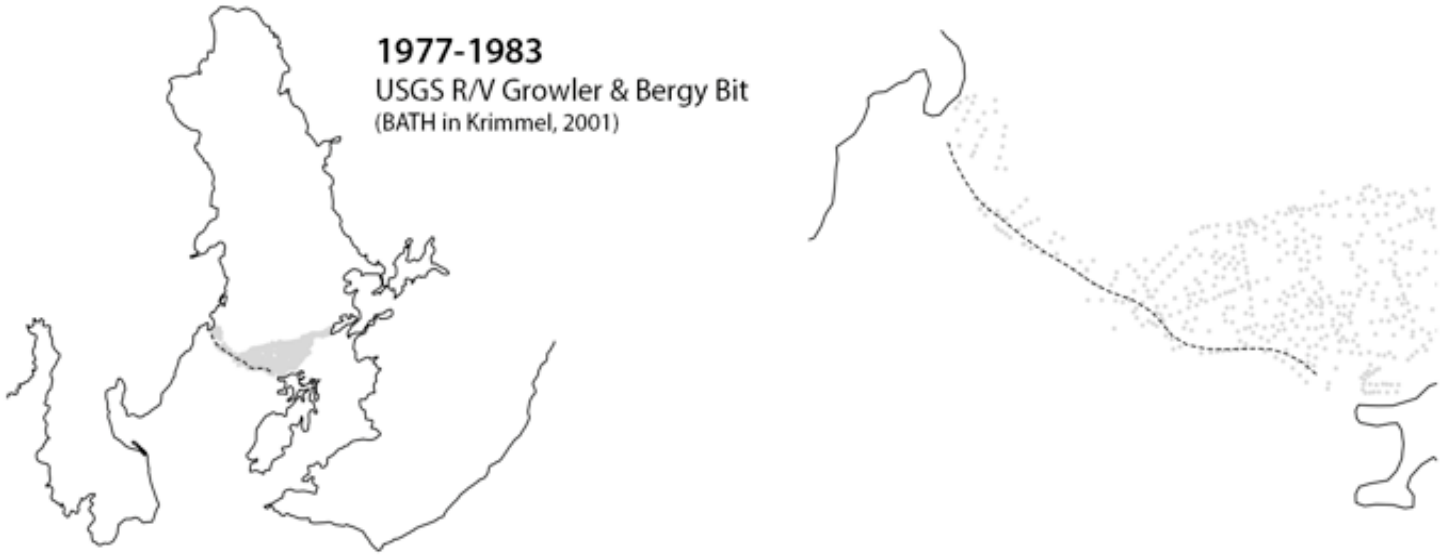
1977-1983
USGS R/V Growler & Bergy Bit
(BATH in Krimmel, 2001)

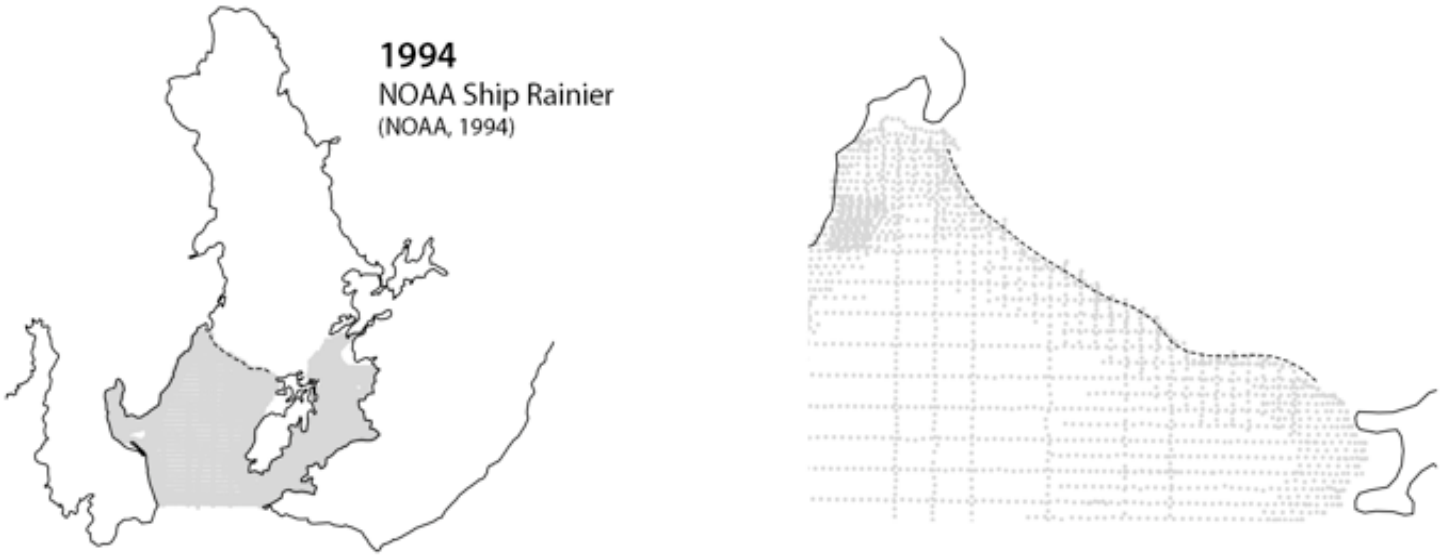
1994
NOAA Ship Rainier
(NOAA, 1994)


1995-1997
Stan Stephens Charters
(BATH in Krimmel, 2001)


2005
NOAA Ship Rainier
(NOAA, 2005)

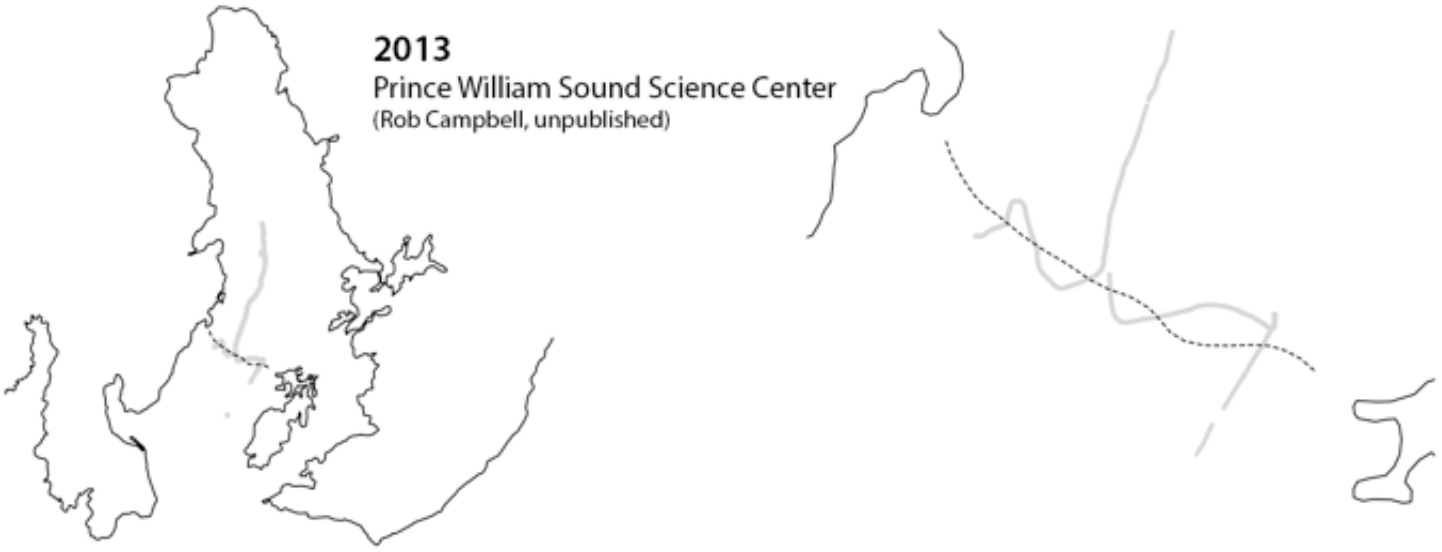
2013
Prince William Sound Science Center
(Rob Campbell, unpublished)

Bathymetric transects of the moraine crest. IMP Open File Report 5 (Post and others, 1998a) illustrated the changes in the moraine shoal as a longitudinal plot, comparing the 1994 NOAA. bathymetry to the 1977 soundings collected by the USGS 15 years earlier.

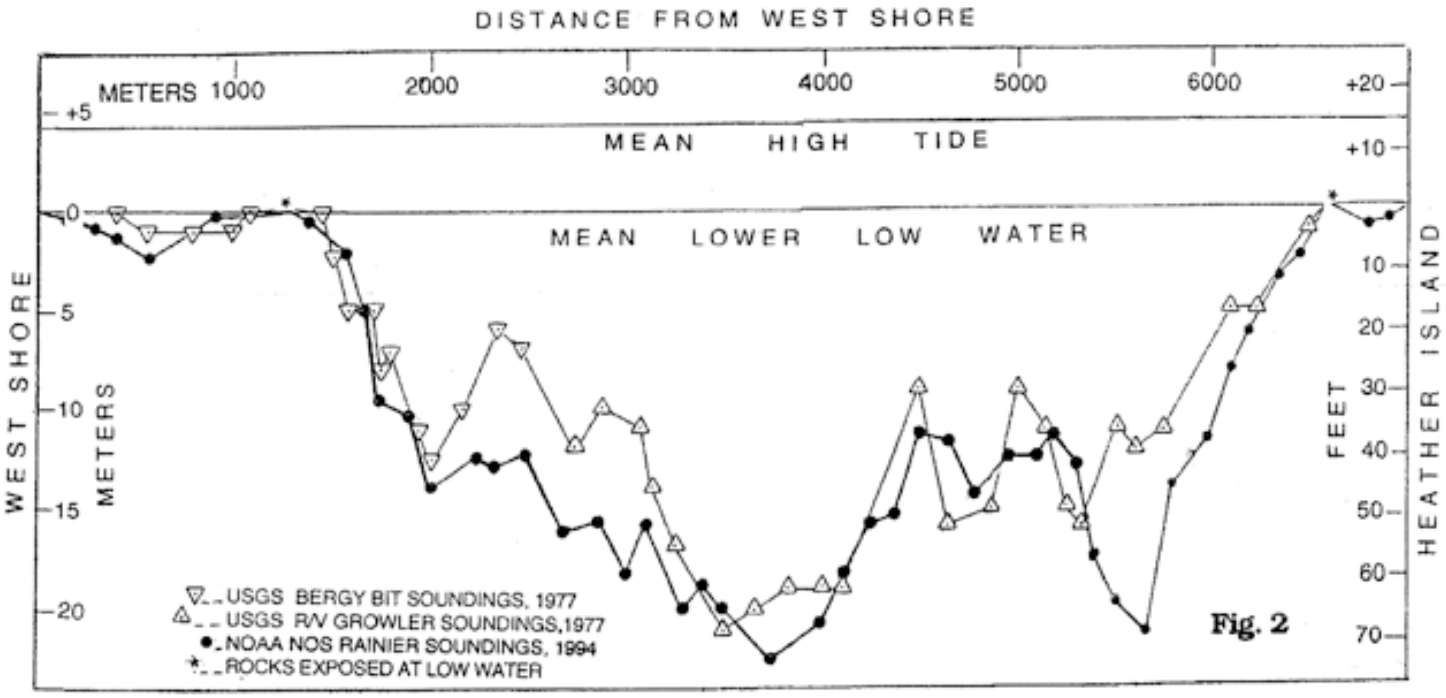

Figure 2-2: Comparison of bathymetric surveys of Heather Bay moraine shoal in 1977 and 1994 (from Post et al, 1998a).

The authors explain the pitfalls of such a comparison, but propose that the apparent lowering of the crest could be real and due to the scouring of the moraine by wave action and current-driven icebergs:

> *The slightly different positions [and tidal datums] of the soundings may account for most of the variations, except between 2000 - 3000 and 5000 - 6000 meters from the western shore. It is likely that here differences may be due to failure to measure the shallowest water on the crest of the moraine during the course of the surveys due to stranded icebergs. It is also possible that the highest points on the moraine shown in the 1997 surveys have been scoured off by storm waves and tidal current-driven icebergs.*

We have recreated the horizontal transect giving rise to the plot, and used it to resample the datasets introduced earlier. In order to correct for the "different positions of the soundings" and to properly sample along the crest of the moraine, the shallowest sounding at each 20-100 m interval falling within 50 m of the transect centerline is used to build each longitudinal profile. Rough agreement between the original figure and the resampled 1977 USGS and 1994 NOAA bathymetry provides a check of transect alignment (each plotted as a pair of lines).

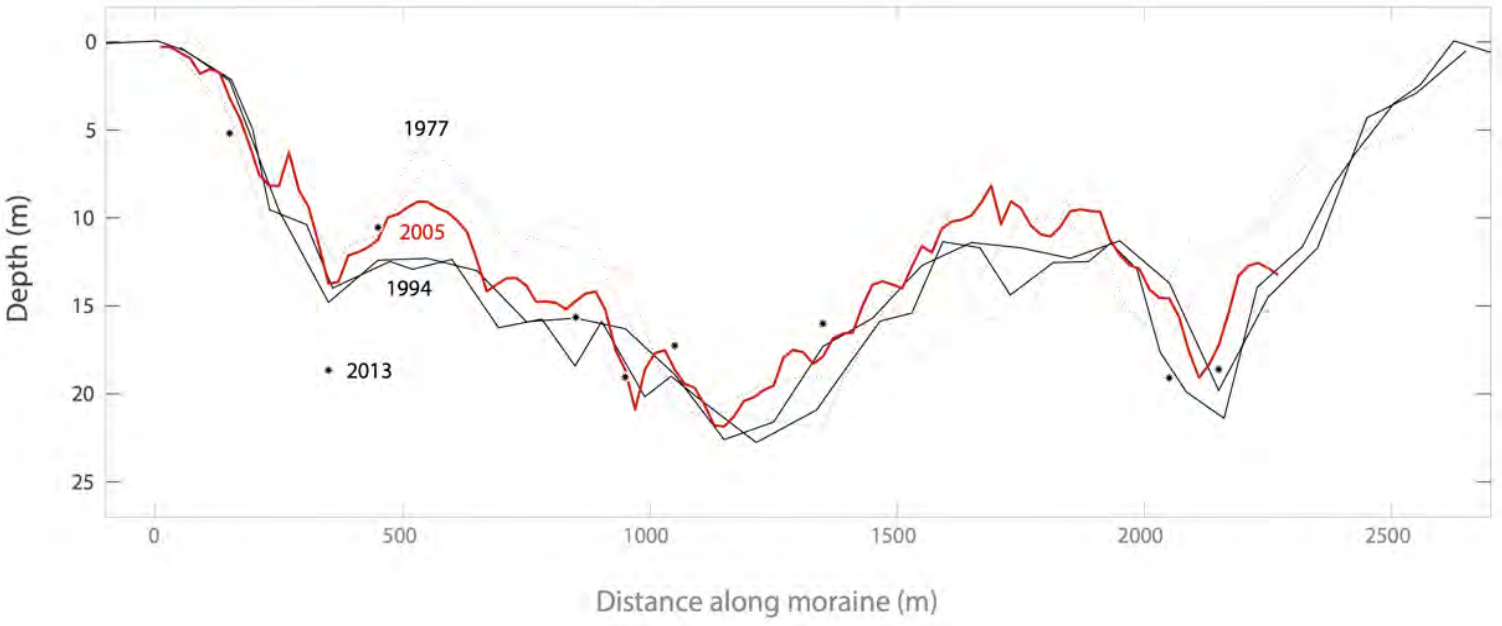

Figure 2-3: Recalculation of bathymetric survey comparison at Heather Bay moraine shoal, 1977 to 1994.

Evidently, the authoritative 2005 hydrographic survey by NOAA Ship Rainier puts to rest earlier suspicions of any major scouring of the moraine shoal. The 10 m spacing between these measurements ensures that the actual crest of the moraine can be reproduced accurately. The overall conclusion of the IMP report remains true today:

> *For several centuries at least, there has been no major submarine avalanching which could have created deep breaks in the moraine. For the foreseeable future, large icebergs will continue to be trapped by the moraine.*

Regional forebay and moraine bathymetry. Comparisons between the 1977, 1994, and 2013 soundings to the gridded NOAA hydrographic survey in 2005 provides a broader view of bathymetric changes. Vertical differences at each point location are colored on a scale expressed in meters per year: black > 0.3 m/yr (shallowing), grey = 0.3 to 0 m/yr, brown = 0 to -0.3 m/yr, red < -0.3 m/yr (deepening). Changes from 1997 and 1994 to 2005 would indicate lowering of the forebay (say, due to the clearing out of fresh, loose glacial deposits) and raising of the moraine crest and distal side (say, due to deposition of scoured sediment). However, the pattern of the 2005 to 2013 changes, measured along the thin, sinuous, but very dense filament of soundings would indicate overall lowering on both sides of the moraine crest.

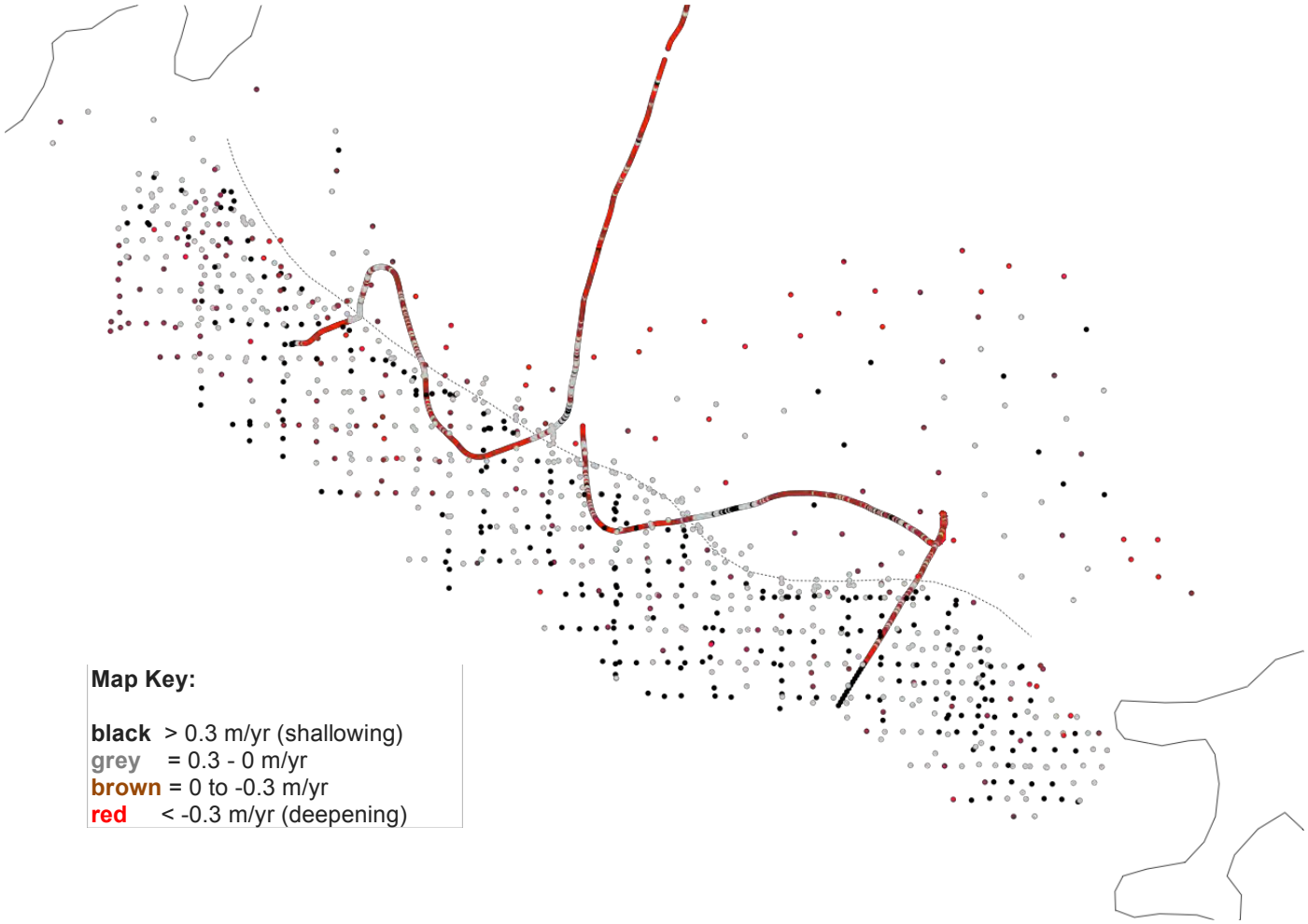

Figure 2-4: Rates of change in bathymetry over survey periods 1977 to 2005, 1994 to 2005, and 2005 to 2013. Data Sources: 1977 USGS R/V Growler and Bergy Bit Soundings (Post, 1978); 1994 NOAA Rainier Gridded Bathymetry (NOAA, 1994); 2005 NOAA Rainier Gridded Bathymetry (NOAA, 2005).

The observed changes are contradictory, and an interpretation, beyond acknowledging the large uncertainties of all but the 2005 survey, is difficult to prescribe. Since the moraine is accentuated by cross-fjord peaks and valleys, and some of these valleys are where currents will be strong, there may be scour and erosion sequences that are spatially limited. The 2005 survey was multibeam, and the raw data is available in the Generic Sensor Format (NOAA, 2005). Looking for textures indicative of scour in the full resolution data, then targeting those locations for a future multi-beam repeat survey may well be the best and only strategy to reconstruct a conclusive narrative of the changes at the moraine shoal.

3. Update on retreat projection

Local (time lapse camera) and satellite (WorldView) imagery have shown several calving terminus embayments, developed over the past several months. These embayments are signs of instability. Visually, the terminus appears to be low in the water, an additional indication of potential instability, and fracturing seems pervasive in regions associated with the main channel and fast flow. Although guided only by intuition, we suspect that there may be an increased potential for a dynamic acceleration in flow, thinning, and calving, perhaps as soon as this summer. A small overdeepening exists upstream of the terminus, and historically, episodes of rapid retreat through overdeepenings have followed periods of temporary stability at pinning points (as is ongoing now). Although we emphasize that this is not a firm prediction for rapid retreat or an abrupt increase in iceberg production, such an event would not be surprising.

Retreat model refinements. The projection model described in Report 1 (December 2012) comprises two alternative procedures, linear and non-linear, for calculating both the future rate of terminus retreat and calving flux, and the time and location of final terminus stabilization after which calving will converge to some steady reduced rate determined by the overall glacier mass balance at that time. Both models are limited to extrapolating past observations into the future, and thus rely on the continued validity of those observations. In the linear model, the average retreat rate over the past decade is assumed to remain true in the future. In the non-linear model, the average thinning rate of the tidewater reach of the glacier over the past decade is assumed to remain constant, and the future calving and retreat rates are calculated from geometric changes driven by that thinning rate. The results of these models are summarized in Table 3-1.

	Linear Model		Non-Linear Model	
Principal Assumption	Fixed Retreat Rate:	0.6 km^3/yr	Fixed Thinning Rate:	0.02 km/yr
Total Ice Volume Calved (km^3)	52.9		66.2	
Date of Stabilization	2029		2036	
Average Calving Rate (km^3/yr)	3.11		2.75	
Maximum Calving Rate (km^3/yr)	5.79		6.2	

Table 3-1: Summary of retreat projection results

Further elaboration of the retreat mechanics beyond what has already been developed in these two models is unwarranted given the weak state of process-derived models for iceberg calving and tidewater hydrological coupling. Extrapolation projections can be robust predictors, however, especially on the comparatively short time scales of interest here (National Research Council, 2012). Our strategy for further model refinement is focused on quantifying the uncertainties in our existing models. The difference between the two projections gives a crude measure of uncertainty, but uncertainties can be quantified in a much more robust fashion by following them from the input assumptions and parameterizations through the calculations to the final projection results. To do this, we will apply formal error propagation analysis and possibly a Bayesian Hierarchical analysis

as well. Table 3-2 lists the variables to be considered in this analysis, with nominal values of those variables as implemented.

Uncertainty analysis of Columbia Glacier retreat models	
Variable	**Nominal Value**
Position of tidewater limit[1]	km 36
Marine-grounded ice volume	12.77 km^3
Future retreat rate (for linear model)	0.6 km/yr
Future thinning rate (for non-linear model)	0.02 km/yr
Divider Gate initial flux	2.6 km^3/yr
Divider Gate final flux	2.0 km^3/yr
Average surface mass balance in tidewater reach	4 m/yr
Instability criterion value (for non-linear case)	1.5

[1]: referred to Columbia Glacier centerline coordinate system

Table 3-2: Variables used in retreat projection models to be included in uncertainty analysis

4. Strategy for quantitative iceberg transport model

4.1 Observational constraints

Time-lapse camera AK10 provides an excellent view of the upper reaches of Columbia Bay nearest the glacier. To begin assembling constraints on future iceberg transport models, we are making a qualitative evaluation of the time-lapse sequences from this camera. Daily and sub-hourly interval movies have been constructed using these images, and analysis is underway to extract patterns of iceberg movement. Some of our preliminary findings include: 1) when larger bergs are calved, they undergo a period of limited motion, sometimes for extended (several hours to days) intervals. This is followed by swift exit from the field of view, generally faster than the 20 minute frame rate. These flushing events are associated with rising tides. 2) ice melange tends to flush in very similar ways. 3) The large bergs tend to ground in the near-glacier fjord, likely due to their release from the now narrow central channel, then drifting laterally into shoals. To the best of our knowledge this type of fjord geometry has not been present since the retreat of the terminus from Heather Island. We also have seen several large bergs grounded in the new West Branch Fjord over the time-lapse sequence.

We are also working to develop methods to characterize and quantify iceberg cover in the fjord from the 11-day repeat TerraSAR-X imagery. To date, we have focused on georeferencing of the high quality radar images and developing image processing techniques to automatically determine fractional ice coverage of the sea surface based on radar reflection intensity. A simultaneous effort is underway to compile time series for external forcing, including tides, sea-surface temperature and wind data over the same time intervals.

4.2 Iceberg calving and transport model strategy

Iceberg ocean transport, and degradation during transport, are substantially better understood than iceberg calving processes. Clearly, however, a critical variable in the transport model is the rate and size distribution of the icebergs originally generated through calving. Research on iceberg transport has been motivated by two distinct objectives: the role of icebergs in marine sediment transport, a topic of substantial interest in marine geology, and a now-abandoned effort of the 1970s and 1980s to determine if icebergs could be towed for long distances as a cost-effective source of freshwater for the world's arid regions. Iceberg hazards to shipping and, more recently, to offshore drilling platforms have also provided motivation. The theory and analysis developed in these fields can be applied directly to the down-fjord transport of icebergs at Columbia Glacier. Adapting process models to a statistical framework for iceberg populations characterized by certain size distributions will provide an efficient method for calculating iceberg population distributions at the down-flow (seaward) end of Columbia Bay. As with the uncertainties in the retreat model, an error propagation analysis will be made to determine which of the many variables used has the greatest influence on the final result, and how uncertainties in those variables influence the final projections. The calving and transport process will be broken down into the following stages:

Calving rate and iceberg size distribution. The future total flux of ice (volume or mass per unit time) will be tied directly to the retreat models reviewed in Section 3. Iceberg size distributions have been described both as log-normal (Weeks and Mellor (1978); Morgan and Budd (1978); Dowdeswell et al (1992) and as power-law (Bahr, 1995; O'Neel at al, 2010). The difference between these distributions lies in the smallest size classes, and is thus of concern here, where bergs small enough to be difficult to detect but large enough to damage a vessel are a prime consideration. Either distribution may be correct; a log-normal truncation at smaller sizes could be either an artifact of undercounting small, hard-to-see, bergs or it may be real and a consequence of their rapid degradation following calving, since melt will eliminate smaller bergs more quickly due to their higher area-volume ratio (Dowdeswell et al, 1992).

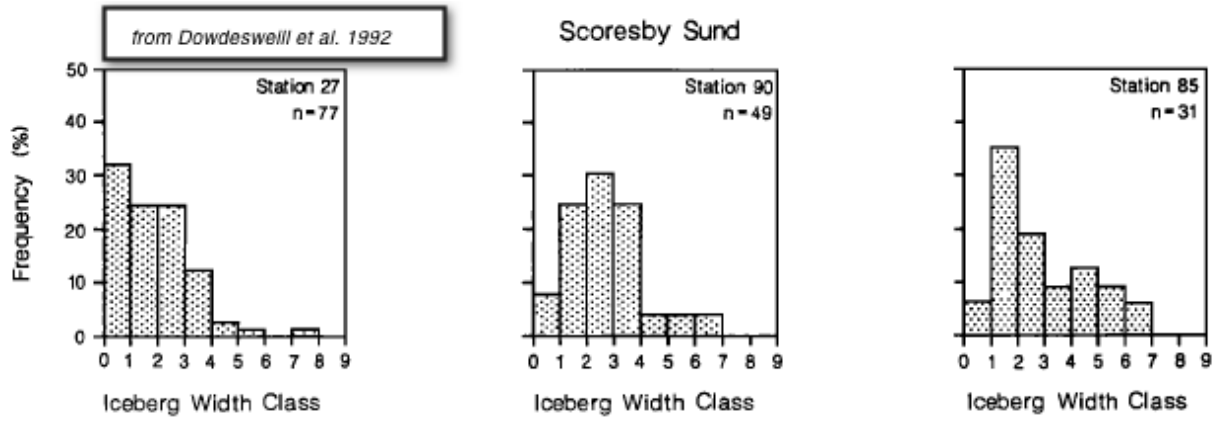

Figure 4-1: Examples of ice size distributions, from Dowdeswell et al, 1992. Station 27 shows a typical power-law distribution, with numbers of bergs increasing monotonically with decreasing size. Stations 90 and 85 show typical log-normal distributions, with frequency declining in the smallest size classes.

Future iceberg size distributions can be generated based on projected total flux and simple assumptions about minimum and maximum berg size. Limits on iceberg size can be obtained from existing imagery, and may be reasonably assumed to be valid in the future, or can be adjusted using simple relationships between berg size and mean terminus ice thickness. Iceberg sizes are abundantly documented in the 1977-2013 catalog of vertical photography at Columbia Glacier, and we are now developing efficient digital methods for measuring berg sizes from the aerial imagery.

Another tool for quantifying size distributions may become available to us through new research being conducted by Tim Bartholomaus, PhD candidate at University of Alaska Fairbanks. Using seismic data gathered by us over the past ca. 8 years at Columbia Glacier, Tim is working on extensions to a seismic filter (originally developed by S. O'Neel and H.P. Marshall at INSTAAR/Univ of Colorado; O'Neel et al, 2007) designed to distinguish iceberg calving from other seismic noise. Tim's research is leading toward algorithms to detect both calving event timing and size (and thus size distributions) from the seismic record. While this tool applies only to observations and has no predictive capacity, it may provide crucial information on size distributions at the time of calving, derived directly from observations. Although much more labor intensive, the size and timing of individual calving events can be extracted from photogrammetric analysis of the time-lapse record, and may be used to spot check the seismic results.

Downfjord iceberg drift. The general equation of motion for an isolated iceberg in the ocean is:

$$M\frac{dV_i}{dx} = -Mf\mathbf{k}xV_i + F_a + F_w + F_r + F_s + F_p$$

where $Mf\mathbf{k}xV_i$ is a term describing Coriolis forces and the remaining terms (F) are applied forces arising from wind (a), currents (w), sea-ice drag (s), waves (r), and a pressure gradient force (p) exerted by the water displaced by the iceberg's mass. Several of these terms can be discarded for the situation in Columbia Bay, where the berg motion is not sufficiently steady for Coriolis forces to significantly alter berg trajectories ($f \rightarrow 0$), and where waves are small ($F_r \rightarrow 0$). The pressure gradient force F_p is a transient force that arises during accelerations of the iceberg relative to the water (e.g. during calving or rolling) but may be neglected when calculating long-term transport.

With these simplifications the general equation of motion reduces to:

$$M\frac{dV_i}{dx} = F_a + F_w + F_s$$

The sea-ice drag term F_s may be modified to represent interparticle forces in the sea ice brash that accumulates in the forebay. In the early years of the retreat, brash ice would form a very dense, tightly packed surface layer (ice melange, or Sikkussaq) covering the entire forebay, with large-scale strength properties that had significant effects on iceberg motion. While still occurring in

portions of the forebay today, rafts of brash ice are far more spatially limited and ephemeral than in the past, and it may not be necessary to include this term in projections.

The forces applied by winds and currents will, under steady state conditions, eventually bring icebergs to a steady velocity mostly equal to the current, but with a second-order influence due to wind. If the time scale of this equilibration is short enough, berg motions can be calculated satisfactorily by assuming that they are carried passively by currents, which can in turn be calculated from knowledge of tides in Columbia Bay (Walters et al, 1988) and modeled freshwater discharge from surface mass balance (Rasmussen et al, 2012; O'Neel, 2012). The required time scale of equilibration was calculated by Sodhi and Dempster (1975) as

$$T = \frac{2M}{\rho_w c_w A_w \Delta V}$$

where M is the iceberg's mass, ρ_w is the density of ocean water, c_w is the drag coefficient of the iceberg in water, A_w is the underwater cross-sectional area facing the flow, and ΔV is the velocity change during equilibration. Iceberg motion will thus be determined primarily by currents in Columbia Bay with velocity equilibration time of duration T introduced during current changes. The effect of wind will be difficult to accommodate (since we have no good way of forecasting wind), but some overall correction may be feasible, knowing, for example, that wind near the glacier terminus will be dominated by down-glacier (katabatic) drainage.

Iceberg degradation by melt. Research in the 1970s and 1980s on the feasibility of towing icebergs to arid regions sought to strike an economic balance between the expense of moving the iceberg and the value of the water contained in the ice. Determining the optimal towing velocity proved to be one of the primary challenges: very slow towing cost less in fuel, but the iceberg had more time to melt on the journey. Fast towing not only increased the fuel costs of towing, but may actually have accelerated melt rate through increased forced convection on the submerged iceberg surfaces. In any case, the problems of heat and mass transfer at a submerged iceberg surface were studied intensively during this time (e.g. Weeks and Campbell, 1973; Weeks and Mellor, 1978; El-Tahan et al, 1987; Chirivella and Miller, 1978; Garrett, 1985; Morgan and Budd, 1978; Smith and Banke, 1983), and a number of simplified parameterizations suitable to the present situation were developed. Among these are an empirical expression for the melt rate on the vertical sides of an iceberg (El-Tahan et al, 1987):

$$\dot{m}_v = 2.78T + 0.47T^2$$

where T is the water temperature (degrees C), and $\dot{m}$ is the melt rate (m/yr). In addition, White et al (1980) derived an expression for wave erosion per degree C water temperature at the berg waterline:

$$\dot{m}_{wave} = 0.000146 \frac{H}{P} \left(\frac{R}{H} \right)^{0.2}$$

where P and H are the mean period and wave height, and R is the wave roughness height. The melt rate $\dot{m}_{wave}$ has units of *m/yr/C.*

Iceberg degradation by fracture. An extensive literature exists on the fracture mechanics of glacier ice, but most analyses are too complex to be applied to the thousands of icebergs carried down Columbia Bay. We will adapt some of the more efficient analyses of stability and fracture to our situation, and determine the probability of failure by fracture based on the probability that an iceberg in a given size class will roll and knowledge of the average strength of glacier ice.

Icebergs roll when melt, both above and below the waterline, alters their shape so as to make them gravitationally unstable. Despite the complex and varied geometry of icebergs, the Weeks-Mellor criterion (Weeks and Mellor, 1978) gives a simple but robust indicator of stability. Rolling will occur when:

$$\frac{L_a}{H} = \sqrt{0.92 + \frac{58.32}{H}}$$

where L_a is the iceberg maximum width and H is its total thickness (m). When melt causes an iceberg of a given size to cross this threshold, the berg is assumed to roll, and the internal stresses and time spent in the roll can be calculated from elementary dynamics. These give a rate of loading (approximately the stress divided by the rolling time), and the loading can be compared to measurements of ice strength (e.g. Schulson, 1999). The iceberg size will determine the stress generated during rolling, so not all berg size categories will experience the same rates of degradation by fracture. On failure the iceberg will simply be assumed to split into two smaller bergs of equal size.

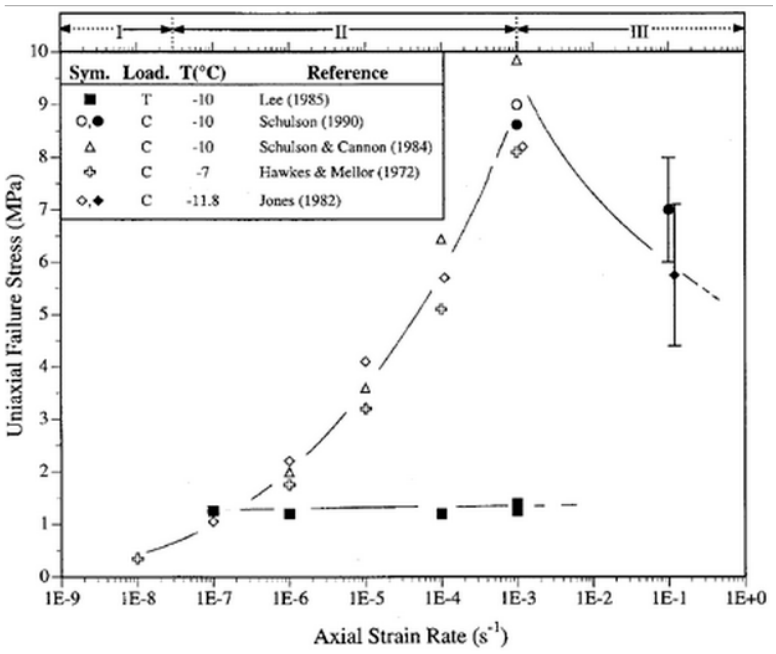

Figure 4-2: Uniaxial failure stress vs. strain rate for polycrystalline glacier ice (from Schulson, 1999)

Iceberg size distribution and passage over Heather Bay moraine. All of the processes described above will generate an evolving size distribution as the iceberg population is advected downstream toward the Heather Bay Moraine shoal. As a means of validation, the down-flow variation of the size distribution can be compared to observations of berg size distribution at positions along Columbia Bay during the course of the retreat. Once imagery has been retrieved from the new Heather Bay moraine camera, the details of iceberg passage over the moraine shoal can be examined in detail. Our current hypothesis is that bergs escape when the water depth over the moraine crest is sufficient for bergs to pass without grounding, and that favorable currents (and possibly winds) are required to move the icebergs. Accordingly, most bergs are hypothesized to escape at some point on the ebb tide, when decreasing water depth and increasing seaward current cross some optimal threshold. Data in the original IMP study will also provide valuable guidance.

5. Heather Island Camera

A digital time-lapse camera was installed inside the USGS cabin on Heather Island on 7 May, 2013. The camera, mounted on one of two survey monuments inside the cabin, is pointed out the window towards the moraine shoal and programmed to acquire an image every 20 minutes (during daylight hours, as determined by a light sensor attached to the camera body). The camera, a Canon 40D equipped with a 24 mm lens, is set to aperture priority (F8) with -1/3 stop underexposure at ISO 200, and loaded with a 32 Gb memory card. The camera clock was synched to Coordinated Universal Time (UTC) by taking photographs of the National Institute of Standards and Technology web clock (www.time.gov) prior to deployment. We verified the system by test-triggering the camera via the camera controller and waiting through three scheduled time-lapse photographs

before departing the cabin. A solar panel was mounted to a tree outside the cabin; the 55 Ahr battery had a 13.5 V charge after the power system was connected. A note was taped to the survey monument explaining the reason for the camera and asking visitors to not disturb or remove it.

Figure 5-1: New time-lapse camera installed at the Heather Bay hut (left), and view of moraine (right).

References

Bahr, D. B. (1995), Simulating iceberg calving with a percolation model, J. Geophys. Res.

Bigg, G. R., Wadley, M. R., Stevens, D. P. & Johnson, J. A. Modelling the dynamics and thermodynamics of icebergs. *Cold Regions Science and Technology* **26,** 113–135 (1997).

Chirivella, J. E., and C. G. Miller (1978), [In: Husseiny, A.A. (ed.), Proceedings of the First Conference on Iceberg Utilization for Freshwater Production. Iowa State University.

Dowdeswell, J. A., R. J. Whittington, and R. Hodgkins (1992), The sizes, frequencies, and freeboards of East Greenland icebergs observed using ship radar and sextant, J. Geophys. Res., 97(C3), 3515, doi:10.1029/91JC02821.

EI-Tahan, M.S., Venkatesh, S., E1-Tahan, H., 1987. Validation and quantitative assessment of the deterioration mechanisms of Arctic icebergs. J. Offshore Mech. Arct. Eng. 109, 102-108.

Garrett, C. (1985), Statistical prediction of iceberg trajectories, Cold Regions Science and Technology.

Hock, R., S. O'Neel, and L. A. Rasmussen (2012), Using surface velocities to calculate ice thickness and bed topography: a case study at Columbia Glacier, Alaska, USA, Journal of ….

Krimmel, R. M., Taylor, P., and Barber, P. (1985). *Time Lapse Observations of the Columbia Glacier, Alaska*. 16mm. Tacoma, Washington: U.S. Geological Survey.

Krimmel, R. M. (2001). *Photogrammetric data set, 1957-2000, and bathymetric measurements for Columbia Glacier, Alaska*. U.S. Geological Survey Water Resources Investigations Report 2001-4089.

Morgan, V. I., and W. F. Budd (1978), In: Husseiny, A.A. (ed.), Proceedings of the First Conference on Iceberg Utilization for Freshwater Production. Iowa State University

National Oceanic and Atmospheric Administration (1994). *Columbia Bay and Heather Bay Hydrographic Survey Sheet H-10567*. NOAA Ship Rainier. Retrieved from http://www.ngdc.noaa.gov/nmmrview/metadata.jsp?xml=NOAA/NESDIS/NGDC/MGG/NOS/iso/xml/H10567.xml

National Oceanic and Atmospheric Administration (2005). *Columbia Bay Hydrographic Survey Sheets H-11493 & H-11494*. NOAA Ship Rainier. Retrieved from http://www.ngdc.noaa.gov/nmmrview/metadata.jsp?xml=NOAA/NESDIS/NGDC/MGG/NOS/iso/xml/H11493.xml

National Research Council, Committee on Sea Level Rise in California, O., Washington, B. O. E. Sciences, Resources, O. S. Board, D. O. Earth, L. Studies, National Research Council (2012), Sea-Level Rise for the Coasts of California, Oregon, and Washington: Past, Present, and Future, The National Academies Press.

O'Neel, S., and W. T. Pfeffer (2007), Source mechanics for monochromatic icequakes produced during iceberg calving at Columbia Glacier, AK, Geophys. Res. Lett.

O'Neel, S., C. F. Larsen, N. Rupert, and R. Hansen (2010), Iceberg calving as a primary source of regional-scale glacier-generated seismicity in the St. Elias Mountains, Alaska, J. Geophys. Res., 115(F4), F04034, doi:10.1029/2009JF001598.

Post, A. (1975). *Preliminary hydrography and historic terminal changes of Columbia Glacier, Alaska.* U.S. Geological Survey Hydrologic Investigations Atlas 559, sheets 1 & 2. Retrieved from http://www.dggs.alaska.gov/pubs/id/13645

Post, A. (1978). *Interim bathymetry of Columbia Glacier and approaches, Alaska*. U.S. Geological Survey Open-File Report 78-449. Retrieved from http://www.dggs.alaska.gov/pubs/id/12041

Post, A. (1982, December). *Columbia Glacier - 1982 Bathymetry*. Hand-drawn map, scale 1:10,000.

Post, A. (1983). *Columbia Glacier - 1983 Bathymetry*. Hand-drawn map, scale 1:10,000.

Post, A., Hallet, B., and Rasmussen, L. A. (1998a). *Bathymetry of the Terminal Moraine Shoal, Columbia Glacier, Alaska*. Iceberg Monitoring Project Open File Report No. 5. Valdez, AK: Regional Citizens' Advisory Council.

Post, A., Hallet, B., and Rasmussen, L. A. (1998b). *Preliminary Bathymetry of the Forebay, Columbia Glacier, Alaska*. Iceberg Monitoring Project Open File Report No. 4B. Valdez, AK: Regional Citizens' Advisory Council.

Post, A., Tangborn, W., and Saint Lawrence, W. (1997). *Iceberg Monitoring Project*. 35mm. Valdez, Alaska: Regional Citizens' Advisory Council.

Schulson, E. M. (1999), The structure and mechanical behavior of ice, JOM.

Sikonia, W. G., and Post, A. (1980). *Columbia Glacier, Alaska; recent ice loss and its relationship to seasonal terminal embayments, thinning, and glacial flow*. U.S. Geological Survey Hydrologic Investigations Atlas 619, sheet 3. Retrieved from http://www.dggs.alaska.gov/pubs/id/13647

Smith, S.D., Banke, E.G., 1983. The influence of winds, currents and towing force on the drift of icebergs. Cold Reg. Sci. Technol. 6, 241-245.

Sodhi, D. S., and R. T. Dempster (1975), Motion of icebergs due to changes in water currents, OCEAN 75 Conference.

Tangborn, W., Post, A., and Soemarmo, R. (2000). *Mitigating Navigation Hazards from Columbia Glacier Icebergs in Prince William Sound*. Iceberg Monitoring Project Report. Valdez, AK: Regional Citizens' Advisory Council.

Walters, R. A., E. G. Josberger, and C. L. Driedger (1988), Columbia Bay, Alaska: an "upside down" estuary, Estuarine, Coastal and Shelf Science, 26(6), 607–617, doi:10.1016/0272-7714(88)90037-6.

Weeks, W.F., Campbell, W.J., 1973. Icebergs as a fresh-water source: an appraisal. J. Glaciol. 12, 207-233.

Weeks, W. F., and M. Mellor (1978), Some elements of iceberg technology. In: Husseiny, A.A. (ed.), Proceedings of the First Conference on Iceberg Utilization for Freshwater Production. Iowa State University, pp. 45-98.

W.T. Pfeffer Geophysical Consultants, LLC

11 November 2013

Report to Prince William Sound Citizen's Regional Advisory Council:
Future Iceberg Discharge from Columbia Glacier, Alaska

Reference PWSRCAC Project #8551
Contractor: W. T. Pfeffer Geophysical Consultants, Nederland, Colorado

Report #3

1. Introduction

Report #3 to PWSRCAC for FY13 consists of two main parts. In part one (Updates), we provide topic-focused progress updates for each component of our ongoing research, drawing on information derived from our time lapse cameras and a variety of remote sensing products. We also use newly available information, both unpublished and in the peer-review scientific literature, including a new paper (Rignot et al, 2013) containing airborne radioecho sounding measurements of ice thickness in the Columbia Glacier East Branch. In part two (Synthesis), we assess all available data and analysis to evaluate the current status of the retreat and make a refined estimate of future retreat, calving, downfjord ice transport, and passage of ice over the Heather Bay Moraine Shoal. While further analysis remains to be done, we are now at a stage where can make qualitative assessments of future retreat, calving, and iceberg transport at a fairly high level of confidence. This assessment appears at the end of this report.

2. Updates: Icebergs at Heather Bay Moraine Shoal, Iceberg transport from Columbia Glacier terminus to moraine shoal, Calving at present terminus, Glacier flow dynamics.

2a. Heather Bay Moraine Shoal (HBMS)

Observations and analysis at HBMS are oriented at understanding how icebergs behave on entering the shallow water approaching HBMS from its landward side, under what conditions bergs are able to pass over the shoal and into the open waters on the seaward side of the shoal, and to characterize or place limits on the size distribution of bergs entering Prince William Sound proper. In report 2, we established that the geometry of HBMS is essentially stable: portions of the moraine have experienced minor erosion and deposition, but few changes exceed the precision of the existing measurements. The obstacle presented to bergs by the moraine itself is thus assessed to be constant over time.

For observation of iceberg behavior at and near HBMS we rely on three principal data sources:

1) High-frequency time-lapse monitoring of HBMS, which began in May, 2013, and has so far provided a continuous 20-minute interval image sequence during daylight hours. Image data was retrieved on 19 September 2013. The camera has been left operating and will be serviced again in late winter 2014. A sample sequence from this camera is included on a flash drive with this report, and is also temporarily posted at

http://ftpext.usgs.gov/pub/wr/ak/anchorage/ONeel/Heather island

2) High-frequency time-lapse monitoring of the lower glacier, from a camera position (camera AK-10) ca. 3 km upstream from the present terminus. The synchronized observations of iceberg production at the glacier terminus and iceberg arrival at HBMS provide constraints on the speed of iceberg transport and berg degradation during downfjord transport.

3) Satellite imagery analysis of glacier motion and of icebergs in the forebay reach between the glacier terminus and HBMS. Imagery from the German TerraSAR-X satellite has high spatial resolution (ca. 1-3 m) and is repeated every 11 to 22 days. Velocity and strain rate fields are obtained by SAR-interferometric methods, providing us with detailed views of changing ice flow conditions in the glacier channel and repeated views of icebergs in the forebay reach, from which iceberg size distributions may be extracted by standard image processing methods.

The HBMS camera operated without failure from May through September, 2013, capturing over 6000 images, and has been left in place to shoot throughout the 2013/14 winter. Ice volume on the inside of the moraine is highly variable, and while the density of icebergs is less than in recent years (and far less than in the first *ca*. decade of the retreat), occasional large bergs continue to be delivered to the moraine. We expect that three factors work to reduce the mean iceberg size at HBMS in recent years: these are 1) increasing distance from the source of icebergs to HBMS as the terminus retreats, 2) smaller initial berg size on calving, since the mean terminus ice thickness has been reduced upon regrounding in shallow water in the Main Branch (ca. summer, 2010), immediately upstream of Juncture and 3) warmer waters in the forebay, which accelerate iceberg melt rates. Warmer waters are partly the result of inflow of warming waters from Prince William Sound and partly due to reduction in iceberg density in the forebay, which allows faster solar heating of surface waters. These factors affect all icebergs traversing the forebay from the glacier terminus to HBMS, but large bergs are still occasionally calved, and under favorable conditions survive the journey to HBMS without loosing a great deal of mass.

The presence of larger icebergs at HBMS is important for the impoundment of ice inside the shoal, because the larger grounded bergs present obstacles to the passage of

smaller bergs that might otherwise pass over the shoal on a high tide. We hypothesize that the absence of large bergs near HBMS may be a factor in the occasional flushing of icebergs from most or all of the forebay, an event first recorded in 1996 and documented occasionally during the IMP1 project. We have not yet identified the mechanism responsible for the flushing events, but the candidate processes include tides, currents in the forebay, water temperature, winds, calving rate, and initial berg size distribution on calving.

As large icebergs that arrive at HBMS melt and fracture, the size distribution of bergs as determined by direct measurements at points along the forebay may be altered significantly. Once grounded, large icebergs are more strongly influenced by tidal forcing than a floating berg. As the tide level changes, the center of gravity of grounded berg shifts, rotating the berg and generating stresses that can fracture it into smaller pieces. A good example of this is visible in the supplied time lapse sequence, between 23 and 25 July, in the center of the field of view. In addition to fracture, rotation of the berg over several tidal cycles can “jack” the berg up the slope of the landward side of the shoal, possibly allowing it to escape into Prince William Sound despite being far to large to be simply floated over the shoal. (The occasional presence of anomalously large icebergs on the seaward side of HBMS suggests that this, or some comparable process, must be occurring.) Submarine melt rates also increase during these grounding episodes due to tidal friction arising from accelerated flow around the iceberg in shallow wtaer.

Our scheme for quantifying submarine melt rates is not yet implemented, but the imagery nevertheless demonstrates that subaerial melt rates are large. In the 23 July grounding events, the grounded berg is noticeably smaller towards the end of the grounding episode. Fracture and melting evidently work in concert to reduce berg size, eventually producing berg fragments small enough to float over HBMS on a sufficiently high tide. In the future, we will be able to use time lapse sequences from Heather Island and camera AK10 (Figure 1) to investigate relationships between iceberg production at the calving terminus and iceberg densities at HBMS. We do not presently know if episodes of calving travel coherently downfjord to the shoal, or if intermediate processes divert and retard some bergs while accelerating others.

2b. Downfjord ice transport

Since early summer, we have been developing image processing methods (such as binary contrast stretching and edge detection) to quantify iceberg size distributions at positions along the forebay. Once completed, a robust and efficient image processing workflow will allow us to extract iceberg size distributions from more than 50 TerraSAR-X images acquired since 2011. A second key goal is to estimate iceberg residence time (travel time from calving to arrival at HBMS), but tracking individual icebergs as they

move over the entire *ca.* 20 km path is proving to be a challenge, due to the spatial limitations of our ground-based time lapse photography and temporal limitations of the TerraSAR-X imagery.

2c. Observations and analysis of calving at present terminus

Sarah Neuhaus, a PhD student at UC Santa Cruz, assisted in the image processing development described above during the summer of 2013, working as a USGS intern supervised by Shad O'Neel. Neuhaus also analyzed time lapse image sequences from camera AK10 (Figure 1) that capture berg motions in the immediate vicinity of the glacier terminus. Iceberg grounding in the immediate vicinity of the terminus can be seen in the imagery, and confirms that newly exposed shallows provide opportunities for bergs to become grounded shortly after calving. Trapping of larger icebergs by grounding in the shoals near the glacier terminus skews the size distribution of bergs leaving the terminus region relative to the size distribution of calved bergs. One unexpected discovery from this time lapse series is the observation that icebergs tend to ground near or shortly below high tide, rather than at low tide. Apparently larger icebergs drift furthest into the shoals near the glacier margins at high tide, and ground as the tide starts to fall. Large bergs also tend to become ungrounded faster than medium and small sized bergs, in part due to their tendency to roll and break up rapidly upon grounding.

Figure 1. View from camera AK10 looking downstream toward Columbia Bay. Locations of iceberg grounding events during summer 2012 are color-coded by size, showing the newly revealed shallow locations in the proximal regions of the fjord. Camera AK10 is maintained through a partnership between the Extreme Ice Survey, WT Pfeffer Geophysical Consultants, and the USGS.

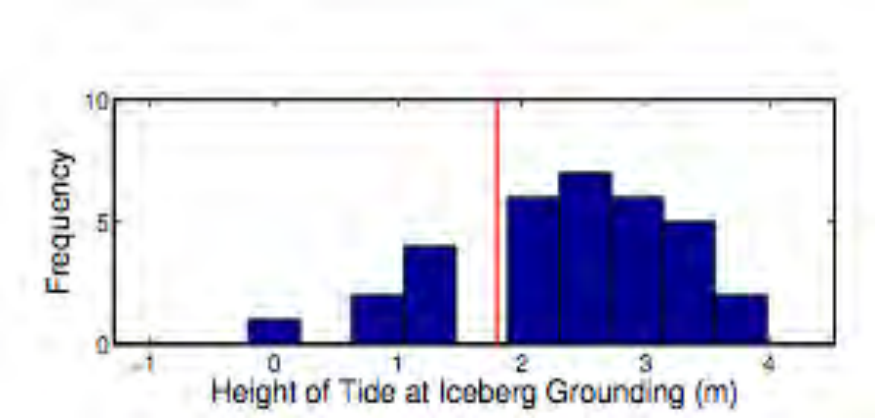

Figure 2. Histogram showing tide height at onset of iceberg grounding events, demonstrating that icebergs tend to drift into otherwise impassable regions during high tide and subsequently become grounded.

2d. Upstream dynamics, future retreat and calving.

When the glacier terminus position is relatively stable over time, as has been the case at Columbia Glacier since summer 2010, changes in flow speed translate directly into changes in calving rate (Figure 3 and Meier and Post, 1987).

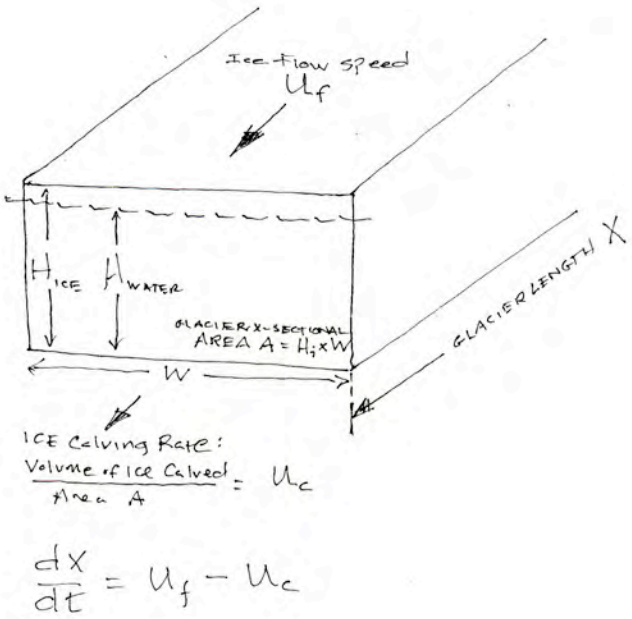

Figure 3. Schematic showing relationship between glacier terminus position, ice flow speed, and calving rate.

Evaluation of the glacier ice flux (volume or mass per unit time pass a reference point on the glacier) requires a complete glacier geometry at a “flux gate” or cross-section of the glacier, as well as a profile of ice motion and measurement or assumption about the variation of flow speed with depth. We define two flux gates, just upstream of the Main and West branch termini (Figure 4). Ice motion at these gates is determined from TerraSAR-X interferometry, using radar data acquired on a nominal 11-day repeat cycle between January 2011 and June 2013. Georectified digital elevation models (DEMs) were calculated from Worldview satellite stereo-pairs collected during 2012. These DEMs, together with swath LiDAR profiles collected by University of Alaska’s NASA Icebridge Mission, constrain the changing surface elevation of the near-terminus region, but on different time steps than the TerraSAR-X-derived velocity is measured. We interpolate the surface elevation change record to common times by linearly fitting the rate of elevation change, applied to the average surface profile geometry. The bed is resolved with a highly data-constrained model (McNabb et al., 2012). We calculate flux as the integrated product of velocity and thickness in 100 m wide cells spanning the entire terminus width, then plot them as a function of time (Figure 5).

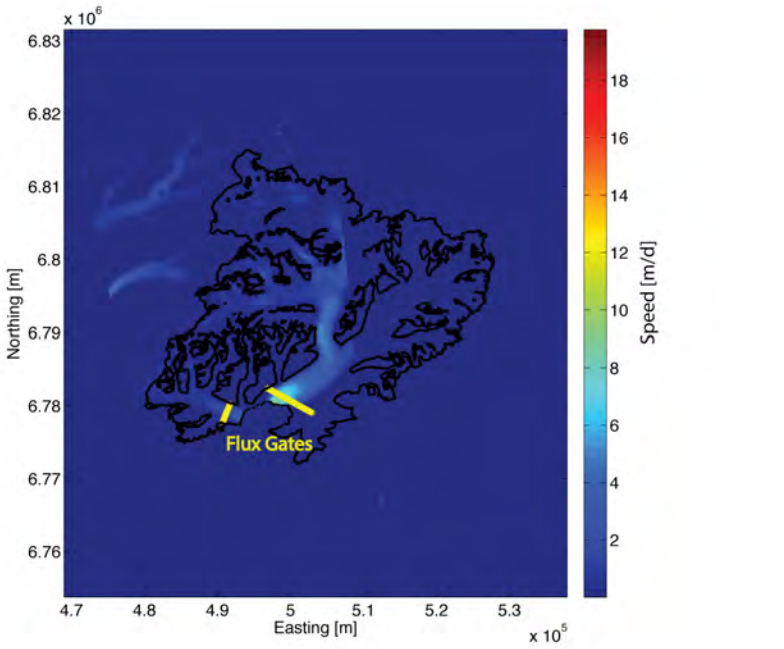

Figure 4. Example of TSX velocity field with Columbia Glacier outline and flux gates overlaid.

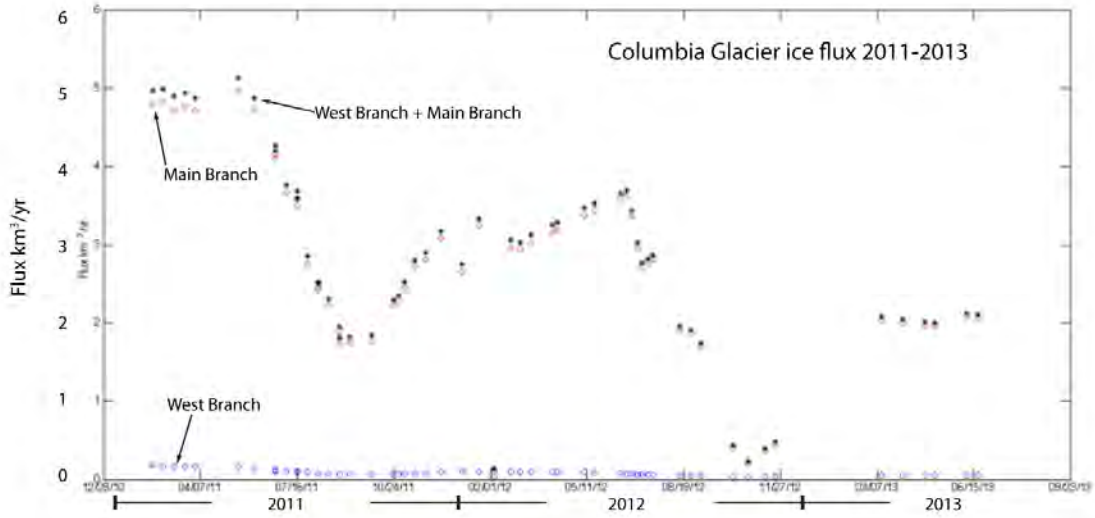

Figure 5. Ice flux (m^3/yr) to the terminus as a function of time (January 2011 through June 2013). Blue circles are from the west branch, red from the main branch, and black stars represent the sum of the two branches.

Average ice flux from both the Main and West branches of the glacier averaged 2.23 km^3/yr from late 2010 to the present (late 2013), with virtually all of the flux coming from the Main branch. (The West branch terminus retreated to very shallow water in *ca*. 2009, and is in addition fed by a much smaller catchment than the Main branch.) Seasonal variability is apparent at *ca.* 1.0 km^3/yr, or *ca*. 45% of the mean flux, superimposed on a secular decreasing trend in flux. This trend is a continuation of the decline in flux observed following a maximum of ca. 7 km^3/yr in the early-mid 2000s as the glacier's terminus entered the deep basin at the West/Main branch confluence. Seasonal variability is characterized by a slow increase in flux during fall through spring, peaking in early summer and falling rapidly to a minimum in late summer.

The sparseness of observations before the TerraSAR-X era (and after the withdrawal of support for regular, multi-annual aerial photogrammetric missions) led to possible under-estimates of ice flux in the mid-2000s (e.g. O'Neel et al, 2005) since the photo missions flown at that time were generally in mid-late summer, when the flux would have been at or near a seasonal low, and no other information existed to apply a seasonal correction.

Short-term (sub-annual) variability in ice flux is primarily forced by speed variations coincident with changes in basal hydraulics (Meier et al, 1994; Kamb et al, 1994). In contrast, the secular trend of reduced flux is a result of thinning of the glacier, which reduces both speed and cross-sectional gate area. Short-term speed variations are coherent over much longer length scales (e.g. high on the Main branch and on tributaries) than stress-coupling theory permits (Kamb and Echelmeyer, 1986a,b; Echelmeyer and Kamb, 1986), implying that ice dynamics are strongly modulated by basal hydrology, the only process available to couple flow dynamics over such long

length scales. Seasonal and shorter time scale changes in motion exhibit maximum variability at the terminus, and decay rapidly upstream.

Comparison with the Krimmel (2001) analysis shows that the timing of seasonal variations in speed is roughly consistent over the history of the retreat. There have been occasional periods during the retreat when the seasonal variation in flux may have diminished or vanished altogether, but the timing of observations has been too sparse at various times during the retreat for these to be interpreted with any confidence. Through the TerraSAR-X era, peak speeds occur *ca.* 2 months later in the year than early in the retreat, but minimum speeds have not shifted in time. Variability in flow speed appears to be fairly consistent over the course of the retreat when measured relative to the terminus position, *i.e.* measured at a position that follows the retreating terminus at a fixed distance (e.g. *ca*. 10 km upstream). The combined effect of these changes is that discharge has become more variable. Indeed, time-lapse imagery and velocity fields both demonstrate that some of the slowdowns nearly stop the ice motion altogether. These slowdowns may be a factor in the occurrence of ice-free forebay conditions.

Our results agree with the conclusions of McNabb et al. (2012), namely, that current discharge rates have fallen significantly since the mid-2000s when the glacier was changing most rapidly. The position of the terminus since ca. 2009 lie outside of the region covered by earlier photogrammetric surveys, so there is no single location where ice flux can be monitored over the entire course of the retreat. However, we can compare migrating near-terminus flux estimates, as described above, to confirm that the discharge flux is declining over time.

The drawdown of the Columbia Glacier reservoir is so considerable that *extended* episodes (> 1 year to decades) of high-volume ice discharge is unlikely in the future. Newly acquired airborne radar results (Rignot et al., 2013) show an overdeepening in the East branch channel some 18 km upstream from the present terminus (Figure 6). This basin comprises a ca. 5 km-long marine-grounded reach of ice lying as much as 300 m below sea level. The basin lies some 2 to 4 km upstream from the originally anticipated upglacier limit of retreat, which was defined as the upstream limit (as determined before the publication of Rignot et al., (2013) of marine-grounded ice.

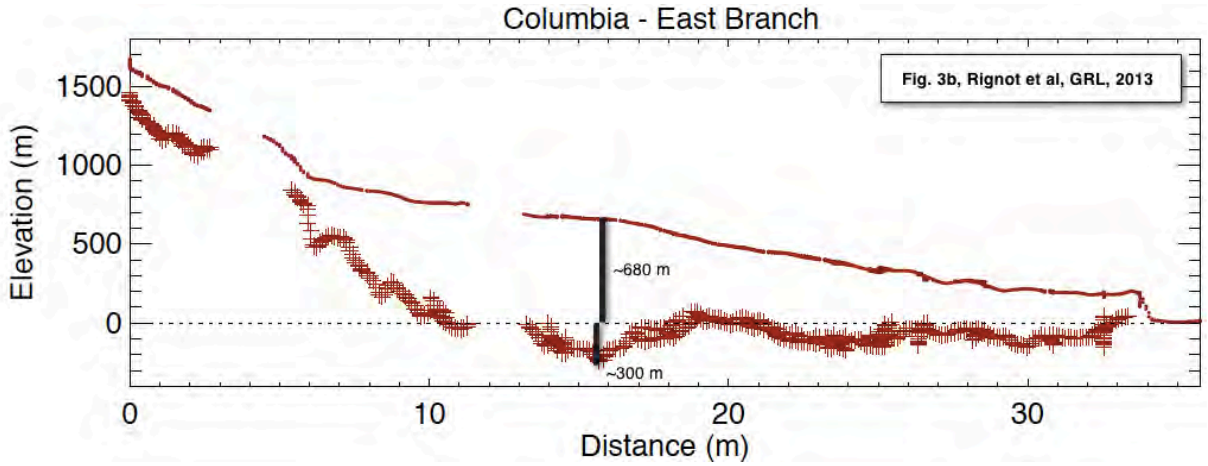

Figure 6. Along-flow profiles of surface elevation and basal topography at the East Branch of Columbia Glacier (from Rignot et al, 2013)

This basin may result in an extension of the glacier's retreat into the East branch for several years, as well as some interval of accelerated flow and increased calving. The timing of terminus retreat into this basin, and duration and magnitudes of accelerated flow and calving during the traverse of the terminus across the basin, are poorly constrained at this time, but several factors suggest that the response of the glacier to this overdeepening may not be large in magnitude or long in duration. These factors include a bedrock sill near or slightly above sea level at the downstream limit of the basin (at km 18-21 in Figure 6) and the fact that at 300 m depth, this basin is comparatively shallow. Further soundings are required to map the lateral extent of the sill; if there is continuous shallow barrier extending across the entire glacier channel, then the retreat will not easily be able to propagate beyond and into the basin. Furthermore, while the ice over the basin at present is very thick (ca. 1000 m), significant thinning will likely have occurred by the time the terminus reaches the basin, and conditions may be similar to conditions today, with modest calving rates.

The overdeepened basin may potentially extend the duration of retreat, and produce some brief (2 year or less) interval of increased flux and calving, but for the moment, we will not change the timing of the forecast retreat as given in our Report#2, pending further information on the basin geometry.

3. Synthesis

In this section of the report, we provide a qualitative synthesis of the current and future status of the retreat, including an evaluation of the potential for future changes in iceberg hazards. While qualitative and somewhat speculative, our synthesis is a compilation of expert opinion, formed over decades of studying the retreat at Columbia Glacier. We adopt language used by the Intergovernmental Panel on Climate Change (IPCC) to assign likelihood in a consistent fashion. The probabilities listed in Table 1 are not determined by calculation, but are estimates of probability assigned to statements to calibrate distinctions such as "likely" *vs*. "very likely."

Table 1. Likelihood Scale	
Term*	**Likelihood of the Outcome**
Virtually certain	99-100% probability
Very likely	90-100% probability
Likely	66-100% probability
About as likely as not	33 to 66% probability
Unlikely	0-33% probability
Very unlikely	0-10% probability
Exceptionally unlikely	0-1% probability

Table 1. IPCC uncertainty language (IPCC, 2013)

Two major shifts have occurred in the past decade in the characteristic calving flux and retreat rate of Columbia Glacier. The first shift, starting about 2006, was the release of the terminus from the constriction in the "Kadin-Great Nunatak Gap," (K-G Gap) when the terminus started a rapid retreat across the deep basin at the West/Main branch confluence. Between ca. 2001 and 2006, the terminus had been in a state of quasi-stability in the K-G gap, when ice flux and calving rate were extremely high but retreat rate low. The second shift started in late summer 2010, when another quasi-stable terminus position was established at the upstream end of the overdeepened basin at the West/Main branch confluence. Since 2010, the ice speed has slowed relative to earlier periods during the retreat, probably in response to thinning and alterations in subglacial hydrology. Current conditions at the terminus - low surface slope, shallow water depths, and thinner ice (but still well about the threshold value for dynamic instability) – all point to continued stability relative to earlier epochs. Radar and model data both agree that the bed remains shallow (with water depths nowhere exceeding ca. 200 - 300 m) from its current position to the tidewater limit, with a number of subglacial pinning points that will anchor the glacier bed, reducing ice speed and along-flow extension, both of which will reinforce stability.

While further modeling and analysis will help to clarify details and reinforce confidence in our conclusions, we judge that the evidence and analysis to date indicates that calving rates during the remaining 14-20 years (duration is **very likely**) of Columbia Glacier's retreat will fall below the levels observed during the 2006-2010 interval. The remaining retreat will **likely** be punctuated by short-lived (months to one year) episodes of increased flux and calving, but even during these episodes calving rates and berg size will **very likely** be less than the maximum values observed in the past.

Our analysis is informed by several data sources, several of which are discussed in detail above. TerraSAR-X radar interferometry provides measures of ice motion on the glacier. Ground-based time-lapse cameras help to fill velocity changes at finer spatial and temporal scales than are available from remote sensing. Several cameras placed at a variety of locations have been documenting changes in glacier motion, terminus position, and iceberg calving characteristics since 2004. Surface elevation on the glacier is derived from optical imagery (e.g. Worldview satellite) and airborne laser altimetry operated by the University of Alaska at Fairbanks. Model estimates of the glacier bed topography are given by McNabb et al., (2012), supplemented by airborne radio echo

sounding measurements (Rignot et al., 2013). The measurements show some important differences from the McNabb modeling, including the presence of thick ice and a marine-grounded basin on the East branch, located above the previously determined tidewater limit. However, further measurements are required to determine the effect this basin may have on future retreat (for example, whether the basin in closed or has a marine connection to the main forebay). Glacier seismicity as documented by The Alaska Earthquake Information Center (AEIC) also plays a role in our assessment. Their continuous monitoring of seismicity in Alaska shows that production of seismicity from Columbia Bay increased dramatically in late summer 2010, at the same time that the glacier terminus re-grounded and stabilized in shallow water. This is consistent with other regional observations, which show that glacier seismicity tends to be associated with tidewater glacier termini grounded in shallow water.

Our recent observations and analysis agree qualitatively with the best understanding of large-scale calving glacier behavior, as outlined, for example, by Amundson and Truffer (2010) and Post et al (2011). These papers describe how tidewater glaciers oscillate between “stable” and “very unstable” during the advance-retreat cycle, but rarely remain in quasi-stable, mid-retreat positions (as Columbia was in 2001-2006 and is now, to a lesser extent) for extended periods. While the retreat of Columbia Glacier terminus has slowed at various times since its onset in the early 1980s, other measures of retreat – rate of mass loss, for example – continued at high rates during these pauses, and nothing resembling a true return to stability has occurred. Long-term stability will be achieved only when the glacier retreats to the tidewater limit, where the bed rises above sea level. At the same time, as discussed above, calving and terminus retreat rates during the remainder of the retreat will **very likely** be smaller in magnitude that the larger episodes (e.g. during 2006-2010) in the past. Even though present-day dynamics are substantially reduced from previous levels, ice discharge remains elevated well above what would be considered stable. In its current state, Columbia Glacier remains one of Alaska’s fast-flowing, most rapidly changing glaciers in Alaska.

An outward sign of the trend toward stabilization is a change in the size and frequency of iceberg production. As stability increases, iceberg production becomes more frequent, uniform, and characterized by smaller bergs (reduced ice thickness at the calving terminus constrains the upper limit on iceberg size). Recent observations show this pattern. Estimates of ice flux to the terminus also support increasing stability. Ice delivery to the calving front has decreased by from peak values by at least a factor of 2, and calving rates are highly erratic (near stoppages of flow).

The final stages of our analysis are ongoing and involve completing the model representation of downfjord iceberg transport and passage over HBMS. Progress on this front is summarized in Appendix 1. Among the most significant factors influencing the fate of icebergs entering the forebay at the glacier’s retreating terminus is the increasing length of forebay and increasing water temperature, both of which exert first-order control on iceberg melt and degradation. Although data are spatially sparse for Prince William Sound, the GAK 1 Buoy near Seward shows a long-term warming trend. Given that fjord circulation involves density gradient driven or “ baroclinic pumping” of water over the sill and circulating it inside the fjord, it is **likely** that ice cliff melting and

berg melting have increased and will continue to increase throughout the remainder of the retreat. Taken together with the reduced initial berg size, the probability of surviving the passage down the entire forebay and the size of icebergs that do make it all the way to HBMS are both declining. On the other hand, smaller mean berg size at HBMS will increase the fraction of bergs passing over the shoal and into Prince William Sound.

Growlers (icebergs with freeboard height of < 1 m) present one of the greatest hazards to shipping traffic, and are hard to detect with radar. Time lapse imagery shows a decrease in berg size from prior to 2006 to 2010, potentially suggesting that more small bergs could be escaping from the fjord. However, the effect of this change on berg sizes in Prince William Sound should have been apparent by now. Analysis of the SERVS ice radar reports may show whether this change was apparent in the tanker shipping lanes. Our top remaining research priorities include characterization of berg melt and degradation in the forebay and passage of bergs over HBMS. Ongoing work on these tasks is summarized in Appendix 1.

4. Summary

In this third report to the RCAC we include a qualitative but informed, expert synthesis of the retreat state. Our primary findings to date include:

- Ice concentrations inside the moraine are higher than expected, but the moraine continues to block most ice from exiting. Although Columbia Glacier still produces some of the larger bergs in the state, the extremely large calving events that were commonly produced in the early 2000s no longer occur due to shallow water conditions at and upstream of the present-day terminus. It is **very unlikely** that extremely large calving events will occur in the future.
- Several processes interact to reduce both the chances of iceberg survival all the way to HBMS and mean size of survivors at arrival at HBMS.
- A new region of ~1km thick ice, grounded in water 200-300 m deep, was discovered in the upper East branch. This ice does not have clear marine-grounded route of access to the forebay necessary to result in another rapid discharge episode, but it is **likely as not** that ice stored here will prolong the duration of overall retreat.
- Delivery of ice by glacier flow to the calving front is declining. We expect that future short-lived episodes of moderately increased flux are **likely**, but prolonged episodes and high calving fluxes are **unlikely** to return to historic levels.
- Time-stamped image sequences that were fundamental to building our understanding of current conditions are being delivered with this report.

Work continues on the more quantitative aspects of the assessment. In particular we continue to 1) develop a quantified iceberg-size distribution, 2) develop a downfjord iceberg-transport model 3) compile a self-consistent analysis of the long-term retreat including terminus position, velocity and geometry changes to identify mechanisms influencing the pace of retreat. The importance of continued funding for TerraSAR-X

imagery cannot be understated as these data ensure that we can continue to measure ice flux, and berg distributions at high space and time resolution in the future

Our work to date has illustrated some important processes ongoing at the Heather Island Moraine. Of particular importance is rapid uplift of the region that is apparent from sparse GPS observations. We are working on establishing a collaboration with UAFs Jeff Freymeuler to assess tectonic uplift. This will be introduced as a new component of the research during spring 2014.

5. References

Amundson, J. M. & Truffer, M. A unifying framework for iceberg-calving models. *Journal of Glaciology* **56,** 822–830 (2010).

Campbell, R.W. PWS Herring survey: Plankton and oceanographic observations. Exxon Valdez Oil Spill Restoration Project Final Report (Restoration Project 10100132A), Prince William Sound Science Center, Cordova, Alaska. (2013)

Echelmeyer, K. A. & KAMB, B. Stress-gradient coupling in glacier flow. II: Longitudinal averaging in the flow response to small perturbations in ice thickness and surface slope. *Journal of Glaciology* **32,** 285–298 (1986).

Kamb, B. *et al.* Mechanical and hydrologic basis for the rapid motion of a large tidewater glacier: 2. Interpretation. *J. Geophys. Res.* **99,** 15231 (1994).

Kamb, B. & Echelmeyer, K. Stress-gradient coupling in glacier flow. I: Longitudinal averaging of the influence of ice thickness and surface slope. *Journal of Glaciology* **32,** 267–284 (1986).

Kamb, B. & Echelmeyer, K. A. Stress-gradient coupling in glacier flow: IV. Effects of the‘ T’ term. *Journal of Glaciology 32, 342-349* (1986).

Krimmel, R. M. Photogrammetric data set, 1957-2000, and bathymetric measurements for Columbia Glacier, Alaska. US Geological Water-Resources Investigations Report 01-4089 (2001).

Hock, R., O'Neel, S. & Rasmussen, L. A. Using surface velocities to calculate ice thickness and bed topography: a case study at Columbia Glacier, Alaska, USA. *Journal of Glaciology* **58,** 1151–1164 (2012).

Meier, M. F. and A. Post, Fast tidewater glaciers. *J. Geophys. Res.* **92,** 9051 (1987).

Meier, M. *et al.* Mechanical and hydrologic basis for the rapid motion of a large tidewater glacier: 1. Observations. *J. Geophys. Res.* **99,** 15219 (1994).

O'Neel, S., Pfeffer, W. T. & Krimmel, R. Evolving force balance at Columbia Glacier,

Alaska, during its rapid retreat. *J. Geophys. Res.* **110**, F3 (2005).

Post, A., O'Neel, S., Motyka, R. J. & Streveler, G. A complex relationship between calving glaciers and climate. *Eos, Transactions American Geophysical Union* **92,** 305 (2011).

Rignot, E. et al., Low-frequency radar sounding of temperate ice masses in Southern Alaska*., Geophys. Res. Lett*. (2013)

APPENDIX
Analysis and Materials Update

A1. Measuring iceberg distribution in the fjord

The most comprehensive source of information available about ice conditions throughout the full length of Columbia Bay is a series of high-resolution (1.8 meter pixel) TerraSAR-X images acquired on 11 to 22 day intervals since February 2011. Quantifying the distribution of icebergs as a function of distance from the terminus is a key first step towards developing a model of iceberg transport.

Results from our preliminary efforts to extract individual icebergs from the October 12, 2013 TerraSAR-X image are shown in Figure A1. As expected, iceberg size and density decline with distance from the terminus, the individual icebergs melting and fracturing on their journeys from the glacier terminus to the moraine shoal. Furthermore, the iceberg sizes follow a power law distribution, as predicted by percolation and particle models of ice calving (e.g. Bahr, 1995; Astrom et al., 2013).

Our image processing strategy, the results of which are shown in Figure 2A and 3A, leverages the brightness of ice and darkness of water in radar images, then makes additional assumptions about shape and texture to further filter the results. Particular care must be taken to not misinterpret swaths of mélange ice as huge individual icebergs.

Since iceberg production and transport cannot be assumed to be in steady state, results from one image are not necessarily representative, and we plan to repeat the same analysis over the full satellite time-series. Furthermore, since the 11 to 22 day time resolution is not be sufficient to resolve the residence time of individual icebergs, the Heather Island (HI), Divider (AK10), and Kadin (AK01) time-lapse cameras will be used to estimate the residence time of icebergs in the fjord and couple instances of iceberg production at the terminus to iceberg transport over the moraine.

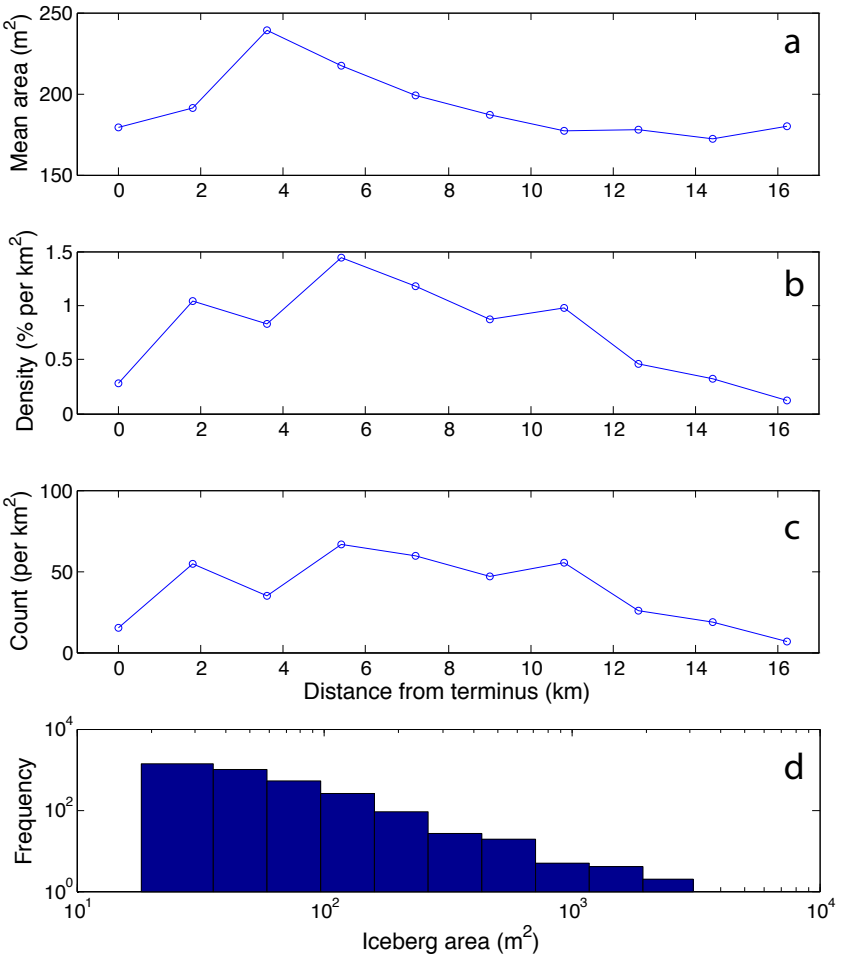

Figure A1. Summary statistics of Columbia Bay icebergs from the October 12, 2013 TerraSAR-X image: (a) mean iceberg surface area, (b) percent of fjord covered by icebergs, (c) number of icebergs per km^2, and (d) log-log histogram of iceberg surface area.

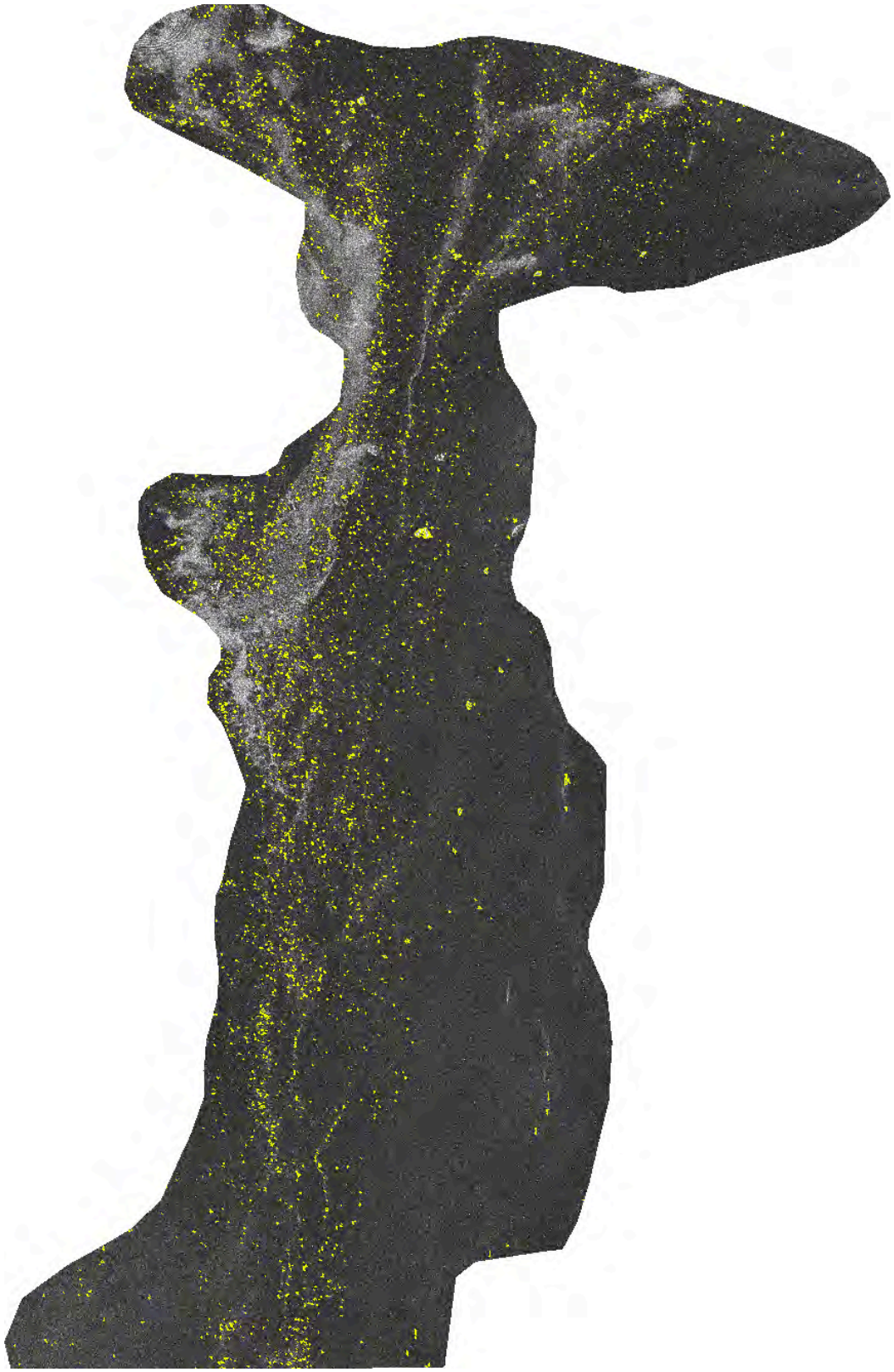

Figure A3. TerraSAR-X intensity image from October 12, 2013 overlaid with the boundaries of the icebergs detected by automated image processing.

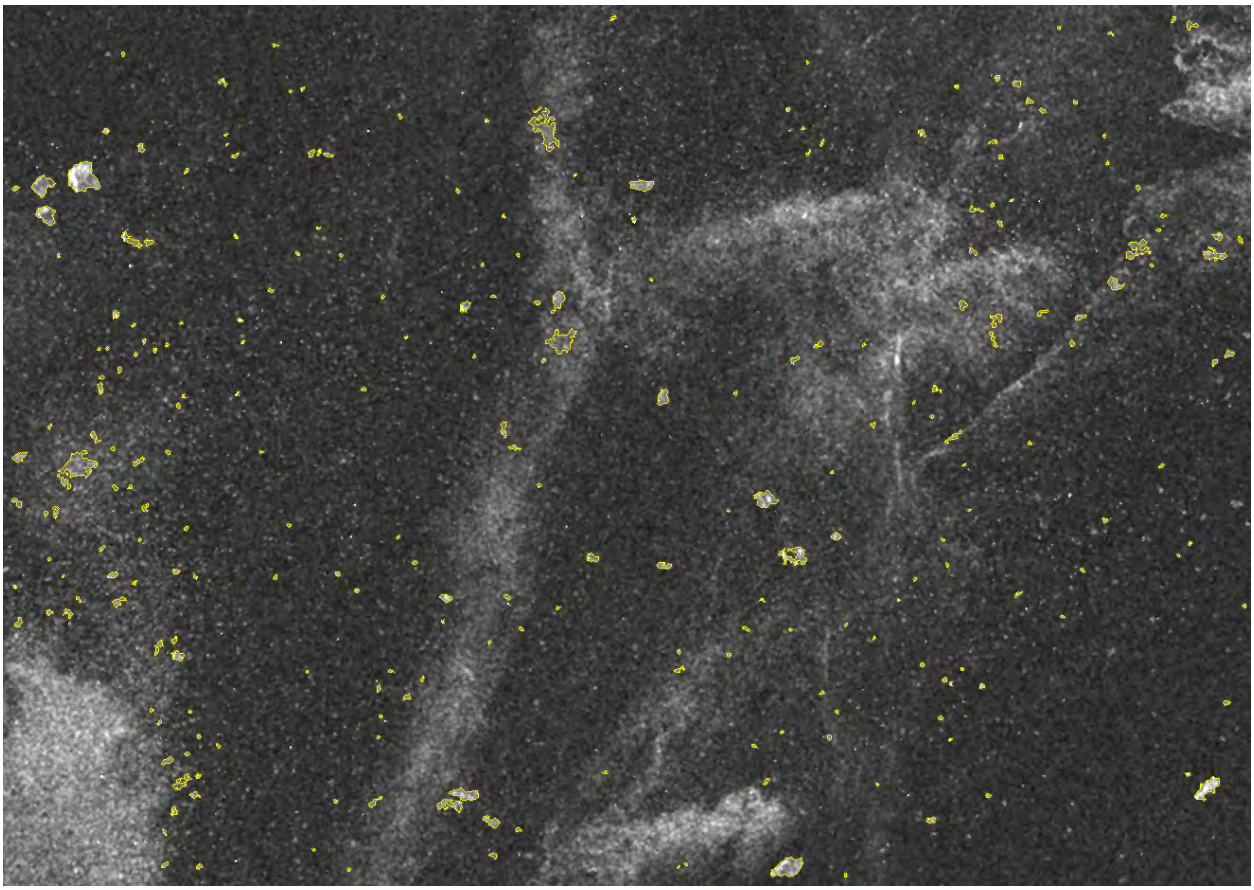

Figure A3. Detail view of the TerraSAR-X intensity image from October 12, 2013 showing the boundaries of the icebergs detected by automated image processing.

A2. Calving event size and time distributions

Over the course of 16 days in June 2005, Shad O'Neel and others watched the calving terminus of Columbia Glacier, recording the time, type, and magnitude of 828 individual events. Of these, 20 were photographed in such a way that the volume of calved ice could be estimated. The resulting size distribution is shown in Figure A4, and approximates a power-law distribution, suggesting that the calving process is scale-invariant. The glacier is capable of calving icebergs of all sizes, limited only to the size of the system itself, from small, frequent subaerial “avalanches” on the order of 100 m^3 to an enormous, very rare 10^8 m^3 event in which the entire terminus broke off at once (to this day the largest event ever observed at Columbia Glacier).

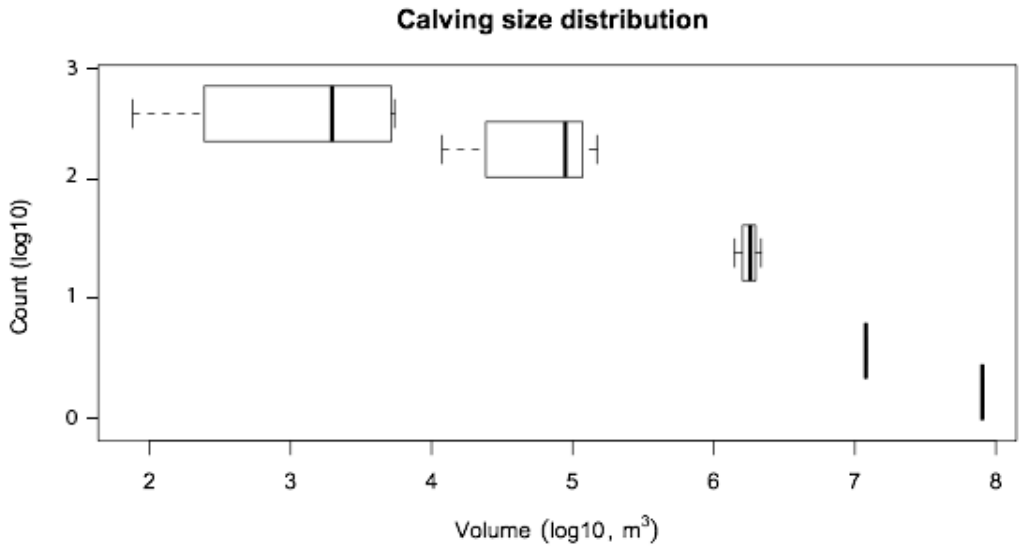

Figure A4. Calving event size distribution estimated from in-situ observations and photographs collected over 16 days in June 2005.

In 2005, the glacier was (just barely) grounded to the bed, a situation that the glacier finds itself in again presently, albeit with thinner ice and shallower water. By summer of 2009, much of the terminus was floating and the glacier reached its highest rate of *area loss* ever observed (as opposed to total *calving flux*). This transition from grounded to floating (and back to grounded) is illustrated in Figure A5.

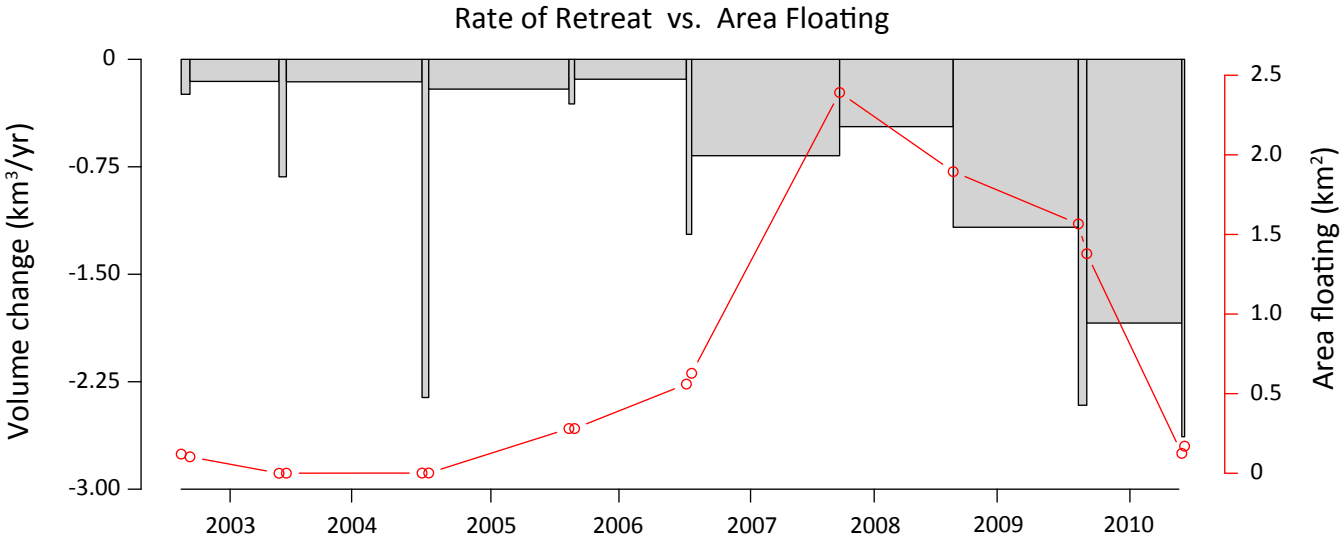

Figure A5. Increase in the rate of retreat following the transition from grounded to floating (and back to grounded) from 2003 to 2010.

As described in Walter et al. (2010), the transition marked a change in calving behavior, from smaller, more frequent calving events while grounded, to fewer and larger calving events while floating. The glacier's floating tongue disintegrated primarily through a sequence of enormous, tabular calving events.

In May to June 2009, a high-speed time-lapse camera was deployed, photographing the terminus every 45 seconds nearly continuously for 23 days – a sequence of 26,719 images ideal for resolving individual calving events. Comparisons of these two calving time-series, 2005 and 2009, confirm and build on our earlier understanding of the differences between the two regimes:

- Huge events were more than twice as frequent during flotation (2009) as they were when the glacier was grounded (2005), even though calving events were as little as half as frequent overall.

- Calving events in 2005 were 25% less likely to occur during low tide than during rising, high, or falling tide, a difference that disappeared in 2009. When the terminus is afloat, tide is expected to have little impact on stability, while when the terminus is very close to the flotation thickness (dH ~ 10m in summer 2005), tide may matter more to calving. Figure A6 illustrates the significance of the tidal period to calving in 2005. Unfortunately, the series is not long enough to potentially resolve longer tidal periods. No peak is present in an equivalent analysis for 2009.

- The time between intervening calving events are, like the size distribution, found to approximate a power law (Figure A7). The results are very similar for both years, but suggest that shorter intervals were more common, and longer intervals less common in 2005, as expected.

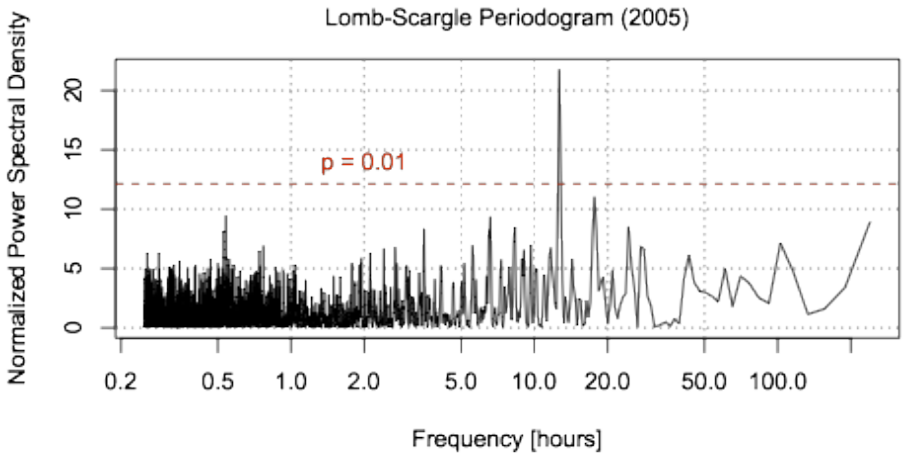

Figure A6. Lomb-Scargle periodogram of the 2005 calving time-series showing a statistically significant peak at 12.7 hours (0.529 days).

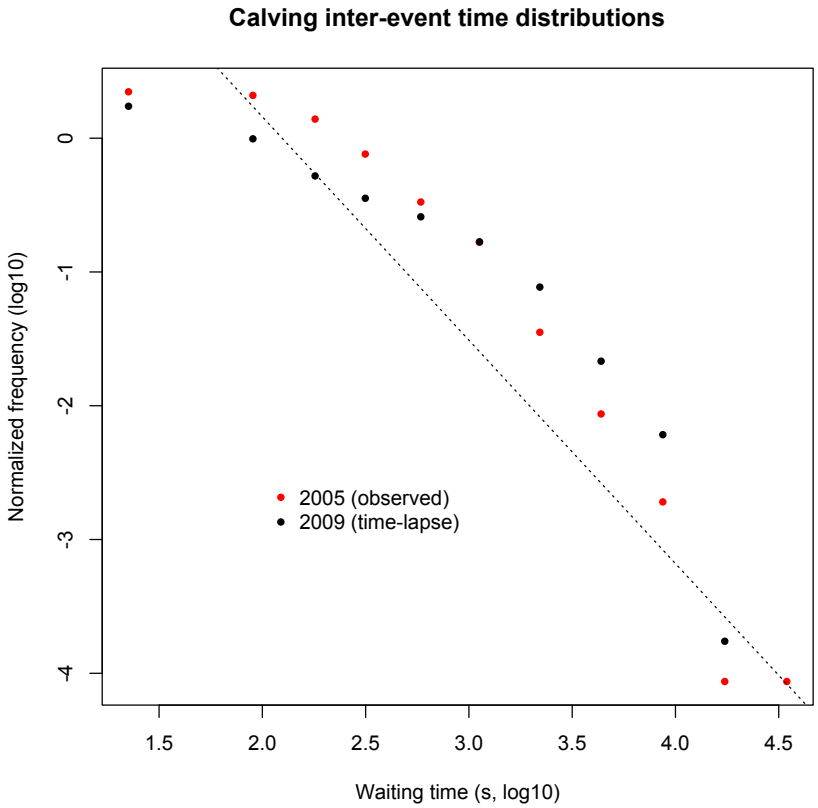

Figure A7. Distribution of inter-event waiting times between consecutive calving events at Columbia Glacier in summer 2005 (red) and summer 2009 (black). The dashed line represents the power law exponent (-1.67) predicted by the discrete particle model developed by Jan Astrom and other (2013). Comparisons between modeled and observed scaling laws in glacier calving are the subject of an upcoming paper O'Neel, Welty, and others are co-authoring with Astrom.

A3. Recovery of historic materials

In 1978-1985, a 16mm film camera maintained by the U.S. Geological Survey (under the direction of Robert M. Krimmel) photographed the glacier front once every hour for seven years (Krimmel and others, 1985). To our knowledge, this is the earliest time-lapse of a tidewater glacier ever produced, but sadly only a tiny fraction of the original film has been found. However, early-production 16mm reels of the video produced by the USGS from the time-lapse footage (which includes only the best frame from each day) have been recovered from both the USGS Washington Water Science Center in Tacoma and the Western Region Offices in Menlo Park, California. One of the best among these has been scanned at 2K (2,000 pixels wide) by Video Producer Don Becker at the USGS Federal Center in Denver, Colorado, paid for by a USGS digital archiving grant. For the first time, this remarkable sequence of images is available to us for analysis. Two of the digitized frames are shown in Figure A8.

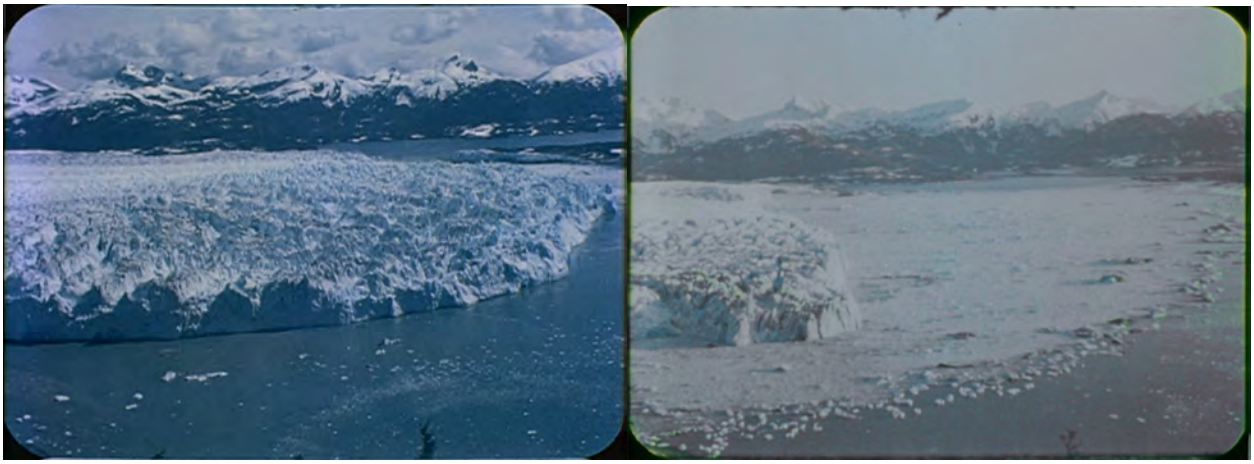

Figure A8. Example frames from the USGS time-lapse sequence, illustrating the onset of the retreat between 1979 and 1983.

References

Åström, J. A., Riikilä, T. I., Tallinen, T., Zwinger, T., Benn, D., Moore, J. C., and Timonen, J. (2013), A particle based simulation model for glacier dynamics, The Cryosphere, 7, 1591-1602, doi:10.5194/tc-7-1591-2013.

Bahr, D. B. (1995), Simulating iceberg calving with a percolation model, J. Geophys. Res., 100(B4), 6225–6232, doi:10.1029/94JB03133.

Krimmel, R. M., Taylor, P., and Barber, P. (1985). Time Lapse Observations of the Columbia Glacier, Alaska. 16mm. Tacoma, Washington: U.S. Geological Survey.

Walter, F., S. O'Neel, D. McNamara, W. T. Pfeffer, J. N. Bassis, and H. A. Fricker (2010), Iceberg calving during transition from grounded to floating ice: Columbia Glacier, Alaska, Geophys. Res. Lett., 37, L15501, doi:10.1029/2010GL043201.

W.T. Pfeffer Geophysical Consultants, LLC

2 October 2014

Report to Prince William Sound Regional Citizens' Advisory Council: Future Iceberg Discharge from Columbia Glacier, Alaska

Reference PWSRCAC Project #8551
Contractor: W. T. Pfeffer Geophysical Consultants, Nederland, Colorado

Report #4

1. Objective

Based on new analysis, evaluate and report on whether ice in the East Branch could be evacuated rapidly and whether any changes to the estimates established in previous reports will be necessary.

2. Introduction

Tidewater Limit *vs.* Grounding Line. The location where the bed of an ocean-ending glacier rises above sea level is referred to as the "tidewater limit." The location where the bed of a *floating* ocean-ending glacier comes in contact with the ocean floor is referred to as the grounding line. These terms are often used interchangeably despite referring to quite different things. We use the terminology *tidewater limit* here. It is the point at which the retreating terminus of a grounded ocean-ending glacier will lose contact with the ocean. It is also the upstream limit of direct influence of the ocean on the glacier's mechanics and hydrology when the glacier is extended past the tidewater limit, although the terminus region can then still communicate with the glacier above the tidewater limit through the glacier's internal hydrology.

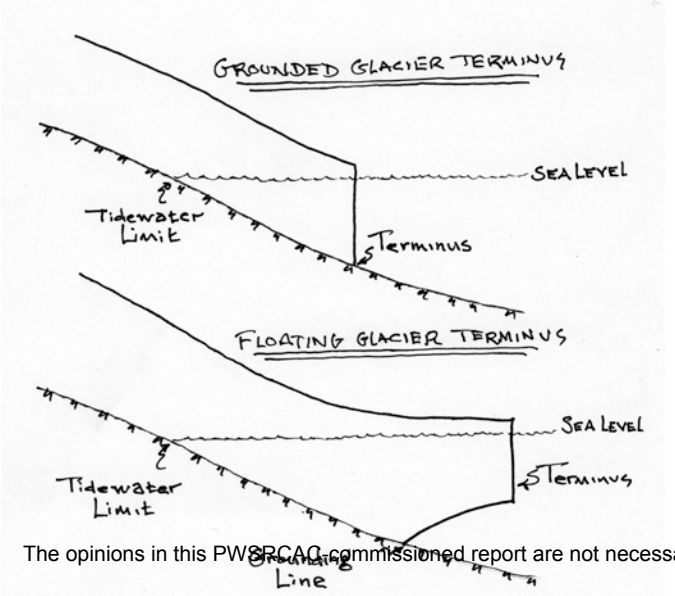

Several new pieces of information concerning Columbia Glacier's subglacial topography came to our knowledge around the time of the release of Report #3 and subsequently. These include the Rignot et al (2013) WISE airborne radar soundings noted in Report #3, seismic surveys of marine sediments near and downstream of the present terminus, and the continued calving retreat of the glacier's West Branch well past the location previously believed to the tidewater limit.

These three factors lead us to believe that the basal topography calculated by McNabb et al (2012) underestimates the depth of true bed throughout, and that the glacier's East Branch in particular (see Figure 1) is substantially deeper than previously indicated. This would result in more ice being stored in the East Branch basin, and provide a source for rapid release of icebergs under the right circumstances. The relevant information

is fairly fragmentary, so the revisions presented here are necessarily rather approximate. A more complete airborne radar survey, coordinated with us, would give us the necessary information, but to our knowledge the operators of the WISE airborne radar have no further plans to fly in Alaska. In the analysis that follows we attempt, as we have done previously, to construct two or more outcomes that bracket the likely actual event.

3. New Information

Knowledge of a tidewater glacier's subglacial topography is fundamental to predictions of the glacier's future behavior, but it is also the most difficult geometric parameter to observe directly. Basal topography in the distal portion of the glacier resting on bedrock below sea level is particularly important for predicting rapid calving and retreat, just as has occurred at Columbia Glacier from the early 1980s to the present. At the time of our earlier reports, our best knowledge of the glacier bed still occupied by ice was the McNabb et al. (2012) 100 m-resolution full glacier bed, modeled from velocity data (Figure 1). But three new findings have cast doubt on the validity of the McNabb bed, and suggests that our earlier projected timing and magnitude of ice discharge require some revision. The most significant changes appear to be in the glacier's East Branch, and our revisions are limited to this region. Of the three new data sources described below, two (West Branch retreat and Post-retreat sedimentary infill) provide evidence that the McNabb bed is flawed, while the third (Airborne Radar Soundings in East Branch) gives new (but incomplete) observational constraints on the bed depth in the East Branch.

a. **West Branch Retreat:** Columbia Glacier's West Branch has always been assumed to be grounded above sea level immediately upstream from the West/Main Branch confluence and therefore not subject to the dynamic instability responsible for the rapid retreat in the Main Branch channel. Following the separation of the West and Main Branches in 2009, the stability of the West Branch terminus was consistent with this assessment. However, over the past year the West Branch terminus abruptly retreated 2.5 - 3 km, well beyond the previously assigned location of the tidewater limit, demonstrating that the bed here is substantially deeper than the McNabb model results suggest (Figure 2).

b. **Post-retreat Sedimentary Infill:** Recent seismic surveys by Boldt et al. (in prep) have found $3.2 \pm 0.6 \times 10^8$ m^3 of fine-grained sediment in the glacier forebay, from 50 to 100 m thick in places (Figure 3). The post-retreat bathymetry in the forebay seaward of the retreating terminus is this shallower than the bathymetry when the forebay was occupied by ice. Subglacial topography inferred from velocity/continuity calculations, as done by McNabb et al (2012), O'Neel et al (2005), and others, used the post-retreat bathymetry as an initial condition, and their calculated subglacial topography is accordingly biased, probably toward shallower depths. Again, this consideration suggests that the McNabb bed, throughout the glacier but on the East Branch in particular, is anomalously shallow.

c. **Airborne Radar Soundings in East Branch**: Newly released radar soundings by Rignot et al. (2013) from the Warm Ice Sounding Explorer (WISE) suggest an average 100 m deeper bed overall, and a previously undetected overdeepening in the fjord up the East Branch. This new data indicated the presence of ice up to 900 m thick lying in 250 m deep water in the East Branch. Given the evidence if the West Branch retreat and the forebay sedimentation, we are inclined to accept Rignot's depths over the McNabb calculated bed at this point.

Since the Rignot radar traces are sparse and located in less-than-optimal locations, we cannot say with confidence what the East Branch subglacial topography is, but we can use the Rignot data as a constraint to estimate both the increased ice volume in the East Branch and to get a rough idea of the potential dynamic instability arising from the bed topography between the present terminus and the revised (Rignot) East Branch tidewater limit. We summarize these estimates in the next section.

4. Preliminary Analysis

In addition to differing depths, the McNabb bed and Rignot profiles conflict in shape as well, and no comprise geometry can be found that satisfies both sources. Nevertheless, we can make a rough estimate of the East Branch ice volume consistent with a channel with the general shape of McNabb's bed but the depth of the Rignot profiles. Using this compromise, we estimate the East Branch ice volume between the Rignot tidewater limit. This volume, using the deeper Rignot bed, is roughly 33 km^3. The volume of ice between the McNabb bed and the Rignot bed as is roughly 15 km^3. The deeper Rignot profile thus entails approximately 15 km^3 more ice than the McNabb bed. At recently observed flux rates of ~ 2 km^3 yr^{-1}, this *additional* ice would be evacuated in ca. 7 to 8 years.

There are two issues to be resolved in predicting the consequences of the deeper East Branch bed. The first of these is the additional ice volume in the East Brach, and in the absence of better and more complete radar bathymetry, the estimates above (33 km3 total) can't be improved upon much. The other issue is the increased likelihood of rapid dynamic discharge from the deeper East Basin. Useful predictions of this aspect require 1) an estimate to the time that rapid discharge will commence, 2) an estimate of the ice volume remaining at that time that is vulnerable to rapid evacuation, and 3) an estimate of ice flux during rapid evacuation. Again, without more complete knowledge of the subglacial topography, these questions can't be precisely addressed, but some simple estimates are possible.

4.1) Time to onset of rapid discharge. Using the instability criterion of Pfeffer (2007), rapid retreat is only possible in those reaches of the East Branch grounded below sea level (show in Figure 6 as regions 1 and 2), and the onset of rapid retreat starts if the ice thickness declines to a certain fraction of the water depth. (The critical ratio, given by model parameters discussed in Pfeffer (2007), is $H_{ice}/H_{water} \approx 1.85$.) This critical thickness is shown as a dashed

blue line in both regions 1 and 2. For region 1, the ice surface height must fall ca. 120 m to 89 m above sea level; for region 2, the surface ice height must fall ca. 500 m to 150 m above sea level. At nominal thinning rates of ca. 20 m yr^{-1}, the time to the critical thickness would be ca. 6 years for region 1 and 25 years for region 2. The future thinning rate in the East Branch is highly uncertain, but on this simple basis, it is reasonable to expect that rapid retreat in these regions could start in ca. 5 years and persist for ca. 15-20 years. Note, however, that rapid retreat will be terminated when regions 1 and 2 are exhausted of ice, which may tale less than 20 years. We will see below that this is likely the case.

4.2) Estimate of ice vulnerable to rapid evacuation. Using the mean ice thickness of regions 1 and 2 at H_{crit} of ~ 250 m, the combined length of the regions of 1.75 km (here the entire span from the downstream edge of region 1 to the upstream edge of region 2), and an estimate of the glacier width at that time of 1 km, the resulting volume is the product of these dimensions, or 0.44 km^3. Note that this is a small fraction of the total ice volume in the East Branch.

4.3) Ice flux during evacuation. Many variables come into play here, and a robust calculation is out of reach, again, without better geometric information; even then, most assessments will rely on comparisons to previous stages of Columbia's retreat. Here, typical ice velocity during other stages of rapid retreat is used to calculate the lifetime of the 0.44 km^3 of ice estimated above, and alternatively, the lifetime is allowed to vary and the corresponding ice flux is calculated.

4.3a. Assume terminus flow speed is 10 m d^{-1}. This is a typical speed for modest rapid retreat seen elsewhere on Columbia Glacier. At the reduced size for rapid retreat, ice would pass through a cross-sectional area of roughly (1 km wide x 250 m thick) = 0.25 km^2, resulting in an ice flux of 0.0025 km^3 d^{-1}. At this flux, the 0.44 km^3 reservoir would be exhausted in ca. 180 days.

4.3b. Vary lifetime of rapid retreat as a parameter. If the duration of rapid retreat varies, the ice flux will vary inversely with it. Using the vulnerable volume of 0.44 km^3 as a fixed parameter, the ice flux is calculated for several choices of lifetime of rapid evacuation, and shown in this table:

Ice flux during rapid evacuation for given lifetime. Ice reservoir fixed at 0.44 km^3.				
Lifetime of rapid evacuation (y)	0.25	.05	1	2
Ice Flux (km^3 $year^{-1}$)	1.76	0.88	0.44	0.22

5. Summary. Without a more completely and carefully planned aerial radar survey a more robust and quantitative analysis of the effects of the added ice volume and greater ice depths

is not feasible. On the basis of the simple constraints described here, however, it appears that the effects in terms of extending the time of Columbia Glacier's retreat are moderate and ice flux from the East Basin will be increased only slightly and will likely be short in duration. The principal findings above can be summarized as follows:

- The ice volume in Columbia Glacier's East Branch is now estimated to be 33 km^3, an increase of ca. 15 km^3 over the ice volume as calculated by McNabb et al (2012).
- At rates of ice flux typical of Columbia Glacier in recent years, the added 15 km^3 will extend the depletion of the East Branch by 7 or 8 years beyond our earlier estimates for this part of the glacier. Note that the retreat of Columbia Glacier's Main Branch may exceed this time; this is not an extension of the overall time to final stability of the entire glacier.
- Assuming a nominal thinning rate of 20 m y^{-1}, the ice thickness in the portions of the East Branch grounded below sea level will reach the critical thickness H_{crit} required for rapid evacuation of ice in approximately 5 years, and rapid evacuation of this additional ice could last as long as 20 years, although depletion of the East Branch reservoir may occur before then.
- Only ca. 0.44 km^3 of ice is located in the deeper portions of the East Branch and below the thickness H_{crit} required for rapid evacuation.
- A very rough estimate of the time to evacuate 0.44 km^3 of ice from the vulnerable portions of the East Branch varies from 3 months to 2 years, with corresponding flux rates ranging from 1.76 to 0.22 km^3 y^{-1}. Again, this timing refers to the East Branch only.

Finally, because of the comparatively thin ice and shallow water in the East Branch, icebergs calved here are likely to be small. This consideration, combined with the fact that the deep basins of the East Branch lie some 15 km upstream from the present terminus position, suggests that any icebergs calved during rapid evacuation of the East Branch basin will be very small or may have melted altogether by they time they reach the Heather Bay Moraine Shoal. The ultimate effects on iceberg hazards in Columbia Bay as therefore probably minimal. One important aspect that should be considered further, however, is the potential for the East Branch to produce bergs in the growler-and-smaller size classes for an extended period at some point, possibly 5 to 15 years in the future.

References

Rignot, E., Mouginot, J., Larsen, C. F., Gim, Y., & Kirchner, D. (2013). Low-frequency radar sounding of temperate ice masses in Southern Alaska. Geophysical Research Letters, 40(20), 5399–5405. doi:10.1002/2013GL057452

Mcnabb, R. W., Hock, R., O'Neel, S., Rasmussen, L. A., Ahn, Y., Braun, M., Conway, H.,

Herried, S., Joughin, I., Pfeffer, W.T., Smith, B., and Truffer, M. (2012). Using surface velocities to calculate ice thickness and bed topography: a case study at Columbia Glacier, Alaska, USA. Journal of Glaciology, 58(212), 1151–1164. doi:10.3189/2012JoG11J249

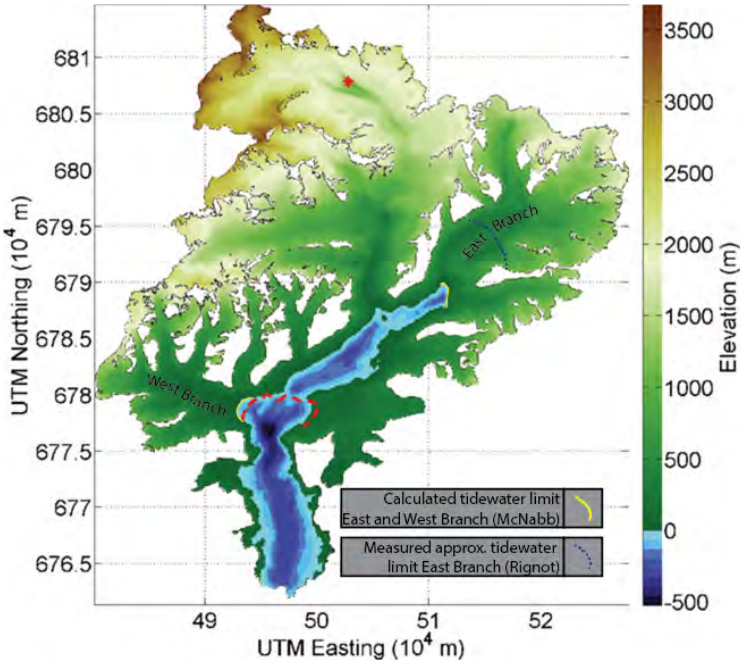

adapted from McNabb et al (2012)

Figure 1: McNabb Calculated Bed – Calculated bed topography from McNabb et al. (2012) showing tidewater limits from both McNabb and Rignot (2013).

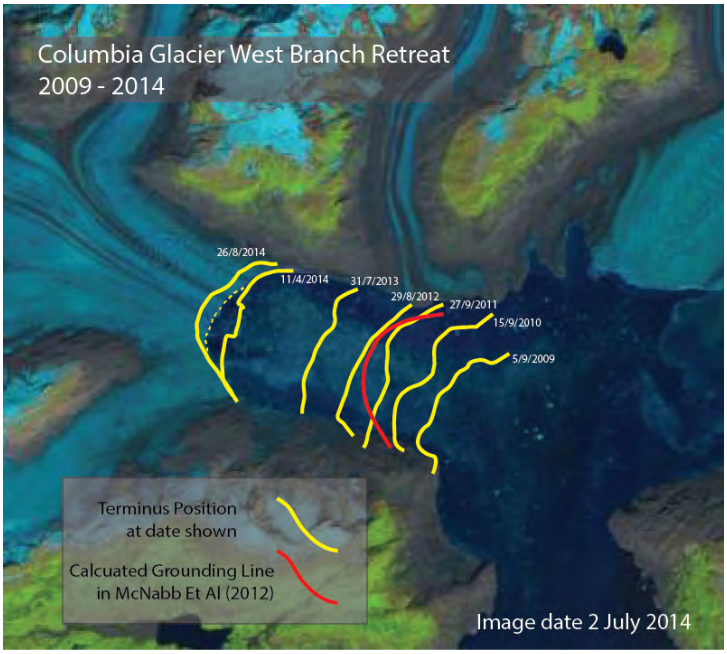

Figure 2: West Branch Retreat – Positions of the West Branch terminus 2009-2014, in yellow, extending well past the grounding line as calculated by McNabb et al. (2012), in red.

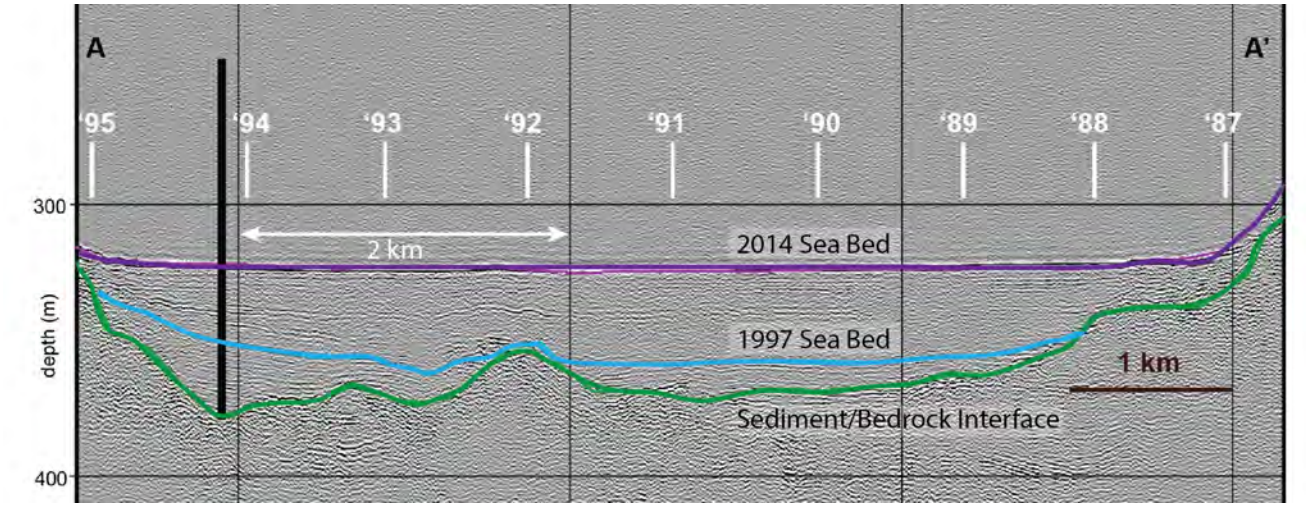

Figure 3: Forebay Sediment – Elevation of the bed (the water-sediment interface) in 1997 and at present (~ 2011), and the sediment-bedrock interface according to seismic surveys by K. Boldt and colleagues from the University of Washington in 2011. The profile runs down the main channel from just seaward of the Kadin-Great Nunatak Gap to the pre-retreat terminus.

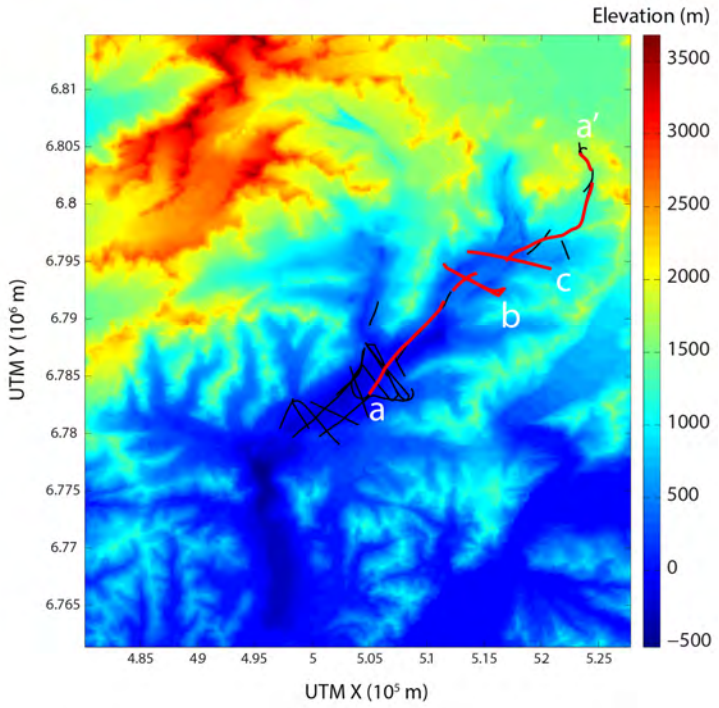

Figure 4: Radar Flight Lines – Warm Ice Sounding Explorer (WISE) radar flight lines from Rignot et al. (2013) on a map of calculated bed elevations from McNabb et al. (2012). The red highlighted profiles are those of (a), (b), and (c) plotted in Figure 5.

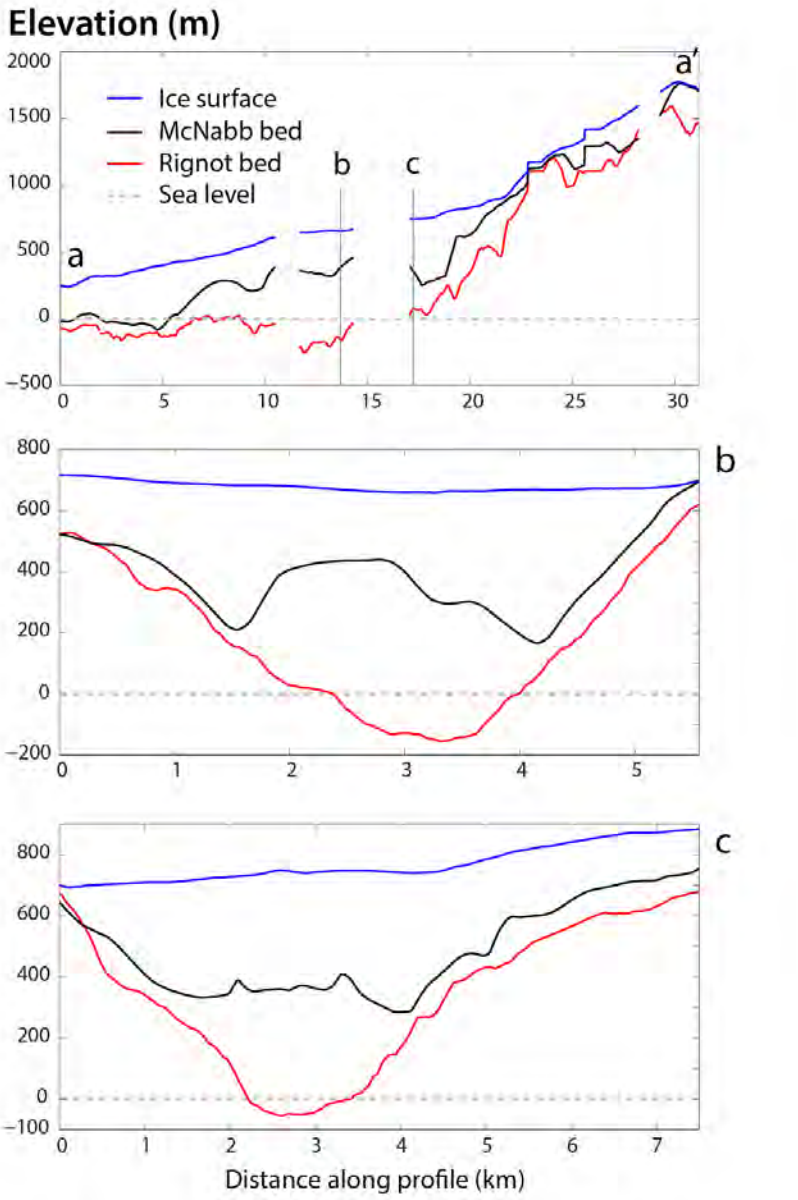

Figure 5: Radar Profiles – Radar (Rignot et al. 2013) and modeled (McNabb et al. 2012) bed elevations plotted alongside ice surface elevation and sea level for the profiles (a), (b), and (c) shown in Figure 4.

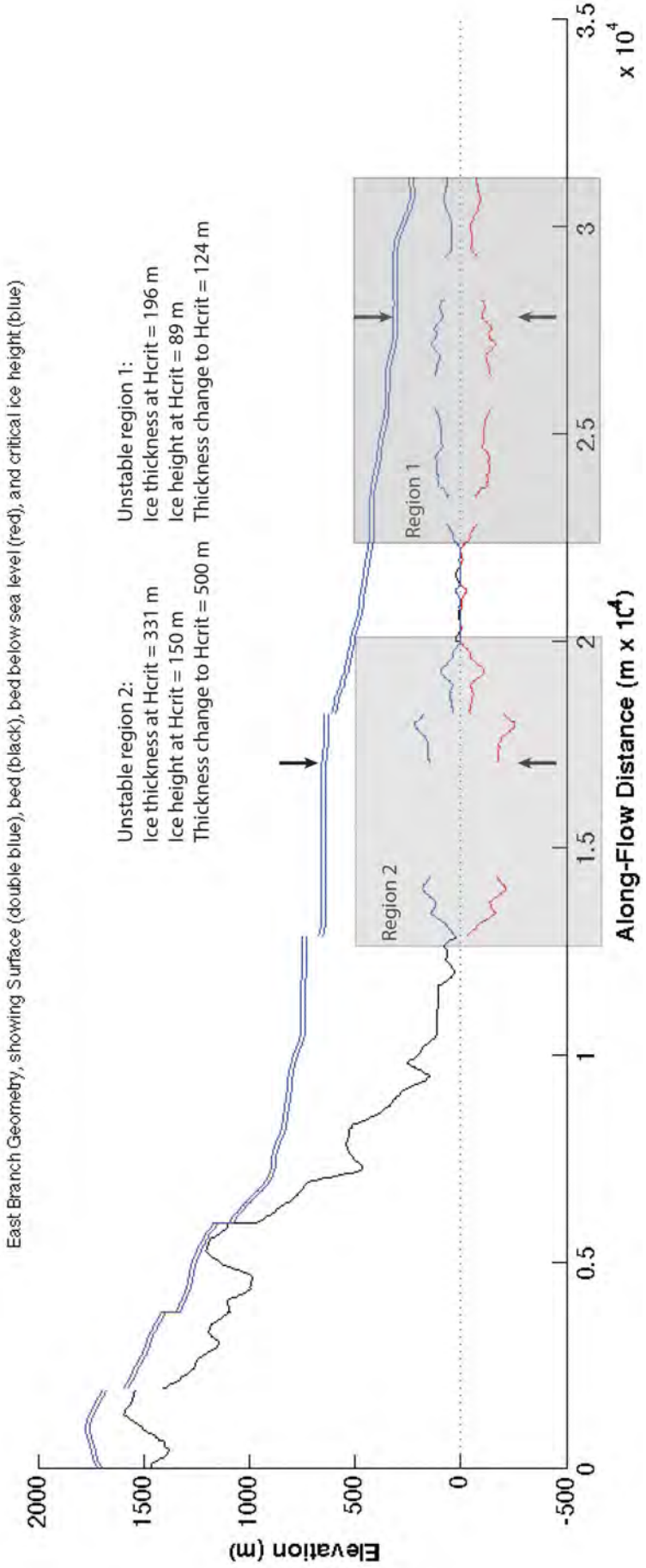

Figure 6: Geometry of East Branch along a-a' transect (Figures 3 and 4). The bed elevation falls below sea level in regions 1 and 2, allowing unstable retreat to occur here. The critical thickness for instable retreat, h_{crit}, is a function of water depth, and is plotted as the blue dotted line in the two regions. Important representative values for the two regions are shown.

W.T. Pfeffer Geophysical Consultants, LLC

2 October 2014

Report to Prince William Sound Regional Citizens' Advisory Council: Future Iceberg Discharge from Columbia Glacier, Alaska

Reference PWSRCAC Project #8551
Contractor: W. T. Pfeffer Geophysical Consultants, Nederland, Colorado

Report #5

1. Objective (from PSA Change Order 3, dated 14 August 2014): "Deliver Report on findings of terminus dynamics evaluation and whether any changes to the estimates established in Report 3 (11 December 2013) will be necessary"

2. Summary Findings: Field observations in October 2014 suggest that an episode of rapid calving and retreat further into the Main Branch is approaching, within 5 years but more likely within 1 year. This marks the incursion of the Main Branch terminus into the ice in the Main Branch Basin, analyzed in Report 1, Part II, but not necessarily the onset of complete evacuation of the Main Branch Basin. Most likely temporary pinning points and stable positions will punctuate this retreat. The analysis of ice in the East Basin is unchanged since Report 4 (October 2014). Iceberg sizes and rates of delivery to Heather Bay Moraine Shoal will vary episodically during the continued retreat, but over the long term, berg population and size will decrease as the glacier retreats.

No further information is available to assess the future behavior of the glacier's West Branch.

3. Summary of additional field operations Since Report 4

(Rob Campbell conducted oceanographic measurements in the Columbia Glacier forebay during October; the results of this work will be reported separately by him.)

During the first week of October 2014, a four-person field team flew to Columbia Glacier and established a camp on Great Nunatak near the present terminus. During the visit, the team operated a Gamma Remote Sensing Ground Portable Radar Interferometer (GPRI), on loan from the University of Alaska at Fairbanks, installed a GPS base station, and serviced the time lapse camera systems. The October timing of the field visit was made in hopes of capturing the response of the glacier and ocean to a heavy fall storm (meteorological records and time lapse sequences recorded during previous fall storms showed large shifts in patterns of flow and calving, which the teamed planned to capture in greater detail). As hoped, the field team was rewarded with five-plus days of heavy rain and snow starting the day after their arrival.

***Weather observations October 7-14*:** The remains of Typhoon Phanfone arrived on day 2 of the field team's visit (8 October) and deposited approximately 5 inches of snow, followed by heavy rain for two more days. Precipitation recorded by National Weather Service near Valdez, at Cannery Creek, totaled 2.1 inches over the period 7-14 October (See Table 1). Temperatures, wind and barometric pressure were recorded by our weather station at the Divider Mountain weather station, located in the glacier's catchment approximately 15 km ENE from the base camp. These data are shown in Figure 1.

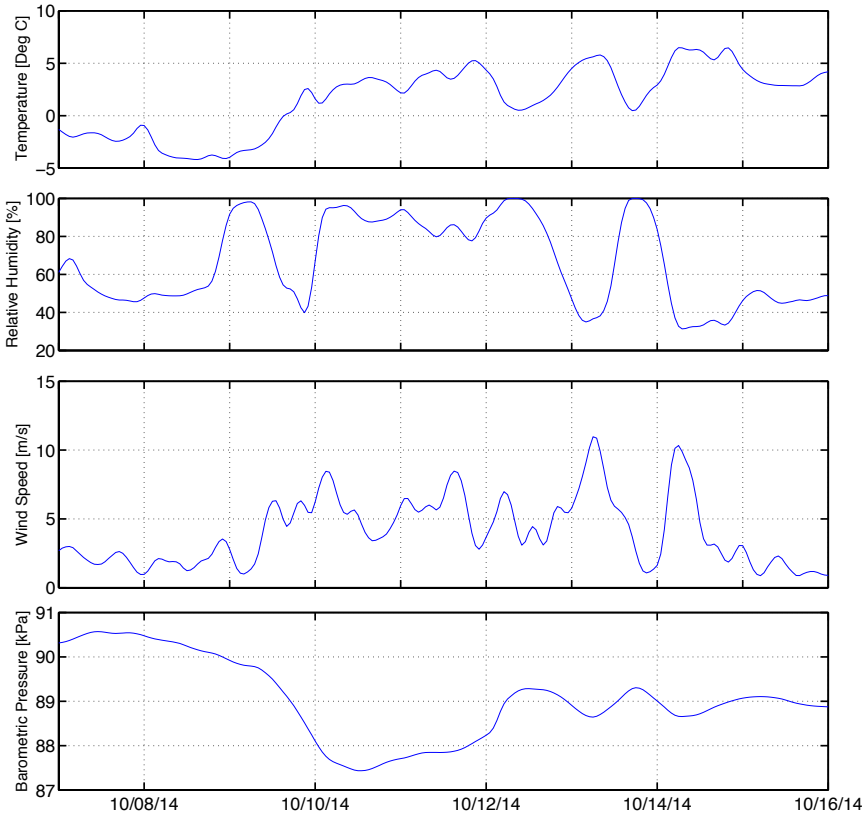

***Figure 1**: Weather data from the trip including daily average temperature, pressure and wind speed, measured at Divider Mountain, 15 km ENE from the glacier terminus.*

Date	Precip (inches)	Description
7/10	0.01	Nice day
8/10	0.01	Overcast, late day snow
9/10	0.06	10-15 cm snow overnight. Rain evening.
10/10	0.51	Rain showers becoming heavy
11/10	0.76	Rain, heavy at times
12/10	0.55	Morning rain
13/10	0.18	Sunny by mid morning
14/10	0.02	Overcast
Total	**2.1 inches**	

Table 1: Daily precipitation at Cannery Creek (27 km distant, at sea level) are given together with a description of observed precipitation by the field party at Columbia Glacier

***Camera Maintenance**:* The two time-lapse camera systems presently operating in Columbia Bay were prepared for winter. Each camera operated on schedule through the 2014 summer. We retrieved 5186 photos from the AK-01b camera and 2403 images from the AK-10b camera. While the field party was on-site, a temporary time-lapse camera was installed at the camp, acquiring images every 3 minutes on a similar schedule as the GPRI (3021 images).

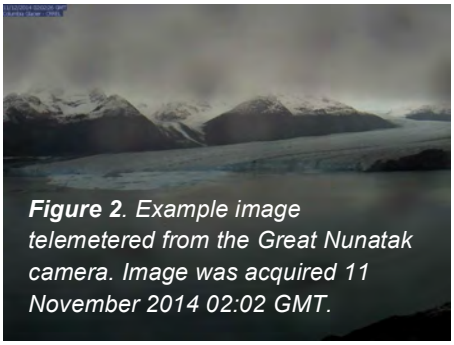

***Figure 2**. Example image telemetered from the Great Nunatak camera. Image was acquired 11 November 2014 02:02 GMT.*

The StarDot/Iridium system above the camp was upgraded to a new camera and logger that allows some 2-way communication as well as on-site recording capacity, ensuring data capture beyond telemetered imagery. This system acquires images hourly, but only transmits 3-4 images a day. It is equipped with a light sensor to avoid capturing images during nighttime hours. The power system was upgraded to a lithium iron phosphate battery, which has improved operating capacity in cold temperatures and a longer shelf life. A sample image is shown in Figure 2.

GPS Base Station: A NetRS geodetic precision GPS base station was installed at the existing seismometer site. A choke ring antenna and radome were installed on a UNAVCO-style polar mount, and an air-alkaline power system was installed to power the instrument through winter. The receiver and antenna are on a long-term loan from Jeff Freymeuller (UAF Geophysical Institute). A tie survey was completed from the GPS station "Base" used in 2004-2010 surveys to determine the position of the new station. Data processing will be possible after the next service of the instrument and will compliment the existing time series of uplift at the site (Figure 3).

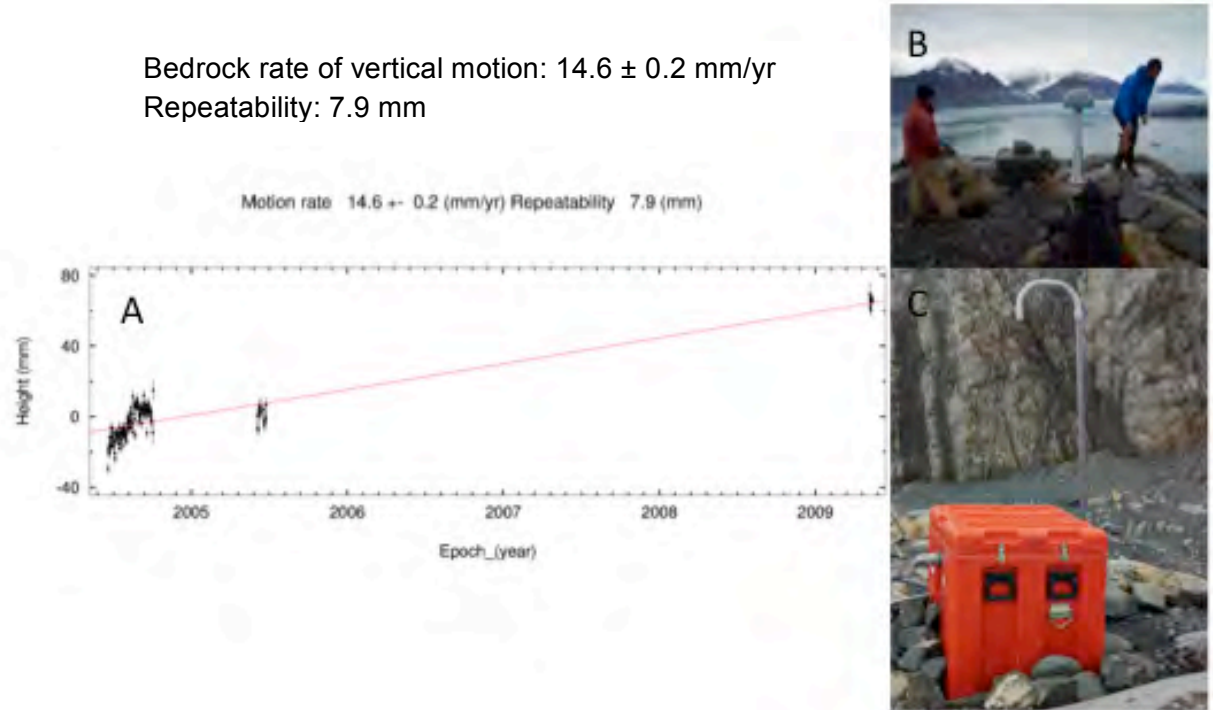

Figure 3*. A) Time series of vertical displacement at the site CGNU located on the Great Nunatak near the 2004-2010 campsite. Processing of these data courtesy of Jeff Freymeuller, UAF. B) Polar mast antenna mount and Radome. C) Instrument and battery vault with ventilation snorkel.*

GPRI Installation: Three 2 m antennas of the instrument transmit and receive radar data on 3-minute intervals to be processed interferometrically. The sensor's range extends to 16 km, and can resolve mm-scale deformation across this range. At 1 km range this senor has an azimuthal precision of ~ 8 meters, and a range precision of 0.75 m. The instrument operated nearly continuously during the week, with 4 data gaps introduced due to high winds. Approximately 700 Gb of data were collected, and are stored in triplicate at the University of Alaska at Fairbanks, the USGS Alaska Science Center in Anchorage, and at the University of New Hampshire in Durham. Both topographic and differential interferograms are output from the sensor allowing construction of digital elevation models (DEMs) and point displacement maps, as discussed below.

Figure 4*. Gamma Remote Sensing Portable (GRSP) Radar Interferometer as installed at Columbia Glacier terminus.*

The GRSP radar backscatter images have been compiled as a movie, available at http://tintin.colorado.edu**;** a frame from this sequence is shown below in Figure 5. In this high-speed movie, calving events and their resulting wave trains and seiches are clearly visible. The measurements span a major fall storm that deposited substantial snow followed by rain. Calving events are clearly visible. Motion of the glacier is obvious if the movie is accelerated. Change in the west branch is evident, but the main branch geometry remained stable. Episodes of tidal mixing are evident, as are intervals of vigorous subglacial discharge. From time to time bergs become grounded in shallow locations of the fjord. Variable transport rates and directions evidence notable differences in iceberg draft. Whether berg motion is a result of current or wind forcing appears to be strongly related to the size of the berg. Newly exposed beaches clearly come and go with the tide. The local tide can be extracted using the slope of the beach and the timing of water level.

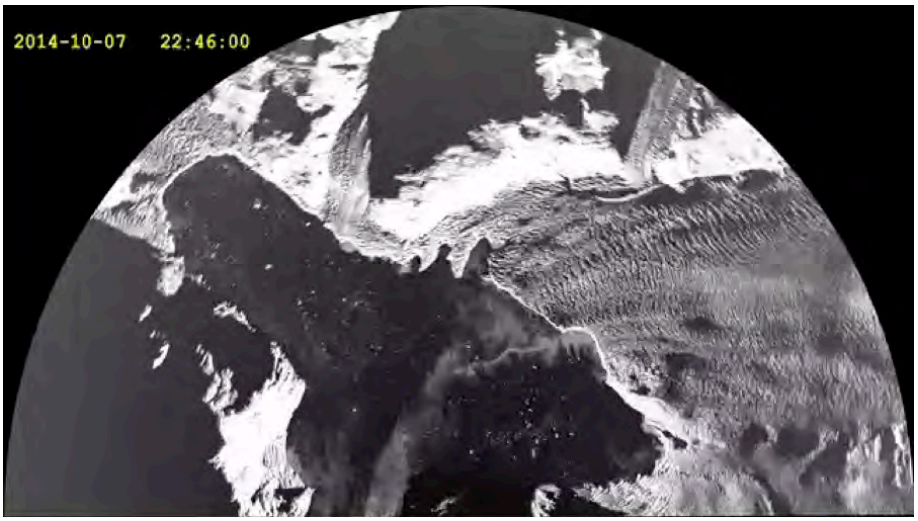

***Figure 5**. Radar backscatter still from the Great Nunatak camp in georeferenced coordinate system. The instrument located at the bottom, center of the frame. The main branch is visible on the right, and the west branch in the upper left of the image space. The sequence is rendered at 1080x or 18 minutes of real time per second of replay. See* http://tintin.colorado.edu *for the sequence.*

Further analysis and projected retreat: Determination of full, georeferenced flow fields will require georectification and referencing of the GRSP images. These will be performed by colleagues at UA Fairbanks; in the meantime we have line-of-sight velocities (i.e. at any given point on the glacier, the component of motion parallel to the vector joining the radar to that point), calculated both as contoured fields in map view (Figure 6) and as time series at various points extracted from the fields (Figure 7). Data are stacked over 1-hour intervals to reduce noise.

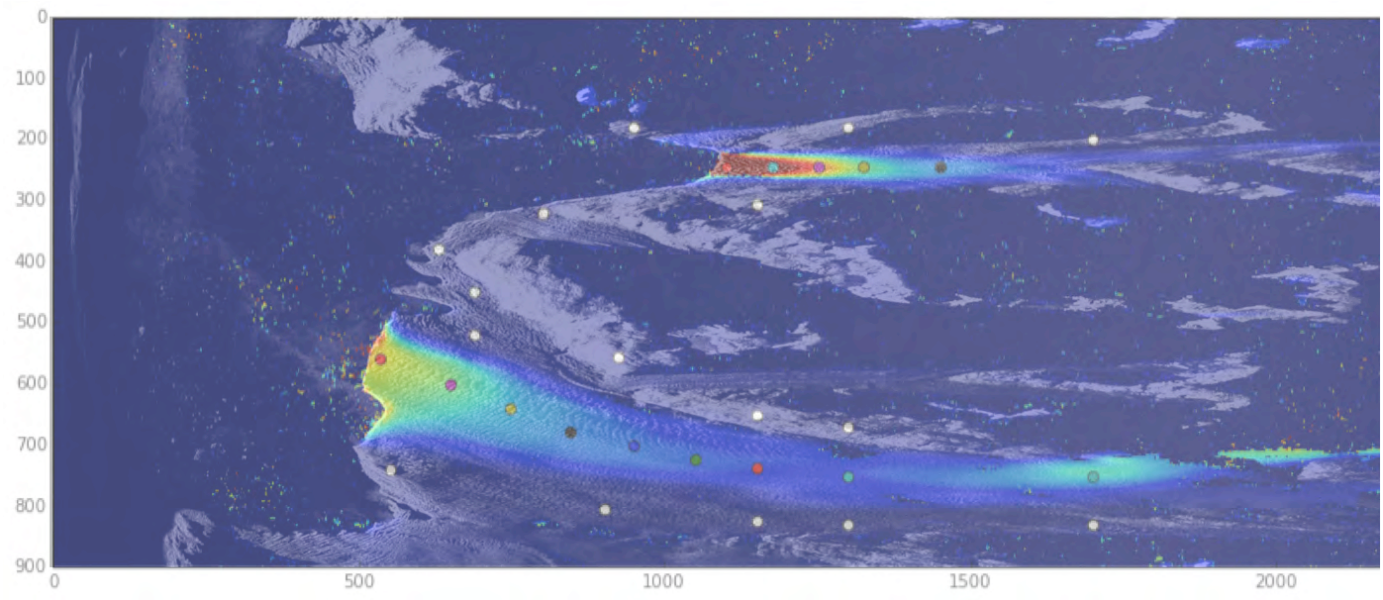

***Figure 6**. Line-of-sight velocity field, where red is the fastest flow (ca. 6 m/d). The image shown here is distorted by rendering the radial space shown in Fig. 5 as a rectangular region. The horizontal axis here corresponds approximately to distance from the radar (equivalent to radial distance in Figure 5); points along the left-hand margin of Figure 6 all map to one point, the location of the radar (at the center of the bottom margin of Figure 5). Faster speeds are shown red and diminish through yellow and green to blue at the lowest speeds. Colored circles indicate the position of time series shown in Figure 7, each plotted in like colors. Note that while the apparent velocity of the West Branch is greater in Figure 6, Figure 5 shows that the radar line-of-sight direction at the West Branch is very nearly parallel to the glacier flow direction, while on the Main Branch the line-of-sight is very oblique to the flow direction; this will cause the apparent flow speed on the Main Branch to be less than the true flow speed.*

Figure 6 shows that the line-of-sight flow speed decreases with increasing distance from the terminus in the Main Branch. From Figure 7, a strong tidal influence on speed is apparent, with maximum speeds at low tide. The amplitude of the tidal influence extends about 2.3 km upstream and decreases with distance from the terminus; the length scale of damping appears to be about 10 ice thicknesses. These are characteristic of grounded tidewater termini, but the amplitude and phase of the tidal signal is unusual: at 30% to 50% of the background velocity, the tidal signal is unusually strong, and there is not strong evidence of a phase lag moving upstream, away from the terminus. These conditions suggest that basal coupling is not strong in the Main Branch, probably caused by increasingly significant buoyancy forces as the glacier continues thinning at annual average rates of 10-20 m/yr.

Taken together with other current and historic observations, our preliminary analysis suggests that the lower glacier is poised for another episode of rapid change, not unlike the period of retreat between ca. 2008 and 2010. Following a period of very rapid flow and calving, but stable terminus position, between ca. 2001 and 2005, the glacier's speed dropped to (relatively) very low values and thinned rapidly near its terminus before beginning a rapid retreat from immediately upstream from the Kadin-Great Nunatak Gap to near its present position just above Juncture. The main branch terminus then stabilized in shallow water around several basal high spots, and has changed only small amounts since then. Following the pattern of the last decade, we expect an episode of retreat to occur, possibly within one year, but very likely within 5 years. Better knowledge of the basal topography of the Main Branch would help predict the glacier's near-term future, but precise knowledge of the onset and speed of this episode of retreat is probably unattainable in any case. Our group will closely monitor the daily image stream to assess glacier stability and will alert RCAC of any notable changes in terminus and iceberg conditions.

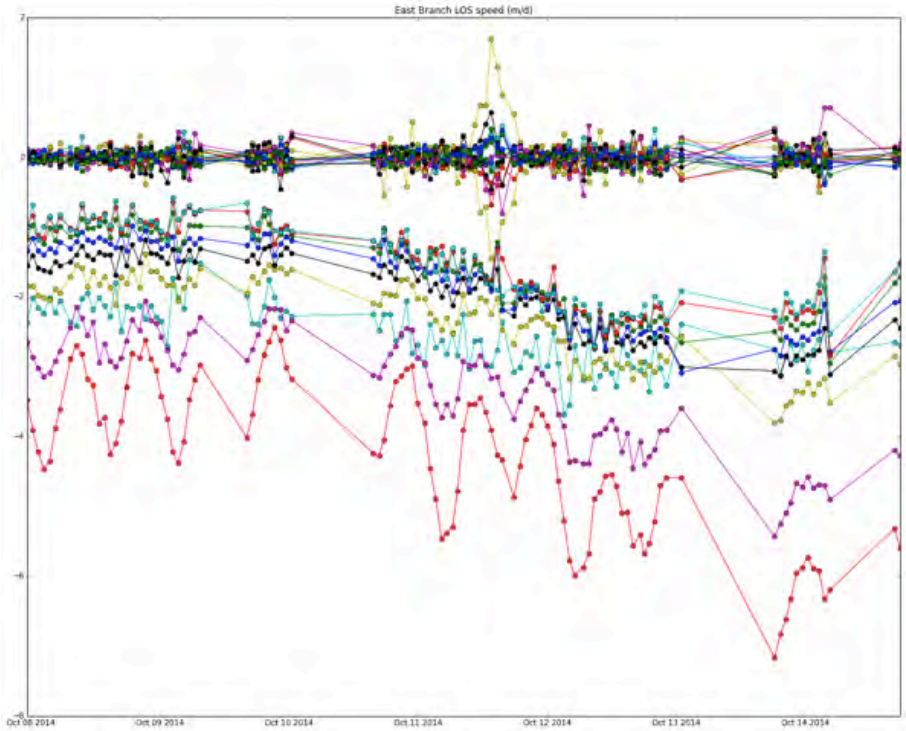

***Figure 7**. Time series of ice motion at colored dots shown in Figure 6. The top cluster of lines are on fixed bedrock points and gives a measure of the noise level in the radar time series following preliminary processing. Nine time series below show time-varying rates of motion toward the radar.*

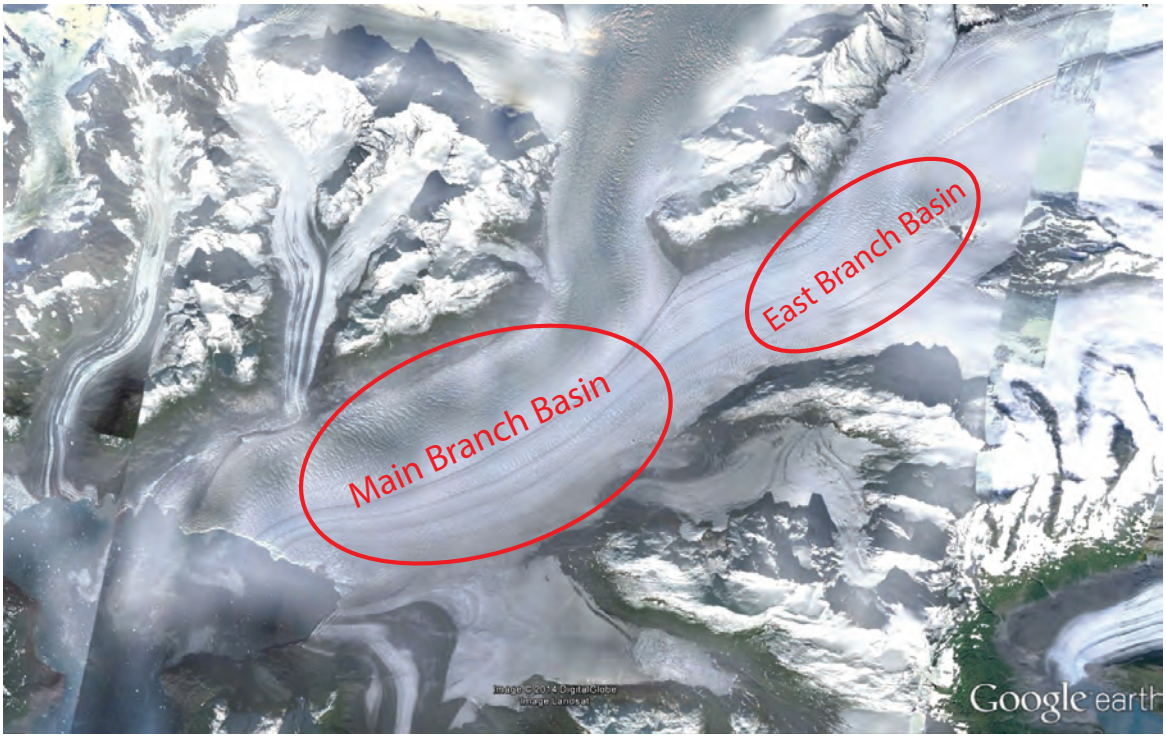

***Figure 8**: Main Branch Basin and East Branch Basin.*

4. Modifications to projections discussed in Reports 3 and 4

The findings of October, 2014, described above, led us to the important conclusion that an episode of rapid retreat and calving of ice from the Main Branch Basin (Figure 8) appears to be set to commence within 1 to 5 years, with the greatest likelihood occurring around one year. This is the first episode of removal of ice from the Main Branch Basin (see Figure 8), where ca. 5.7 – 7.2 x 10^{10} tons of ice are stored (see Report 1, Part II), but this does *not* necessarily represent the onset of the flushing of that entire basin. Without further measurements of the bed topography in the Main Branch Basin, we cannot determine if pinning points are present upstream where temporarily stable terminus positions might be reached. The approximate knowledge of the bed in the reach (e.g. through McNabb et al, 2012) indicates that the bed geometry is complex, with ridges and some local high spots, favoring temporary stabilization during a longer episode of retreat (Report 1, Part II)

The assessment of deeper ice in the East Branch Basin than given by earlier analyses, as detailed in Report 4, is unchanged here. The removal of ice from the East Branch Basin will clearly not commence until the Main Branch Basin is opened up, but nothing in the observations over the past two months alters our assessment given in Report 4.

No further analysis of the future behavior of the glacier's West Branch can be made at this time.

Current understanding of the transport and delivery of icebergs down Columbia Bay and to the Heather Bay Moraine Shoal (HBMS) was outlined in Report 3, and those findings are unchanged. Recapping the summary of Report 3 on iceberg transport:

While calving rates are declining over the long term, Columbia Glacier continues to produce icebergs at a rate faster than most Alaskan tidewater glaciers, and those icebergs are larger than icebergs produced at most other locations. Most of the calved ice is retained behind HBMS until the bergs deteriorate to smaller sizes or unless a high tide sweeps a cluster of bergs over the moraine (not uncommon). For these reasons alone, Columbia Glacier merits continued surveillance as it continues retreating, but other factors are at work to reduce iceberg sizes, including declining berg sizes at the time of calving (due to thinning ice), increasing distance from the glacier terminus to HBMS, and possible trapping of icebergs at shallow parts of either the Main or East Branch Basins. All of these conditions point toward prolonged but episodic future rates of iceberg calving and diminishing size of icebergs over time.

15 June 2015

Report to Prince William Sound Regional Citizens' Advisory Council:
Future Iceberg Discharge from Columbia Glacier, Alaska

Reference PWSRCAC Project #8551
Contractor: W. T. Pfeffer Geophysical Consultants, Nederland, Colorado

Report #6 FINAL REPORT

Abstract

Columbia Glacier, in the northeastern corner of Prince William Sound and ca. 12 miles distant from the path of tankers leaving the southern terminus of the Alaska Pipeline, has been in a state of rapid tidewater retreat since the early 1980s. Icebergs discharged by the glacier during the retreat have largely been contained within the moraine shoal at the position of the terminus prior to the glacier's retreat, but the fraction of icebergs crossing the moraine and entering Prince William Sound proper still pose a potential hazard to ship traffic in the Sound.

This study assesses the current and future status of iceberg discharge from Columbia Glacier. There is a long history of glaciological research at Columbia Glacier that we can draw on, much of it conducted by the US Geological Survey in the 1970s and 1980s. In addition to these resources, starting in 2012 and continuing at present, we have worked on the glacier and in the fjord collecting and compiling new datasets, including time-lapse photography, weather data, tectonic uplift, ice motion (diurnal to annual time scales), bathymetry, ocean water properties, and ice surface topography. The details of these investigations are described in our five earlier reports to PWSRCAC, but the overall conclusions of the project are stated here, and we make our final assessment of Columbia Glacier's future retreat, the characteristics of iceberg discharge, and our judgment of the primary hazards posed by the glacier in the future. We estimate that the tidewater retreat phase of Columbia Glacier may continue for as long as another 20 years, but that icebergs discharged from the retreating terminus in future will be reduced both in size and number. The increasing distance that icebergs must traverse between the retreating terminus and the moraine shoal at Heather Island (where the vast majority of icebergs are trapped and prevented from escaping into the Sound proper), as well as increasing water temperature, will also contribute to further degradation of icebergs before they reach the shoal. Risk to tanker traffic from icebergs will thus likely be reduced, but not absent, in the next two decades. In addition to risk to tankers, however, a new class of risk may be developing to other boat traffic in the inner Columbia Fjord, as this area becomes more accessible with declining iceberg density.

Introduction

This project is focused on assessing the current and future status of iceberg discharge from Columbia Glacier, a large tidewater glacier that terminates in Prince William Sound, Alaska. The Prince William Sound Regional Citizen's Advisory Council (PWSRCAC) initiated Project #8551 with W.T. Pfeffer Geophysical Consultants, LLC in 2012 as a follow-up to the 1996-1998 Iceberg Monitoring Project (IMP) conducted by Austin Post and Wendell Tangborn. The principal objectives of the present study are to summarize the glacier's retreat since 1996-1998, reevaluate methods for assessing and projecting glacier retreat and iceberg calving, estimate the duration of remaining glacier retreat, and project iceberg production and drift for the next decade (to 2022). To these ends, we have worked on the glacier and in the fjord collecting and compiling new datasets, including time-lapse photography, weather data, tectonic uplift, ice motion (diurnal to annual time scales), bathymetry, ocean water properties, and ice surface topography. Our report also discusses colleagues' findings, including fjord sedimentation, ice thickness, and mass balance measurements. All are aimed at understanding the present stability of the Columbia Glacier and improving forecasts of the continued retreat over the coming decade.

Background

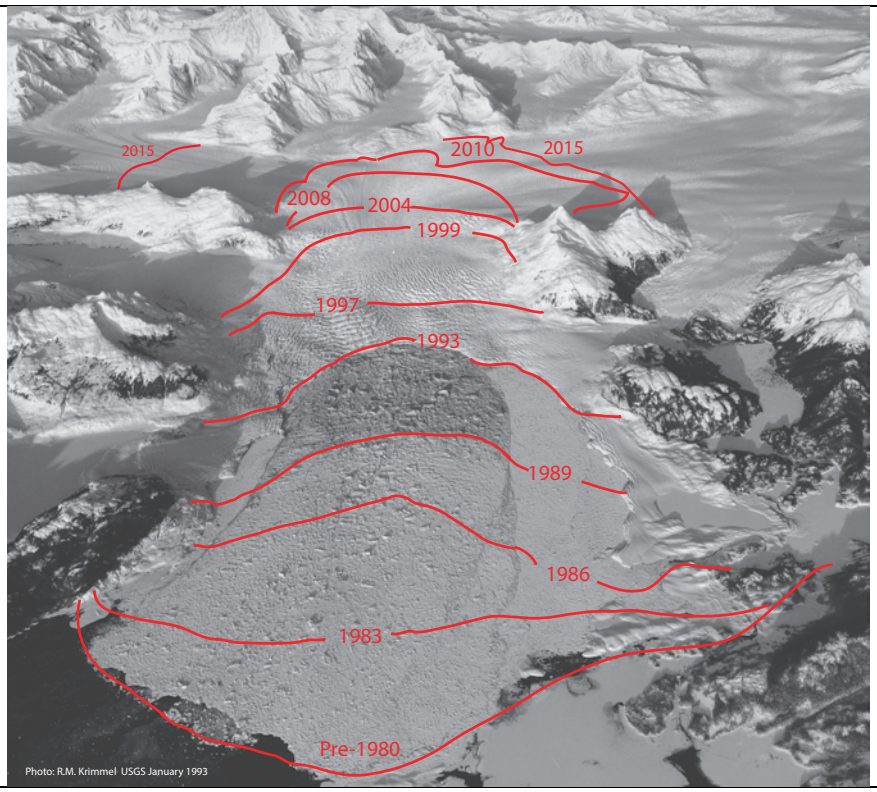

Figure 1. Columbia Glacier in 1993 with terminus positions throughout the retreat overlaid.

Columbia Glacier began rapidly retreating in the early 1980s. Since 1982, the glacier terminus has retreated over 20 km. Rapid thinning and discharge has reduced the total volume of the

glacier by about 50% (**Figure 1**). The data compiled during this period represents the most detailed observational record of tidewater glacier retreat ever assembled (**Figure 2**).

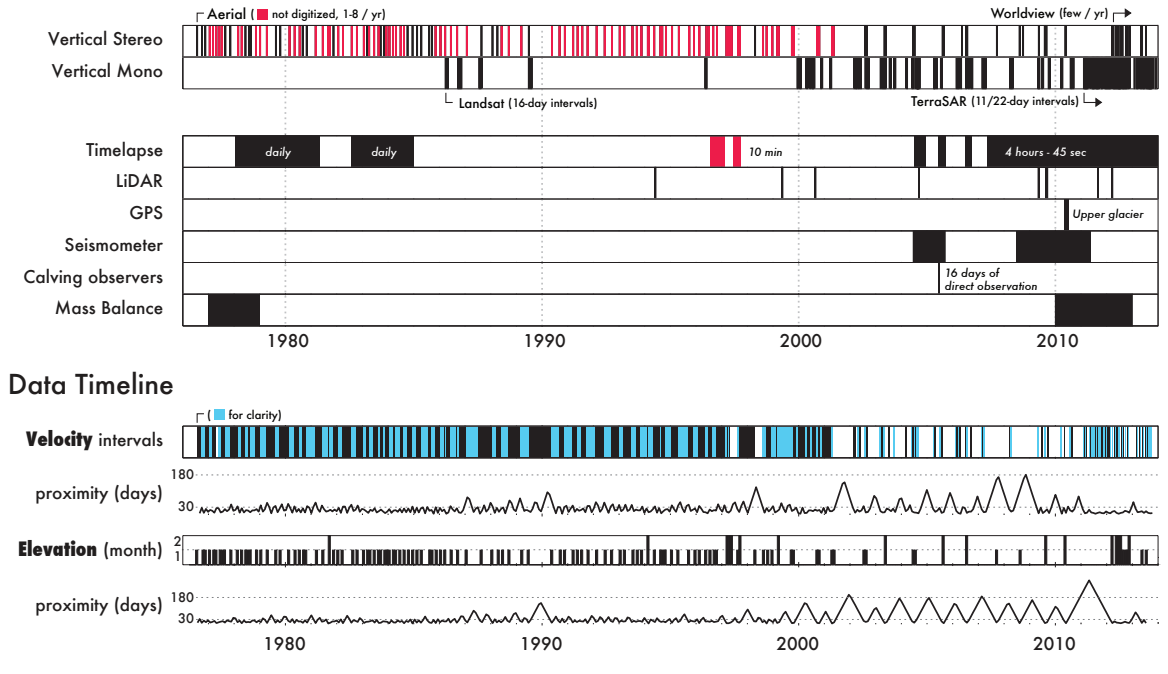

Figure 2. Distribution of principal observational time series over the lifetime of Columbia Glacier research, from 1976-2012

Columbia Glacier is one of the fastest changing landforms on Earth. The rate of ice loss is spectacular relative to the glacier's total size, and for nearly a decade (between 1998 and 2007) accounted for roughly 1% of global sea level rise (Rasmussen et al., 2011). The processes characterizing the retreat provide insight into other tidewater and outlet glacier retreats around the globe. Locally, icebergs calved from Columbia Glacier have been a hazard to ship traffic in eastern Prince William Sound, while the combined flux of ice and meltwater almost certainly have a significant influence on salinity and acidity in the Sound (Evans et al., 2014).

Iceberg hazards have been an issue of great concern to stakeholders in Prince William Sound. Accordingly, our wide-ranging investigations at Columbia Glacier, although serving a number of valuable scientific goals, also bear on the question of present and future iceberg discharge into the Sound. We describe our investigations in general terms below, and address the specific iceberg hazard issues that motivated this work in the Summary Evaluation and Recommendations.

Data Collection and Interpretation (since RCAC Report 5)

Time-lapse photography

Four time-lapse cameras have been in operation since Report 5 was delivered to RCAC in December 2014. These cameras were last serviced in March 2015. Although power supply issues plagued the telemetered camera through winter, the power system was replaced and improved and the camera is operating once again. The DSLR camera at Kadin(AK-01) operated through winter. A solar panel failure at the upglacier DSLR camera (AK-10) caused a gap in photographic coverage, but this was repaired in March. The Heather Island camera also had a short gap in coverage during the winter (potentially from limited sunlight), but was operating when we arrived. This camera was removed in March 2015, after having recorded over 20,000 images since its deployment in May 2013.

Geodetics

A geodetic GPS base station was installed during the October 2014 field visit (see Report 5) and operated from October 2014 to February 2015; the collected data has been sent to Jeffrey Freymueller (University of Alaska) for processing, including a survey tying the new antennae location to an older reference point (established 2004). Despite efforts to ventilate the air-alkaline batteries, insufficient airflow is likely to have caused the premature failure of the station. The receiver was brought back to Anchorage in March 2015, and a new power system is being designed using funds leveraged from other projects. The station is scheduled to deploy in June 2015 with a rechargeable lithium iron phosphate (LiFePo) battery and solar power system.

Ice motion

Since Report 5 (December, 2014), we have performed ice motion observations on a range of time scales. Ground-based portable radar interferometry (GPRI) data was collected over a weeklong, 3-minute repeat interval survey in fall 2014, and analysis is ongoing (**Figure 3**).

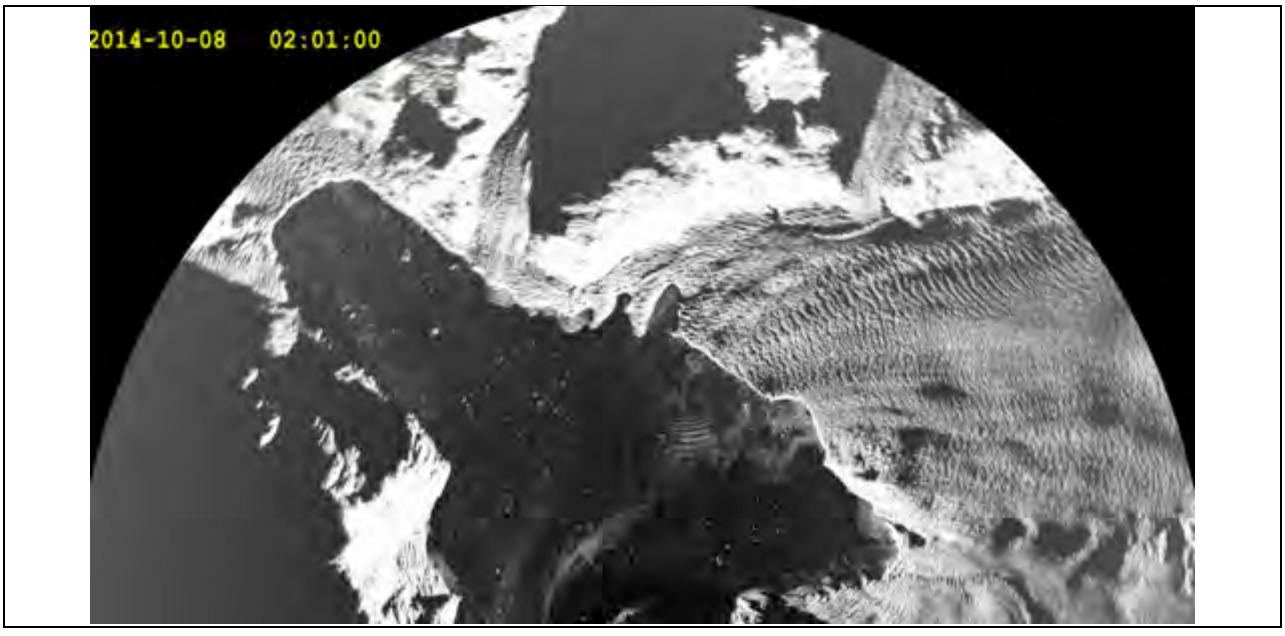

Figure 3. Radar backscatter still image from the Great Nunatak camp. The ground-based radar interferometer is located at the center of the bottom edge of the image, and collects data in a radially symmetric pattern. In this reference frame the main branch is located on the right hand side of the image, and the west branch on the left side of the image.

PhD student Ryan Cassotto (University of New Hampshire) is leading this work, and the algorithms needed to process such data are being developed with NSF funding (once ready, they could be used to process the data collected last fall). The data are presently in a line-of-sight (LOS) reference frame, complicating the location of features in the imagery, but we expect only small changes to our interpretations of ice motion when the data is transformed to a standard, gridded coordinate system.

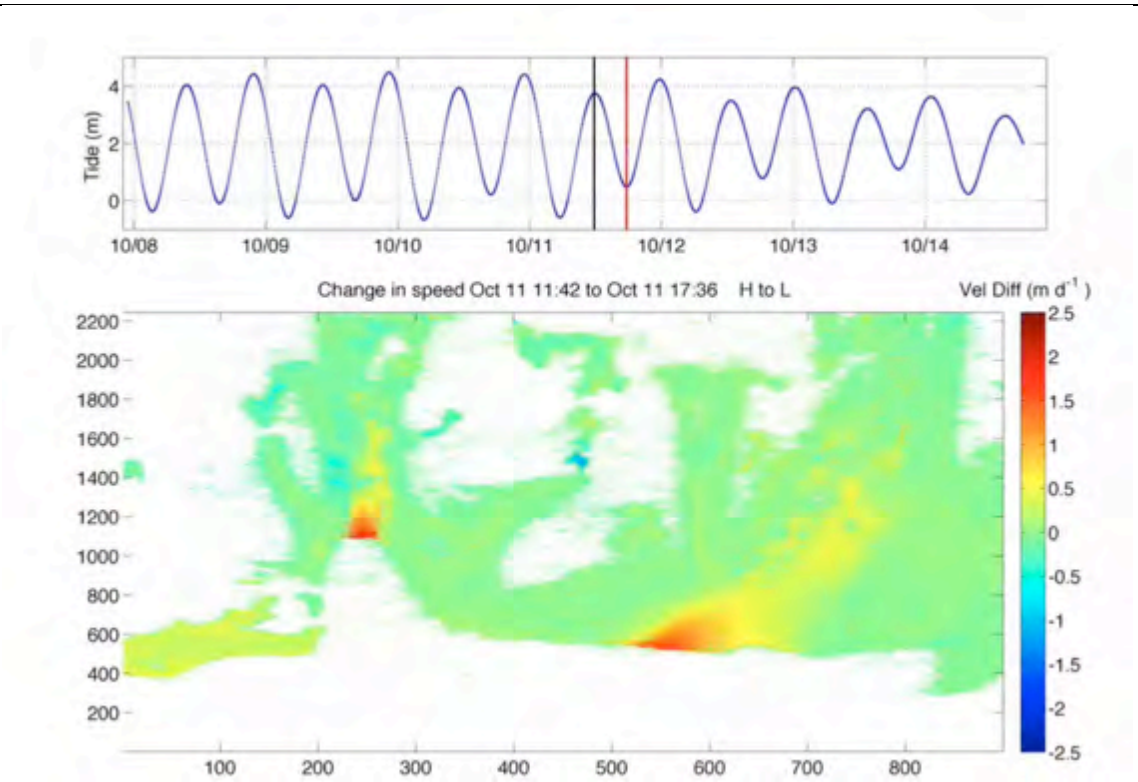

Figure 4. Tidal variations in motion. The top panel shows the regional tide with vertical bars indicating the timing of the two scans that are differenced in the color plot below. This example shows the difference between high and low tide on October 11 and the associated speed up at the West and Main calving fronts. Red colors indicate faster motion for the second interval, blue colors slower motion.

So far, our analysis has confirmed that tides force velocity variations in the glacier (**Figure 4**), with slower speeds occurring at high tide and faster speeds occurring at low tide. This is expected of grounded tidewater glaciers (e.g., Walters and Dunlap, 1987; O'Neel et al., 2001);

however, the velocity perturbation reaches further upstream than we expected (**Figure 5**). Precipitation may also have a very large influence on glacier speed: the lower glacier accelerated up to 300% beginning 1-1.5 days after the onset of sustained rainfall (**Figure 6**). Walters and Dunlap (1987) analyzed along-flow speed variations at Columbia Glacier very early in the glacier's retreat and reported an "e-folding" (1/e ≈ 0.37) damping length scale of ~2 km. The damping lengths we observe today are ~5 km (**Figures 4,5**), meaning that velocity fluctuations are propagating more than twice as far up the glacier now as they did in the 1980s.

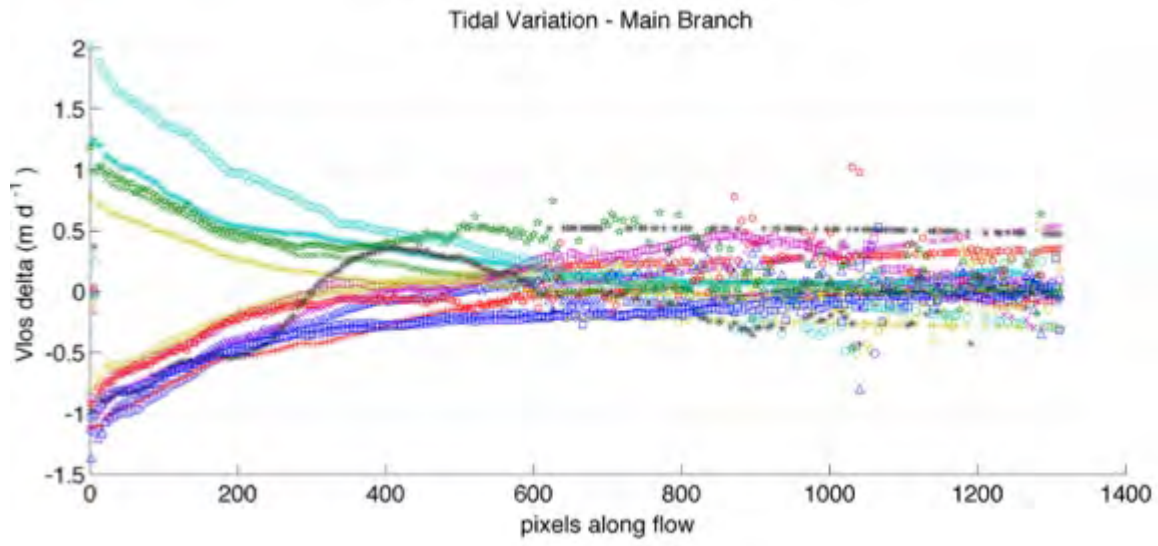

Figure 5. Ice flow velocity plotted vs. along-flow distance, approximated by pixel positions in the images. The 1300-pixel length of the profile corresponds to roughly 10 km in the upstream direction.

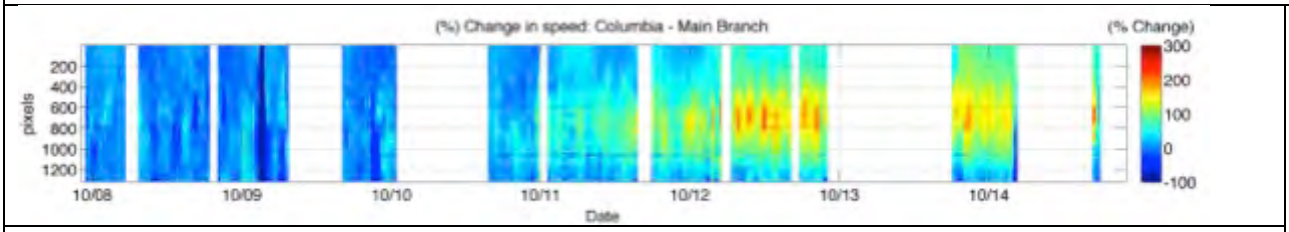

Figure 6. Influence of precipitation on ice motion is shown as a percent deviation from initial speed. The terminus is across the top (pixel 0) and speeds are shown along the centerline profile extending up the main branch. Accelerations up to 300% the initial speed are seen after water inputs, which began on the evening of 10/9 and persisted through the morning of 10/12.

We have also obtained TerraSAR-X velocity fields (through 25 July 2014) from UW collaborator Ian Joughin (**Figure 7**). These data show that overall glacier velocities are continuing to decline over time. The glacier continues to exhibit strong seasonal fluctuations in flow speed, with a rapid spring acceleration, culminating in the fastest observed speeds, followed by a slow decline through summer and into fall, followed by a slow acceleration through the winter (**Figure 8**).

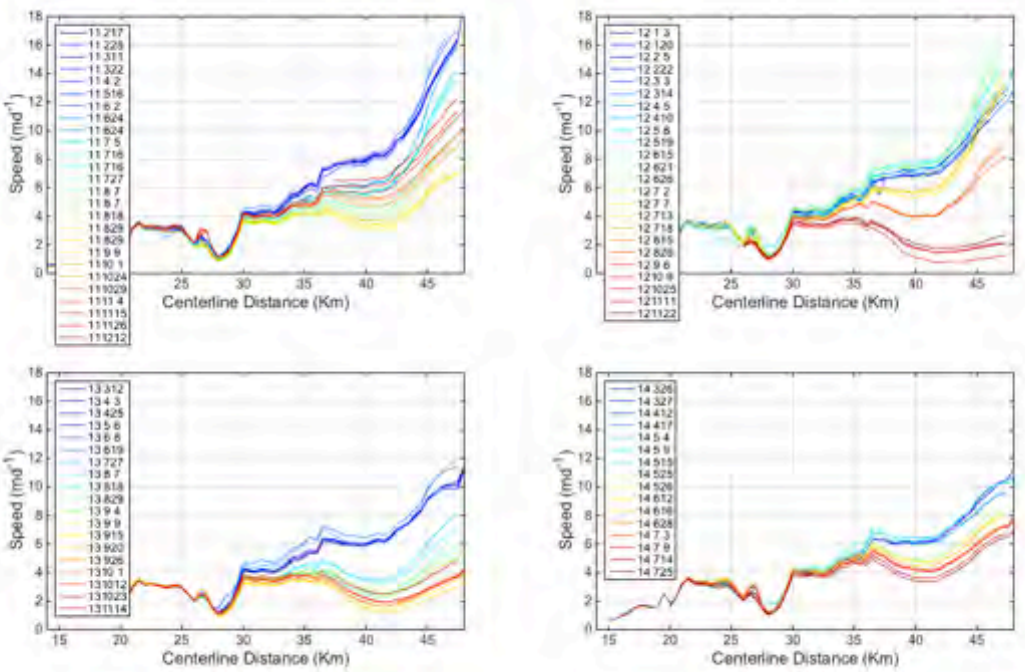

Figure 7. Centerline speed profiles extracted from TSX velocity fields. For 2011 – 2014. Note the general decline in terminus speed since 2011.

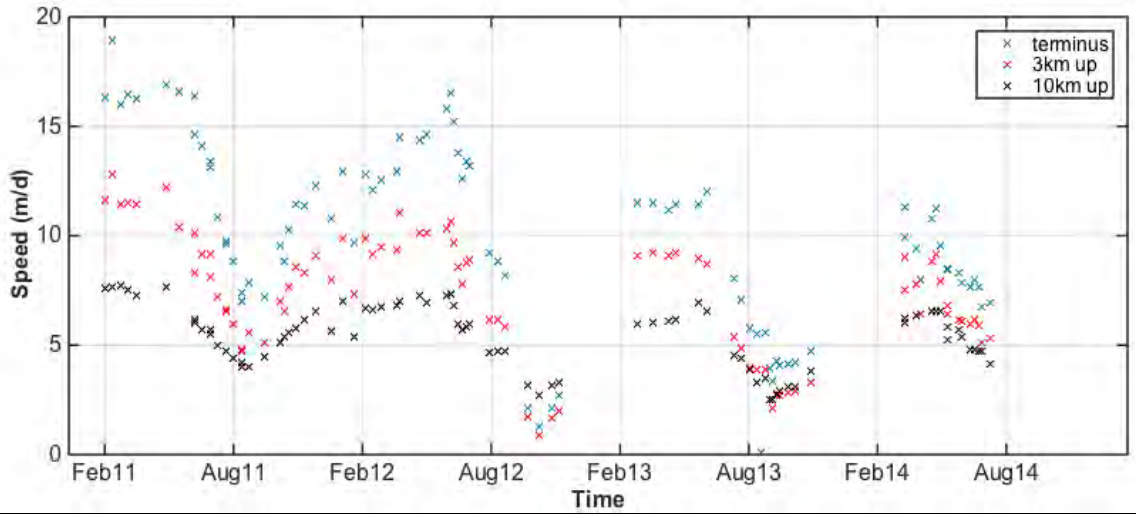

Figure 8. Time series of centerline speed (m/yr) over the 2011-2014 interval. Speed has been increasing slowly through spring and summer but has tended to decelerate rapidly in late summer. Over the three years of TSX acquisition, there is an overall trend of reduced speed and lower amplitude seasonal variability.

Overall Project Summary

Over the lifetime of this project (2012-present), we analyzed existing data, collected new data, and incorporated data from other investigators to make predictions about the discharge of icebergs from Columbia Glacier in the future. We recovered a significant volume of early photogrammetric data, conducted an extensive time-lapse survey of the glacier, and installed an iridium-telemetered timelapse camera to monitor the terminus for signs of destabilization in real-time. The images are viewable on the site glacierresearch.org, which has been moved to a more stable server and redesigned with a greatly improved interface.

Stability of the moraine shoal

Early in our work, we investigated whether or not the moraine shoal west of Heather Island has been substantially eroded (Report 2 and Figure 9). Within the precision of the data, which was limited by the poorly resolved tide stages of the 1977 and 1994 surveys, we found no large-scale changes to the topography of the shoal, which continues to be the main obstacle to large icebergs escaping from the Columbia fjord into Prince William Sound. Although the size distribution and rate of iceberg production at the terminus remain important variables in determining the size distribution of icebergs reaching the Sound (see Report 2), melt and fragmentation of the icebergs during their journey to the shoal are becoming critically important processes as the distance from the terminus to the shoal increases as the glacier retreats.

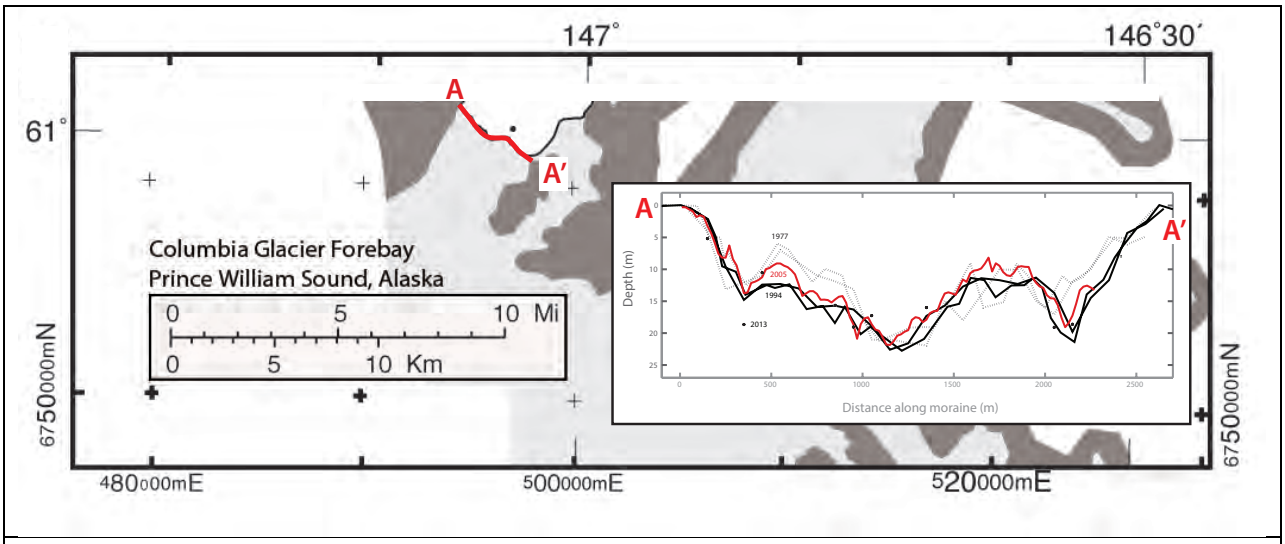

Figure 9. Bathymetric profiles across the Columbia Bay Entrance Sill the west shore of the fjord (0 m) to Heather Island (3000 m).

Iceberg calving and transport

The calving flux discharged by Columbia Glacier over the nearly 30-year lifetime of the retreat to date has been marked by variations closely tied to changes in the fjord geometry in the immediate vicinity of the retreating terminus (Figure 10). The future long-term thinning of the glacier and retreat of the glacier terminus into narrower and shallower waters constrains the

future rate and size of icebergs discharged into the fjord. The glacier has thinned over 500 m at the current terminus position since the onset of retreat. The deep-water channel to which the terminus is exposed has narrowed significantly (from ~5 km in 1982 to ~2 km at the Kadin-Great Nunatak gap, for example) and water depths in the vicinity of the present terminus are variable and generally shallow (less than 200 m). All of these changes suggest that the terminus will produce smaller and smaller icebergs over the long term and that the larger icebergs will be more likely to become grounded in their journey down-fjord to the moraine shoal.

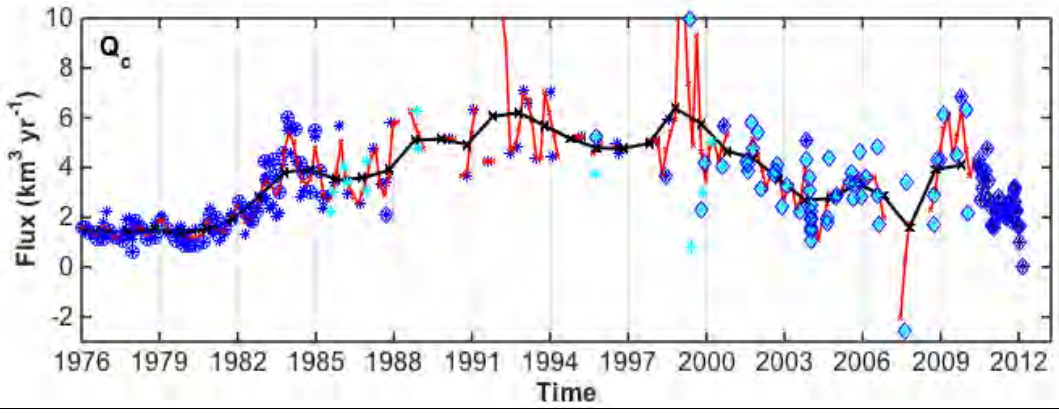

Figure 10. Columbia Glacier calving flux estimates over the history of the retreat produced using a flux gate analysis (described below). The red curve is smoothed over 3 month intervals, and the black curve depicts annual smoothing.

However, periods of increased – and possibly dramatically increased – rates of calving are still possible. Since the rapid opening of the inner fjord in 2007-2010, the terminus position of the Main Branch has remained relatively stable (with minor adjustments and embayments but no significant change in position). The glacier is also flowing and thinning at comparatively slow rates. However, relative to the past ca. 2 years, variations in speed have become well correlated over large horizontal distances (i.e., a perturbation in speed near the terminus is reflected several km upstream with little delay). This coherence suggests that basal drag is presently very low and that the glacier is near flotation over a large region upstream from the present terminus. Judging from past behavior and our latest observations, the glacier may soon enter a period of rapid terminus retreat, increased iceberg production, and larger iceberg sizes.

In 2006, when the glacier terminus was thicker but located at a similar pinning point in the fjord, iceberg size increased dramatically as the glacier thinned, transitioned to flotation (2007), and retreated out of the pinning point and the deeper water immediately up-fjord (2008-2009). During the 18-month period the terminus was floating, many of the icebergs produced were "tabular," a classification describing icebergs that are much wider than they are thick. The tabular icebergs were heavily fractured, and rapidly disintegrated into smaller icebergs, but some potential remains for large, thin icebergs to be carried over the moraine shoal and into the Sound.

However, other changes in the fjord will reduce the likelihood of large icebergs escaping. The inner fjord (the recently opened reach up-fjord of the Kadin-Great Nunatak Gap), and in particular the Main Branch side of the inner fjord, contains a number of shallow reefs, features not present in the main, or outer, fjord, downstream from the constriction between Kadin Peak and the Great Nunatak (referred to here as the "Kadin-Great Nunatak Gap"). Grounding on these reefs not only slows the passage of icebergs down-fjord, but also subjects them to strong tidally-forced rotations which tend to break the icebergs into smaller pieces. In turn, the increased surface-to-volume ratio of the smaller bergs accelerates melt, further reducing the total volume of ice reaching the moraine shoal.

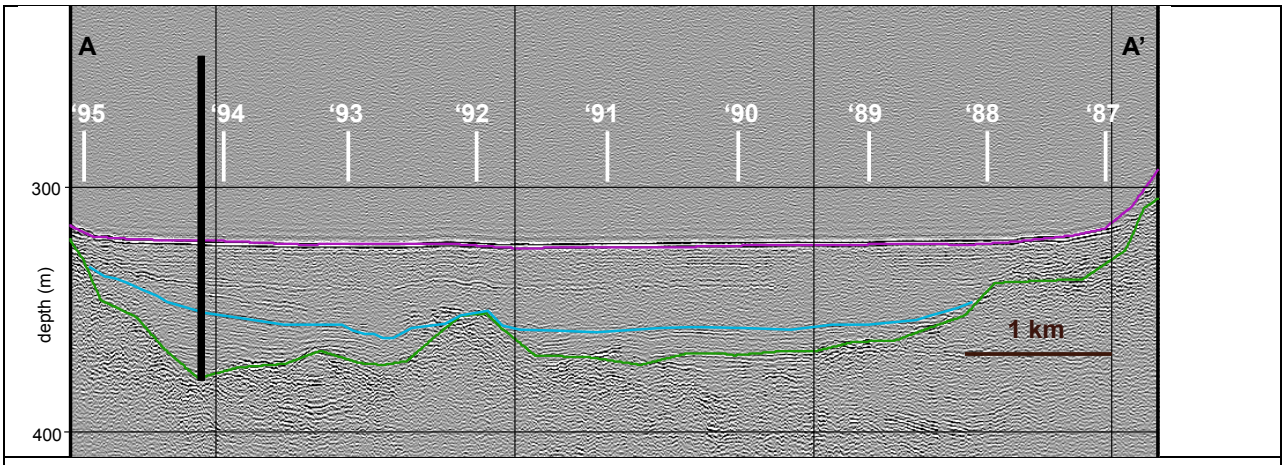

Figure 11. Active-source seismic mapping of bedrock and sediment geometry along the centerline of the outer bay of Columbia Glacier's fjord. White bars show the location of the terminus in year indicated. The black line represents the position and depth of a 1987 borehole (Meier et al., 1994). The base of the sediment deposit is shown with a green line. The blue line indicates seabed depth in 1997, and the pink line shows the seafloor in 2011.

Sedimentation in the fjord

A study of sedimentation rates and processes by colleagues at the University of Washington (UW) is nearing submission to the Journal of Glaciology (Boldt et al., in prep). Their work shows that sedimentation is very rapid, with sediment fluxes upwards of 19 million cubic meters per year, or an average sedimentation rate of 20 cm/yr throughout the fjord. The sedimentation rate is episodic, with variations linked more closely to changes in the fjord geometry near the current terminus position than to variations in ice flux or calving speed. A new model developed by the UW team is able to reproduce the spatial and temporal patterns observed in the fjord stratigraphy (**Figure 11**), and their results should give us valuable insights into subglacial erosion, spatial variations in basal sliding, and – possibly of greatest interest to RCAC – insights into processes governing the delivery of sediments, associated nutrients, and changes in water chemistry not only to the Columbia fjord but to Prince William Sound.

Measurements of bed topography

Recently discovered errors in the subglacial topography produced by McNabb et al. (2012) are proving to have a significant effect on many important results and predictions. In 2014, the West Branch retreated suddenly and unexpectedly to a position where the bed was earlier predicted to be 100 m above sea level, whereas bathymetric data collected in fall 2014 showed that the water depth in fact approaches 300 m in this location (**Figure 12**). We suspect that the large modeling errors in McNabb et al. (2012) are largely the result of not considering the magnitude of changes in bathymetry caused by deposition and evacuation of basal sediments – conditions that we had no knowledge of prior to the work by Boldt et al. (see above). There is also a trend toward larger errors as the terminus retreats further upstream, away from the bathymetric measurements made in open water earlier in the glacier's retreat and used as initial conditions in the model. The recent bathymetric measurements by Rob Campbell in the inner fjord will provide new constraints if and when the McNabb bed model is improved and re-run.

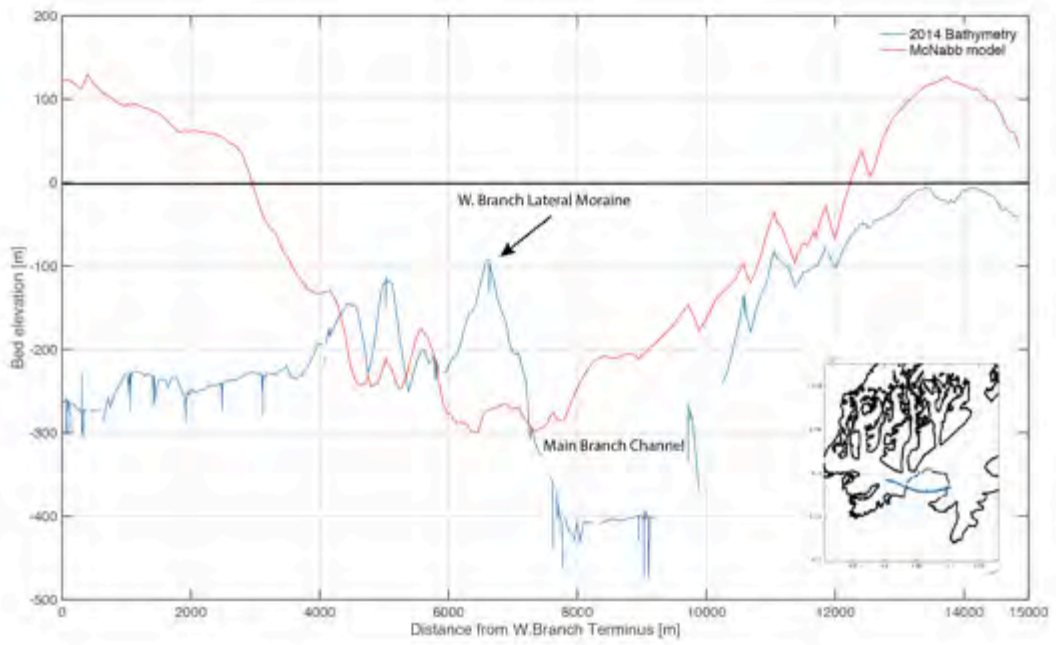

Figure 12. The 2012 bed model (McNabb et al., 2012) is plotted along a bathymetric profile taken perpendicular to the fjord and extending up into the west branch as shown in the inset figure. At the location of the October 2014 survey, the model estimate was ~350 m shallower than measured. The reverse slope bed in this location is an indication of continued susceptibility to unstable flow and calving.

Tectonics

The GPS record of uplift at the Great Nunatak site extends back to 2004 (Figure 13). The time series of elevation at that site reveals that local uplift from ice unloading is rapid, 14.6 mm/yr, or roughly half as fast as the fastest rates ever recorded near Glacier Bay (Motyka et al., 2007).

The observations and analyses summarized above and in our 5 previous reports form the core knowledge that we draw from to answer those questions about future iceberg calving and transport most relevant to the RCAC. In the sections that follow we address those questions more explicitly, first with a synthesis of the various observations in context, then with a list of recommendations and a final statement about the projected future retreat.

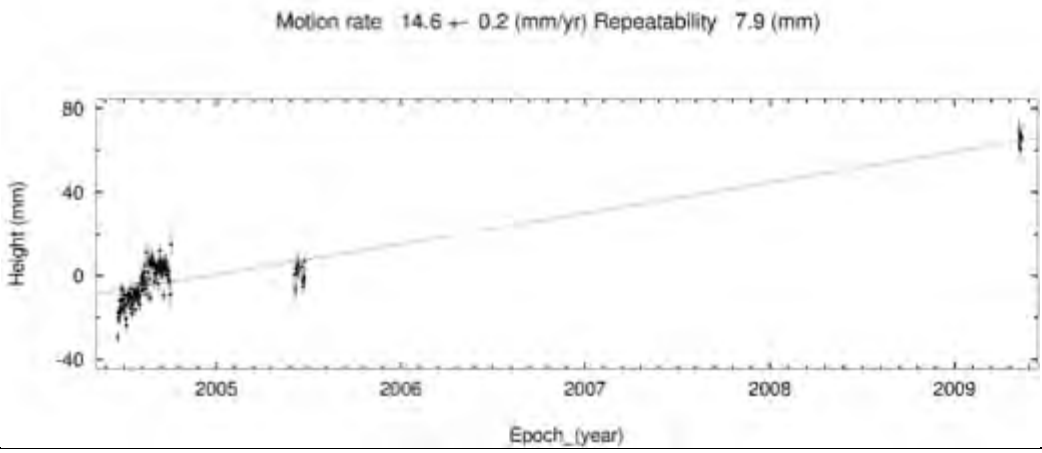

Figure 13. GPS-derived elevation of benchmark BBB at Great Nunatak, Columbia Glacier, Alaska, showing tectonic uplift of ca. 14.6 mm per year.

Discussion: Integrated Insight

We assembled a long-term record of calving discharge through the retreat using the Krimmel (2001) aerial photogrammetry data set (1977-1999), LANDSAT visible imagery (1986-2010), WorldView visible imagery (2008-2014), and TerraSAR-X radar imagery (2011-2014). The flux record is shown in **Figure 10**, where calving flux (Q_c) is plotted vs. time from 1976 to 2013.

The calving flux is calculated as the sum of the incoming ice flux (Q_{in}) passing through a "gate" located some distance upstream from the terminus and the volume change (dV/dt) in the region between the gate and the terminus:

$$Q_c = Q_{in} - dV/dt \quad (1)$$

The incoming flux at the upstream gate Q_{in} was calculated by multiplying the observed cross-glacier-average surface ice speed u at the gate (assumed equal to the depth-averaged speed) by the glacier's cross-sectional area at the gate (A):

$$Q_{in} = A \cdot \vec{u} \quad (2)$$

The cross-sectional area A was determined from the difference between the measured surface topography and the calculated subglacial topography (from McNabb et al., 2012) at the gate. Several gates were used to calculate Q_{in} to accommodate the long distance traversed by the retreat over the 37-year record. We defined a set of 4 gates, and for each time interval estimated Q_{in} at all gates upstream of the terminus position. Volume change (dV/dt) in the region between any gate and the terminus was calculated from the corresponding map-plane area change measured in the imagery. The measured area changes were multiplied by ice thickness (H) then scaled by the time interval (Δt) over which they were made:

$$dV/dt = \Delta A * H/\Delta t \quad (3)$$

Ice motion varies strongly over seasonal time scales, and the temporally inconsistent sampling challenges interpretation without introducing aliasing biases related to the sampling time. For example, a change in speed over a year may be misrepresented if one image in a pair was captured at maximum speed and the second captured at mean speed rather than at the time of minimum speed. Our annual estimates of speed are resolved with confidence but seasonal changes are often poorly constrained.

Our results indicate that the highest calving flux of the entire retreat to date, 8-10 $km^3\ yr^{-1}$, occurred during the early stages of entrapment of the terminus in the Kadin-Great Nunatak Gap (1998-2000). Comparable fluxes occurred in the early 1990s and during the opening of the inner fjord in 2008-2010. Since then calving flux has declined to essentially pre-retreat levels (2 $km^3\ yr^{-1}$). Since the onset of retreat, more than 150 km^3 of ice has been lost to a combination of melt and calving, with calving dominating melt by a factor of 3 to 2 (Rasmussen et al., 2011). However, despite the high rate of retreat, the incoming flux Q_{in} still dominated the volume change at the terminus (dV/dt) over most of the retreat. This means that the high iceberg discharge was mostly drawing from large reservoirs of ice far upstream and the rate of terminus retreat was slower than it otherwise would have been.

The spatial and temporal patterns in the discharge data illustrate of how fjord geometry is a primary control on discharge. Early in the retreat, when the glacier terminus was located in the shallow regions around the moraine shoal, ice flow was generally stable, with seasonal retreats and recovering advances. Meanwhile, long-term climatically-forced thinning of the lower glacier (not visible in the glacier-wide mass balance) was leading the near-terminus glacier geometry

toward a dynamically unstable configuration (defined by Pfeffer (2007) as approximately 3/2 of the flotation thickness), and in 1982-1984 the pattern of seasonal retreat and advance was replaced by accelerating retreat, thinning, flow speed, and calving rate. Sustained retreat, modulated by modest seasonal re-advances, persisted through the 1990s as the terminus retreated upstream through the broad and deep lower fjord. Not until the terminus started to engage with the Kadin-Great Nunatak gap, around 1998-1999, did the retreat rate slow down, although ice flux through the terminus (i.e. calving) remained initially high.

Peak discharge rates exceeding 10 km^3 per year occurred in 1999-2000, coincident with the retreat of the terminus onto a steeply reverse-sloped bed in the deepest portion of the outer fjord, at the Kadin-Great Nunatak Gap. While the terminus position was temporarily pinned by lateral convergence in the Gap (2001-2006), ice flux declined and the West-Main Branch confluence immediately upstream of the constriction thinned until the ice reached flotation again, leading to the opening of the inner fjord (2007-2010). This episode of thinning, flotation, retreat, and restabilization in the shallow water of the Main Branch was analyzed in detail in Report 2. The pattern seems to be somewhat cyclic, and the glacier terminus, which has continued to thin since 2010, now may be approaching another episode of instability. We discuss this further below.

Hydrographic and bathymetric measurements performed in October 2014 by Rob Campbell in Columbia Glacier's inner fjord reveal several further links between the ocean and the glacier. As discussed above, the sudden 1.5 km retreat of the West Branch was a surprise. Not only is the ice in the West Branch ~400 m thicker (and the fjord 400 m deeper) than previously thought, but the new bathymetry reveals that the fall 2014 terminus was located on a reverse-slope bed (where bed depth increases with distance upstream), a geometry known to be unstable (e.g. Meier and Post, 1987; Cuffey and Paterson, 2010).

The reverse bed slope explains the continued West Branch retreat through winter 2014-2015. However, it is unlikely that the bed extends below sea level for much further upstream, and unlikely that the West Branch will continue to retreat for much longer, as the bed rises steeply immediately upstream of the present terminus and rock is showing through the ice in one location. Campbell's measurements also show large differences in water circulation and heat transport between the eastern and western parts of the inner fjord. A counterclockwise circulation, possibly linked to the predominant winds and resulting Eckman transport in the inner fjord, limits the circulation of warm water into the West Branch, while allowing warm upwelling in the Main Branch. Iceberg trains and plumes of brash ice visible in the GPRI image sequences (Figure 3) suggests that three initially independent water masses are mixing in the open area between the Kadin-Great Nunatak Gap and Juncture. These are the two freshwater inputs from the West and Main Branches, and the ocean water carried up the fiord by tidal currents.

The 2014 bathymetry also provides strong constraints on the geometry of the Main Branch. Like the West Branch, a narrow segment of the Main Branch channel is deeper than previously thought by at least 50 -100m, although deep water in this region has been hypothesized as early as Engel (2008) but never confirmed.

Vertical profiles of temperature obtained from Campbell's measurements show that warm water was present in Columbia Bay in October 2014. Although the atmosphere generally cools by this time of year, ocean temperatures remain warm substantially later in the year, which results in elevated rates of iceberg melt. Warm water is also an important driver for melting along the submarine ice cliff. This kind of submarine melting can account for 50% of the total mass flux discharged at the terminus (e.g. Motyka et al., 2013) when the warm water is convectively mixed by freshwater subglacial discharge. Turbidity measurements from the same observations suggest that freshwater is being discharged by the glacier, but the vigorous estuarine circulation seen in other glacierized fjords is not obviously present here. Similar data collection at a coarser scale in 2006 was interpreted as indicating estuarine circulation, comparable to data from LeConte and Yahtse glaciers. These new data suggest that the submarine melt process may have a strong seasonal component.

Iceberg processes

Our observations of the moraine shoal indicate that erosion at the crest has been inconsequential since the onset of the glacier's retreat. Within the limited precision of the earlier bathymetric surveys, the moraine geometry has remained constant and the limit imposed by the moraine on the size of escaping bergs thus has not changed. The largest icebergs that do escape pass through a low trough (Report 2, Figure 2-3, 18 m below Mean Lower Low Water) in the moraine. Our qualitative assessment of iceberg passage over the moraine (from time-lapse photography) indicates that icebergs are flushed quasi-periodically through this gap and over the moraine, with both tides and wind governing their escape.

Characteristics of future iceberg discharge

Given the stability of the moraine shoal, the factors that will control the number and size of icebergs reaching Columbia Bay and Prince William Sound in the future are (a) the number and size of icebergs produced at the terminus of Columbia Glacier, including the possibility of transient episodes of accelerated calving and ice flux, and (b) the rate of fragmentation and melt of icebergs as they travel down-fjord to the moraine shoal.

Our original research plan included the development of a transport model for icebergs moving down-fjord from the calving terminus to the moraine shoal; the number density and size distribution of icebergs was to be calculated based on fluid mechanics and heat transfer principles, providing the sizes and numbers of icebergs arriving at the moraine shoal. Subsequent observations of currents in the fjord, and especially those observations made by

GPRI in the inner fjord, revealed a far more complex and unpredictable pattern of currents than we originally estimated, and this model ultimately proved to be intractable. However, our observations also gave us important insights to the processes driving iceberg transport and degradation on a qualitative level, and from these we are confident in drawing conclusions that constrain the characteristics of icebergs arriving at the moraine shoal in the future. We discuss those conclusions here.

The largest icebergs calved at the terminus of Columbia Glacier in the future will almost certainly be smaller than the largest icebergs recorded in the past. The part of the glacier resting below sea level is significantly thinner than the ice passing through the terminus in the past, both because of the shallower bed upstream of the present terminus and the thinning of the glacier throughout the tidewater reach over the course of the retreat. Smaller icebergs have a smaller mass to be melted and have a larger surface-area to volume ratio, making them more susceptible to melt by contact with a warm environment. Furthermore, the journey from the glacier terminus to the moraine shoal is much longer now than it was in the early years of the retreat. Not only is the distance is greater, but the path is more circuitous and icebergs may be caught in gyres that carry them up- and down-fjord repeatedly as tides and winds change. This effect was amplified following the opening of the inner fjord (2007-2010), and the mixing of currents producing high vorticity relative to the outer fjord. The inner fjord also contains shallow reefs where icebergs are regularly seen to ground at high falling tide and fracture under their own weight with continued tidal fall.

Finally, the rate of iceberg production, while generally reduced in magnitude, is likely to remain episodic for the remaining future of the retreat. Ice flux and ice speed vary strongly with the seasons, with the peak calving rate typically occurring in spring, and multi-year intervals of accelerated retreat (like those seen at Columbia Glacier in the past) will continue to occur. In fact, the geometric conditions indicative of an episode of retreat are once again taking shape. The near-terminus ice is approaching flotation thickness (as indicated by the long propagation up-glacier of velocity variations at the terminus, as discussed above), and the bed is believed to be deeper immediately upstream of the present terminus (although the bed in the Main Branch above the present terminus position is imperfectly known).

The “tidewater limit” – the upstream point at which the glacier bed rises above sea level – marks the upstream extent of the glacier’s susceptibility to the ocean. In the upper Main Branch, which climbs rapidly to the west of Divider Mountain into the upper reaches of Columbia Glacier (See Report 1, Figures 1a, 1b), the tidewater limit lies another 8-10 km upstream of the present terminus. We anticipate that the glacier terminus will reach this tidewater limit by 2029 – 2036 (Report 2), with modeled maximum calving rates as high as 6.2 $km^3\ yr^{-1}$ during brief (less than one year) episodes of accelerated retreat. Predicting calving rates and retreat for a separate terminus moving up the glacier’s East Branch (passing to the east of Divider Mountain) will be difficult given the very large uncertainty for the ice thickness in the East Branch (see Reports 4

and 5). When the glacier's terminus reaches this basin, likely sometime after 2035, another episode of rapid calving and retreat may occur, possibly in thick ice. That event is distant enough in time that no quantitative prediction of ice flux can be made, but three significant points can be noted. First, the terminus by that time will be more than 35 km from the moraine shoal, exposing icebergs to yet more melt and degradation over the extended path to the shoal. Second, the inner-fjord shoals in the vicinity of the present terminus will trap a significant fraction of any large icebergs coming from the deep water of the East Branch. Third, thinning may have progressed to the point that, by the time the terminus enters the East Branch basin, the remaining ice below the tidewater limit may be in a state of so-called "disarticulation" (Molnia, 2007) distinguished by the absence of a clearly defined calving terminus and disintegration of all floating ice more or less simultaneously. If this occurs with a shallow barrier, or sill, on the downstream side of the basin (and radar data suggests that such a sill exists, as discussed in Report 4), the disarticulated icebergs may be trapped in the basin and subject to much higher melt rates (by their increased surface-to-volume ratio) relative to intact ice.

All of these factors work towards reducing the likely future iceberg flux and iceberg size coming from the East Branch basin at some point in the future. This is the last known reservoir of thick ice grounded below sea level and subject to rapid tidewater retreat. However, our evaluation is that the probability of large or numerous icebergs issuing from this reservoir at some future time is very low.

Summary Evaluation and Recommendations

The series of 6 reports we have submitted to the Prince William Sound Regional Citizen's Advisory Council form the scientific basis of the following evaluation and recommendations regarding future hazards arising from icebergs originating from Columbia Glacier.

- The retreat of the Columbia Glacier is predicted to cease by 2029 – 2036 (Report 2).
- The maximum calving rate (ice flux at the terminus) during the remainder of the retreat is estimated to range from 5.8 to 6.2 $km^3\ yr^{-1}$ (Report 2).
- More episodes of elevated calving flux are expected, with one episode imminent (Report 5).
- Efforts to construct an explicit iceberg transport model failed, due to the increasing complexity of ocean circulation in the fjord (Report 6).
- Despite the absence of a transport model, a number of factors all act to reduce the initial size of calved icebergs, increase the residence time of ice in the fjord, and increase water temperatures, leading us to these further qualitative conclusions:
    - Individual initial iceberg size is estimated to be smaller in the future than at present (2012-2015) (Reports 3-6).
    - The degradation of icebergs between the time they are calved from the terminus to the time the arrive at the moraine shoal is very likely to increase significantly in the future, meaning that the total ice flux arriving at the shoal, as well as the size distribution of icebergs, will be yet smaller than the predicted ice flux and size distribution predicted for the calving terminus itself.
- Bathymetry at the moraine shoal (Report 2) indicate that the shoal has not suffered erosion over the course of the retreat.
- The likelihood that the shoal will be eroded in the future is extremely low. Erosion would occur from the dragging of iceberg keels across the top of the shoal, but the size and number of icebergs present at the moraine shoal was vastly larger in the past than it is today (and is predicted to be in the future) and no erosion has yet occurred. These observations suggest (with a high degree of confidence) that the capability of the shoal to block the passage of large icebergs out of the fjord and into Columbia Bay will continue undiminished in the future.
- Note that the factors detailed above all act toward reducing the size of icebergs arriving at the Heather Island moraine shoal. This also means that a larger fraction of icebergs may have sufficiently shallow drafts to be able to escape over the moraine. The combined effect of smaller but more numerous icebergs in Columbia Bay proper on overall risk to ship traffic depends in part on what size classes of icebergs are viewed as posing the greatest hazard to ship traffic moving in and out of Port Valdez. We do not address this question.

Risks Icebergs crossing the moraine shoal in Columbia Bay and Prince William Sound proper will continue in the future, but at lower and declining rates, both in terms of iceberg size and frequency of occurrence. Episodes of significantly elevated ice flux in the Sound are possible but infrequent, but will be composed of icebergs generally smaller in size than what is observed today. Our model projections suggest that the retreat will persist for another ca. 20 years at most, at which time the ocean-ending termini of the glacier will have retreated to the tidewater

limit. At this point continued calving will occur, but at rates comparable to other retreated glaciers in the Sound.

The primary increase in risk associated with Columbia Glacier's continued retreat may not be to ship traffic in Prince William Sound proper, but rather to boat operations (e.g., private operators, tour boats) entering upper Columbia Glacier fjord and being exposed to icebergs and waves produced in calving events at the glacier terminus, and to already-calved icebergs that roll or split. This has been a hazard ever since the ice mélange in the fjord upstream from the moraine shoal was clear enough to allow boats access to the terminus, but the risk of encounters will most likely increase in the future as the fjord grows in size, becomes more accessible, and becomes a more popular and desirable destination.

References

Cuffey, K. M., & Paterson, W. S. B. (2010). *The Physics of Glaciers, Fourth Edition* (4th ed.). Academic Press.

Engel, C. S. (2008). *Defining basal geometry and force balance at Columbia Glacier, Alaska* (M.S.). University of Colorado at Boulder.

Evans, W., J. T. Mathis, J. N. Cross (2014). Calcium Carbonate Corrosivity in an Alaskan Inland Sea. Biogeosciences 11(2): 365–379.

Krimmel, R. M. (2001). *Photogrammetric data set, 1957-2000, and bathymetric measurements for Columbia Glacier, Alaska* (No. 2001-4089) (p. 50). U.S. Geological Survey. Retrieved from http://pubs.usgs.gov/wri/wri014089/

McNabb, R. W., Hock, R., O'Neel, S., Rasmussen, L. A., Ahn, Y., Braun, M.,Truffer, M. (2012). Using surface velocities to calculate ice thickness and bed topography: a case study at Columbia Glacier, Alaska, USA. *Journal of Glaciology*, *58*(212), 1151–1164. http://doi.org/10.3189/2012JoG11J249

Meier, M. F., and Austin Post. (1987). Fast Tidewater Glaciers. Journal of Geophysical Research: Solid Earth 92(B9): 9051–9058.

Meier, M., Lundstrom, S., Stone, D., Kamb, B., Engelhardt, H., Humphrey, N., ... & Walters, R. (1994). Mechanical and hydrologic basis for the rapid motion of a large tidewater glacier: 1. Observations. Journal of Geophysical Research: Solid Earth (1978–2012), 99(B8), 15219-15229.

Molnia, B. (2007). Disarticulation of Temperate Glaciers-The Dynamics of Passive Calving. In *Geophysical Research Abstracts* (Vol. 9, p. 09788). Retrieved from http://meetings.copernicus.org/www.cosis.net/abstracts/EGU2007/09788/EGU2007-J-09788.pdf

Motyka, R. J., Larsen, C. F., Freymueller, J. T., & Echelmeyer, K. A. (2007). Post Little Ice Age Glacial Rebound in Glacier Bay National Park and Surrounding Areas. *Alaska Park Science*, *6*(1), 36–41.

Motyka, R. J., Dryer, W. P., Amundson, J., Truffer, M., & Fahnestock, M. (2013). Rapid submarine melting driven by subglacial discharge, LeConte Glacier, Alaska. *Geophysical Research Letters*, *40*(19), 5153–5158. http://doi.org/10.1002/grl.51011

O'Neel, S., K.A. Echelmeyer, and R.J. Motyka (2001). Short-Term Flow Dynamics of a Retreating Tidewater Glacier: LeConte Glacier, Alaska, U.S.A. Journal of Glaciology 47(159): 567–578.

Pfeffer, W. T. (2007). A simple mechanism for irreversible tidewater glacier retreat. *J. Geophys. Res*, *112*.

Rasmussen, L. A., Conway, H., Krimmel, R. M., & Hock, R. (2011). Surface mass balance, thinning and iceberg production, Columbia Glacier, Alaska, 1948–2007. *Journal of Glaciology*, *57*(203), 431–440. http://doi.org/10.3189/002214311796905532

Walters, R. A., & Dunlap, W. W. (1987). Analysis of time series of glacier speed: Columbia Glacier, Alaska. *Journal of Geophysical Research: Solid Earth*, *92*(B9), 8969–8975. http://doi.org/10.1029/JB092iB09p08969